

Examining the role of the adenosine monophosphate-activated protein kinase α_2
(AMPK α_2) subunit on sarcoplasmic reticulum calcium-ATPase (SERCA)
expression and function in sedentary and exercise-trained mice.

by

Marc Morissette

A Thesis submitted to the Faculty of Graduate Studies of
The University of Manitoba
in partial fulfilment of the requirements of the degree of

MASTER OF SCIENCE

Faculty of Kinesiology and Recreation Management
University of Manitoba
Winnipeg, Manitoba, Canada

Copyright © 2013 by Marc Morissette

Abstract

This thesis determined whether changes in adenosine monophosphate-activated protein kinase (AMPK) activity would influence sarcoplasmic reticulum Ca^{2+} -ATPase (SERCA) content and function in left ventricle (LV) and skeletal muscle isolated from sedentary or exercise trained mice. The data indicate that AMPK α_2 kinase dead transgenic (KD) mice, as compared to wild-type (WT) mice, were characterized by reduced SERCA1a, SERCA2a and higher phospholamban (PLN) protein levels in both cardiac and skeletal muscle. Notably, exercise-training up-regulated myocardial SERCA2a protein content by 43%, as compared to sedentary WT mice. In contrast, exercise-training did not alter myocardial SERCA2a protein content in KD mice. Even so, exercise-training up-regulated SERCA1a protein content in skeletal muscle in both WT and KD mice. Based on these data, it appears that an AMPK α_2 -mediated mechanism influences SERCA2a content and function in the heart and skeletal muscle, which may contribute to the pathophysiology of models characterized by impaired AMPK activity and impaired calcium-cycling.

Acknowledgements

Over the past 10 years at the University of Manitoba, I have had the chance to work alongside many people that have helped me mature both academically and personally.

I would first like to acknowledge my graduate supervisor, Dr. Todd Duhamel. Todd has always taken the time to help when hurdles appeared in my way. He has been supportive of any decisions I have made and has helped me achieve specific academic and professional goals. I hope that one day I may be able to influence others the same way that Todd has influenced me.

Secondly, I would like to acknowledge of Dr. Gordon Glazner for giving me my first summer student position and introducing me to the world of scientific research. Furthermore, I would also like to acknowledge Dr. Jason Schapansky, Dr. Darrell Smith and all other lab members I worked with in Dr. Glazner's lab for guiding and helping me during my time at the St. Boniface Hospital Research Centre. They always took the time to answer my questions and put up with many of my mistakes. Without these people I would have never continued on this path, and for that I am extremely grateful.

I must also acknowledge all those who have helped me complete the work contained within this thesis. Shanel Susser, Teri Moffatt, Pat Sheppard and Andrew Stammers have all played a big part in helping me along and without them around this wouldn't have been possible.

Acknowledgement must also be given to the Natural Sciences and Engineering Research Council of Canada (NSERC; Alexander Graham Bell Canada Graduate Scholarship) and the Government of Manitoba (Manitoba Graduate Scholarship) for their financial support during my time in Dr. Duhamel's lab. I would not be able to write this document without their funding and their support has helped avoid any financial stress.

Finally, I would like to acknowledge my family. They have been nothing short of amazing in providing support and encouragement throughout my academic career. I have had to make tough decisions and have sometimes felt discouraged; however they have always been by my side and helped me through rough patches. While I have made sacrifices over the past few years, they have as well. Everything you have done for me is greatly appreciated.

Dedication

I would like to dedicate this work to all my family and friends; specifically Aura, Danielle, grandpa (Ray), mom (Janice), and dad (Ron). Whether it be personal, financial or academic problems, I have always had someone to talk to and you have always shown your support. I can honestly say that without any of you, I would never have made it this far.

List of Abbreviations

- A wave – Atrial ventricular filling velocity
- ACC – Acetyl-CoA carboxylase
- AMP – Adenosine monophosphate
- AMPK – Adenosine monophosphate activated protein kinase
- AMPKK – AMPK kinase
- AMPK α_2 KD – AMPK α_2 kinase dead
- AMPK α_2 KO – AMPK α_2 knockout mice
- AMPK α^{Thr172} – AMPK α threonine 172
- ATP – Adenosine triphosphate
- BCA – Bicinchoninic acid
- Ca²⁺ – Calcium
- CaMK – Ca²⁺/calmodulin-dependent protein kinase
- CaMKK – Ca²⁺/calmodulin-dependent protein kinase kinase
- CICR – Ca²⁺-induced Ca²⁺ release
- COX – Cytochrome C oxidase
- CPA – Cyclopiazonic acid
- DHPR – Dihydropyridine receptor
- DT – Deceleration time
- E wave – Early ventricular filling velocity
- EDL – Extensor digitorum longus
- EF – Ejection fraction
- HEK-293 – Human embryonic kidney 293 cells
- GLUT4 – Glucose transporter-4
- HR – Heart rate

KD+Ex – AMPK α_2 kinase dead +exercise

KD+Sed – AMPK α_2 kinase dead+sedentary

LC – Loading control

LCM – Laser capture microdissection

LV – Left ventricle

LVIDd – Left ventricular internal dimension in diastole

LVPWd – Left ventricular posterior wall dimension

m/min – Meters per minute

MCK – Muscle creatine kinase

MI – Myocardial infarction

PBS – Phosphate buffered saline

PhB – Phosphate buffer

PKA – cyclic-AMP-dependent protein kinase

PLN – Phospholamban

PLN^{Ser16} – Phospholamban serine 16

PLN^{Thr17} – Phospholamban threonine 17

PVDF – Polyvinylidene fluoride

qPCR – Real-time polymerase chain reaction

RyR – Ryanodine receptor

SERCA – sarcoplasmic reticulum Ca²⁺-ATPase

SIRT1 – Sirtuin 1

SIRT3 – Sirtuin 3

SLN – Sarcolipin

SLN^{T5A} – Sarcolipin threonine 5 mutant

SLN^{Thr5} – Sarcolipin threonine 5

SR – sarcoplasmic reticulum

TBST – Tris-buffered saline tween

TDI – Tissue Doppler imaging

VO₂ – Oxygen utilization

WT – Wild-type

WT+Ex – Wild-type+exercise

WT+Sed – Wild-type+sedentary

Table of Contents

Abstract	i
Acknowledgments	ii
Dedication	iv
List of abbreviations	v
Table of contents	viii
List of tables	xi
List of figures	xii
Chapter 1: Literature review	
• The importance of muscle contraction	1
• Fiber-type differences	2
• What is the SR calcium-ATPase?	3
• How is SERCA regulated?	5
• Acute exercise down regulates SERCA function	10
• Exercise-training enhances SERCA expression and function	11
• AMPK is a major energy regulator in cardiac and skeletal muscle	16
• Does AMPK exert regulatory control over SERCA?	21
• Fiber-type recruitment patterns	22
Chapter 2: Study design and methods	
• Statement of problem	25
• Rationale	25
• Hypotheses	25

• Animal model	26
• Exercise-training	27
• Graded exercise test	29
• Oral glucose tolerance test	30
• Echocardiography	31
• Tissue removal	31
• Western blot analysis	32
• RNA isolation from left ventricle tissue	33
• Left ventricle qPCR	34
• Immunohistochemistry	35
• Laser capture microdissection	37
• RNA isolation from microdissected muscle samples	38
• qPCR from microdissected muscle samples	39
• SERCA activity assay	41
• Statistical analyses	42
Chapter 3: Results	
• General characteristics of animals	43
• Graded exercise treadmill test	45
• Left ventricle metabolic marker protein abundance	45
• Gastrocnemius metabolic marker protein abundance	46

• Left ventricle SERCA2a, PLN, p-PLN ^{Thr17} and p-PLN ^{Ser16} protein levels	48
• Gastrocnemius SERCA1a, SERA2a, PLN, p-PLN ^{Thr17} and p-PLN ^{Ser16} protein levels	49
• Left ventricle mRNA expression	52
• Laser captured gastrocnemius mRNA expression	53
• Calcium-dependent SERCA activity in left ventricle and gastrocnemius samples	63
• Echocardiography	66
Chapter 4: Discussion	
• AMPK α_2 KD mice are characterized by a down-regulation of AMPK signaling	68
• AMPK α_2 KD transgene and exercise-training affect exercise capacity	69
• Regulation of SERCA2a in cardiac tissue	71
• Regulation of SERCA1a and SERCA2a in skeletal muscle	74
• Fiber-type specific differences in various protein content	75
• Regulation of PLN	79
• AMPK α_2 KD mice are characterized by a prolonged cardiac deceleration time	82
• The link between AMPK and SERCA	83
• Limitations	86
• Conclusion	88
References	92

List of Tables

Literature review

Table 1. Tissue distribution of various proteins in mouse cardiac, as well as slow-twitch and fast-twitch muscle.	5
Table 2. Phospholamban and sarcolipin mRNA and protein distribution in mouse cardiac and skeletal muscle.	8
Table 3. Acute exercise effects on SERCA expression and function in cardiac and skeletal muscle.	11
Table 4. Exercise-training effects on SERCA expression and function in cardiac and skeletal muscle.	13

Study design and methods

Table 5. Forward and reverse primers for left ventricle qPCR.	35
Table 6. TaqMan gene expression assays.	40

Results

Table 7. General characteristics of C57BL/6J mice used in this study at time of tissue collection.	44
Table 8. Five month graded exercise treadmill test.	45
Table 9. Echocardiography parameters at 20 weeks.	67

List of Figures

Literature review

- Figure 1. Graphical representation of Calcium-dependent SERCA activity. 6
- Figure 2. Illustration of proposed phospholamban and sarcolipin regulation in cardiac and skeletal muscle. 7
- Figure 3. Proposed exercise-mediated regulation of adenosine monophosphate-activated protein kinase in cardiac and skeletal muscle. 18

Study design and methods

- Figure 4. Mouse running wheel (Coulbourn Instruments; ACT-551). 28
- Figure 5. Mouse treadmill (Columbus Instruments; Exer-3/6 Treadmill). 30
- Figure 6. Slow, skeletal myosin (Sigma-Aldrich; M8421) immunostained mouse gastrocnemius cross-section. 37
- Figure 7. Gastrocnemius cross-section pre- and post-LCM. 38

Results

- Figure 8. Representative Western blots and graphs depicting left ventricular protein expression of AMPK, p-AMPK^{Thr172}, p-AMPK^{Thr172}/AMPK ratio, p-ACC and COX IV from sedentary and exercise-trained animals. 46
- Figure 9. Representative Western blots and graphs depicting gastrocnemius protein expression of AMPK, p-AMPK^{Thr172}, p-AMPK^{Thr172}/AMPK ratio, p-ACC and COX IV from sedentary and exercise-trained animals. 47
- Figure 10. Representative Western blots and graphs depicting left ventricular protein expression of SERCA2a, PLN, p-PLN^{Thr17} and p-PLN^{Ser16} from sedentary and exercise-trained animals. 49
- Figure 11. Representative Western blots and graphs depicting gastrocnemius protein expression of SERCA1a, SERCA2a, PLN, p-PLN^{Thr17} and p-PLN^{Ser16} from sedentary and exercise-trained animals. 51
- Figure 12. Quantitative PCR data characterizing left ventricle mRNA expression of SERCA2a, PLN and RyR2 from sedentary and exercise-trained animals. 53

- Figure 13. Quantitative PCR data characterizing mRNA expression of MHC-1 β from laser captured gastrocnemius of sedentary and exercise-trained animals. 55
- Figure 14. Quantitative PCR data characterizing mRNA expression of PGC-1 α from laser captured gastrocnemius of sedentary and exercise-trained animals. 57
- Figure 15. Quantitative PCR data characterizing mRNA expression of SERCA1a from laser captured gastrocnemius of sedentary and exercise-trained animals. 59
- Figure 16. Quantitative PCR data characterizing mRNA expression of SERCA2a from laser captured gastrocnemius of sedentary and exercise-trained animals. 61
- Figure 17. Quantitative PCR data characterizing mRNA expression of RyR1 from laser captured gastrocnemius of sedentary and exercise-trained animals. 62
- Figure 18. Calcium-dependent SERCA activity from left ventricle samples isolated from sedentary and exercise-trained animals. 64
- Figure 19. Calcium-dependent SERCA activity from gastrocnemius samples isolated from sedentary and exercise-trained animals. 65
- Figure 20. The link between AMPK α_2 and SERCA expression and function in cardiac and skeletal muscle. 85

Chapter 1: Literature review

The importance of muscle contraction

Muscle contraction and relaxation allow us to perform movements essential for our existence (eg; walking, eating or cardiac cycle). The process that regulates muscle contraction is known as excitation-contraction coupling. In general, excitation-contraction coupling processes are similar between cardiac and skeletal muscle; however, there are some differences. For example, in cardiac muscle, an action potential allows extracellular calcium (Ca^{2+}) to enter the sarcomere through the dihydropyridine receptors (DHPR). Upon influx of Ca^{2+} , a specialized receptor known as the ryanodine receptor (RyR) releases Ca^{2+} from the sarcoplasmic reticulum (SR)¹, which acts as a storage site for intracellular Ca^{2+} . The release of Ca^{2+} from RyR triggers other RyR proteins to open, causing a large release of Ca^{2+} into the cytoplasm. Collectively, this process is known as Ca^{2+} -induced Ca^{2+} release (CICR) (as reviewed by Lamb²). However, CICR does not regulate Ca^{2+} release in skeletal muscle. Upon depolarization of skeletal muscle, DHPRs are directly activated, resulting in the opening of the RyR in the SR. This causes a release of Ca^{2+} from the SR into the cytoplasm of the skeletal muscle cell (as reviewed by Lamb²). Upon release from the SR, Ca^{2+} plays an important cell signalling role in both cardiac and skeletal muscle.

Two main proteins involved in muscle contraction are actin and myosin. At rest, a protein complex consisting of troponin C and tropomyosin prevent actin and myosin from interacting with each other, thereby inhibiting muscle contraction. Following the release of Ca^{2+} from the SR, intracellular Ca^{2+} binds to troponin C and causes a conformational change to tropomyosin. This process exposes the actin-binding site and allows actin-

myosin cross-bridges to form, leading to muscle contraction³⁻⁵. In order for rhythmic muscle contraction to occur, the process of actin-myosin cross-bridge cycling must happen multiple times, which involves the utilization of adenosine triphosphate (ATP) by the myosin ATPase located on the S1 segment of the myosin heavy chain (as reviewed by Geeves⁶). Cellular energy demand increases by ~100-fold when transitioning from rest to exercise⁷, with ~90% of this increase in energy requirement being accounted for by skeletal muscle contraction⁸. Therefore, muscle contraction consumes a significant amount of energy and challenges ATP homeostasis.

Fiber-type differences

It should be noted that skeletal muscle consists of different fibre types, which contributes to differences in functional characteristics for each fiber type. In mice, skeletal muscle is classified as being composed of either slow-twitch (type I) or fast-twitch (type II) muscle fibres, with type II fibers being subdivided further to type IIa, type IIx/d and type IIb⁹. Specifically, the gastrocnemius consists of 54% type IIb fibers, 19% type IIdb, 12% type IIad, 6% type IIa fibers, 6% type I fibers and 2% type IId fibers in the C57BL/6J mouse strain¹⁰. The speed of muscle contraction is dependent on myosin ATPase activity, with slow-twitch muscles having lower activity compared to fast-twitch muscles¹¹. In general, type I and type IIa fibres have the highest mitochondrial content^{12, 13}, indicating that these two fiber-types are the most oxidative and resistant to fatigue. Furthermore, type IIb fibers were found to have a high glycolytic capacity, with type IIx fibers having a moderate glycolytic capacity between the levels observed for type IIa and type IIb fibers^{9, 14}.

What is the SR calcium-ATPase?

In order for muscle relaxation to occur, intracellular Ca^{2+} must be removed from troponin C to restore tropomyosin's inhibitory effect on the actin-myosin complex. A protein known as the SR Ca^{2+} ATPase (SERCA) is primarily responsible for the reuptake of Ca^{2+} back into the SR following muscle contraction¹⁵. This reuptake of Ca^{2+} occurs against a concentration gradient, thus SERCA activity requires energy whereby two Ca^{2+} ions are transported back into the SR at the cost of one ATP molecule³. However, several other types of Ca^{2+} pumps and exchangers are also responsible for regulating intracellular Ca^{2+} levels, including plasma-membrane Ca^{2+} -ATPase, sodium- Ca^{2+} exchanger¹⁶, DHPR² and inositol 1, 4, 5-triphosphate receptor¹⁷. Even so, SERCA is the most important Ca^{2+} transporter during muscle relaxation because it is responsible for removing up to ~92% of intracellular Ca^{2+} ¹⁸. Without proper SERCA function, muscle relaxation would be disrupted, potentially leading to problems in both skeletal and cardiac muscle function. Recently, Tupling et al.¹⁹ utilized isolated extensor digitorum longus (EDL) and soleus muscle preparations incubated in a solution containing the SERCA inhibitor cyclopiazonic acid (CPA) to estimate the proportion of energy utilization that can be attributed to SERCA-mediated Ca^{2+} -transport. In their experiments, CPA maximally inhibited SERCA activity and reduced muscle oxygen consumption by 30%. Importantly, CPA treatment did not alter high-energy phosphates and metabolites in resting muscle, which indicates that the observed differences in oxygen utilization (VO_2) were not a result of impaired oxidative phosphorylation. A search was conducted to identify SERCA's contribution to ATP consumption during muscle contraction; however, no information was found. Even so, Tupling et al.¹⁹

estimate that SERCA pumps account for ~30% of resting metabolic rates in mice. Thus, the importance of SERCA activity and function in regulating energy homeostasis is significant.

Several different SERCA isoforms are known to exist in mammals, namely SERCA1a, SERCA1b, SERCA2a, SERCA2b, SERCA3a, SERCA3b and SERCA3c. Notably, the variety of SERCA isoforms appear to be expressed in a tissue specific manner. First described by Brandl et al.²⁰, a difference in SERCA protein isoforms was found between cardiac muscle and fast- and slow-twitch skeletal muscle fiber-types. Using rabbit muscle, they demonstrated that cDNA from one SERCA isoform hybridized to mRNA from slow-twitch and cardiac muscle; whereas, a different SERCA isoform's cDNA only hybridized to mRNA isolated from fast-twitch muscle. Indeed, additional literature has confirmed that SERCA2a is expressed in mouse slow-twitch skeletal and cardiac muscle; whereas SERCA1a is expressed in mouse fast-twitch skeletal muscle²¹⁻²⁴ (Table 1). This muscle specific expression pattern has since been confirmed in other animal models.

Table 1. Tissue distribution of various proteins in mouse cardiac, as well as slow-twitch and fast-twitch muscle.

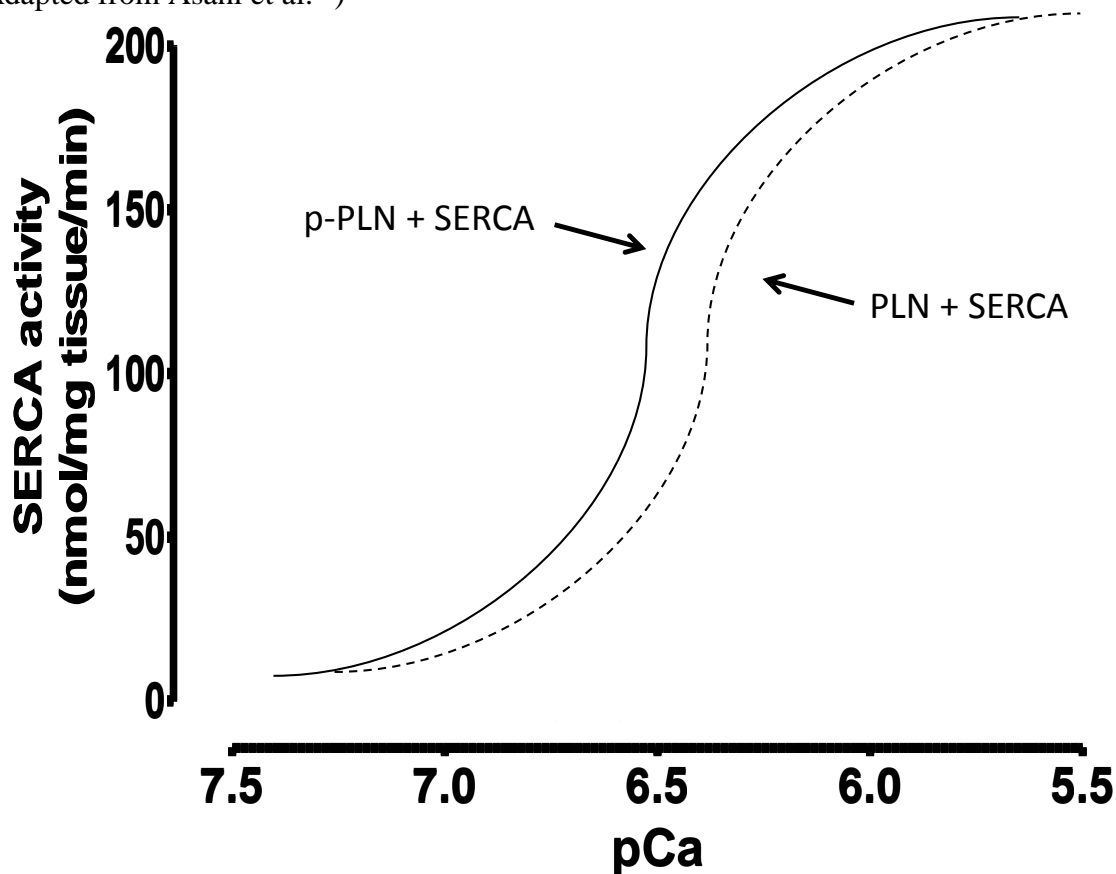
	Cardiac	Slow-twitch	Fast-twitch
MHC	MHC1 α ^{25, 26} MHC1 β ^{25, 26}	MHC1 β ^{9, 27}	MHCIIa ^{9, 27} MHCIIb ^{9, 27} MHCIIc/x ^{9, 27}
RyR	RyR2 ¹	RyR1 ¹	RyR1 ¹
SERCA	SERCA2a ²¹	SERCA2a ²¹	SERCA1a ²¹
PLN	PLN ²⁴	Not detected ²⁴	
SLN	SLN ^{24, 28}	SLN ²⁸	
AMPK	AMPK α ₁ ²⁹ AMPK α ₂ ²⁹ AMPK β ₁ ³⁰ AMPK β ₂ ³⁰ AMPK γ ₁ ³¹ AMPK γ ₂ ³¹	AMPK α ₁ ^{29, 32} AMPK α ₂ ^{29, 32} AMPK β ₁ ^{30, 33} AMPK β ₂ ^{30, 33} AMPK γ ₁ ³¹ AMPK γ ₂ ³¹ AMPK γ ₃ ³¹	AMPK α ₁ ^{29, 32} AMPK α ₂ ^{29, 32} AMPK β ₁ ^{30, 33} AMPK β ₂ ^{30, 33} AMPK γ ₁ ³¹ AMPK γ ₂ ³¹ AMPK γ ₃ ³¹
LKB1	LKB1 ³⁴	LKB1 ³⁵	LKB1 ³⁵
CaMKK	CaMKK β ³⁶	CaMKK α ³⁷ CaMKK β ³⁷	CaMKK α ³⁷ CaMKK β ³⁷

MHC, Myosin heavy chain. **RyR**, Ryanodine receptor. **SERCA**, Sarcoplasmic reticulum calcium ATPase. **PLN**, Phospholamban. **SLN**, Sarcophilin. **AMPK**, Adenosine monophosphate-activated protein kinase. **LKB1**, Serine/threonine kinase 11. **CaMKK**, Calcium/calmodulin-dependent protein kinase. **Superscript**, reference.

How is SERCA regulated?

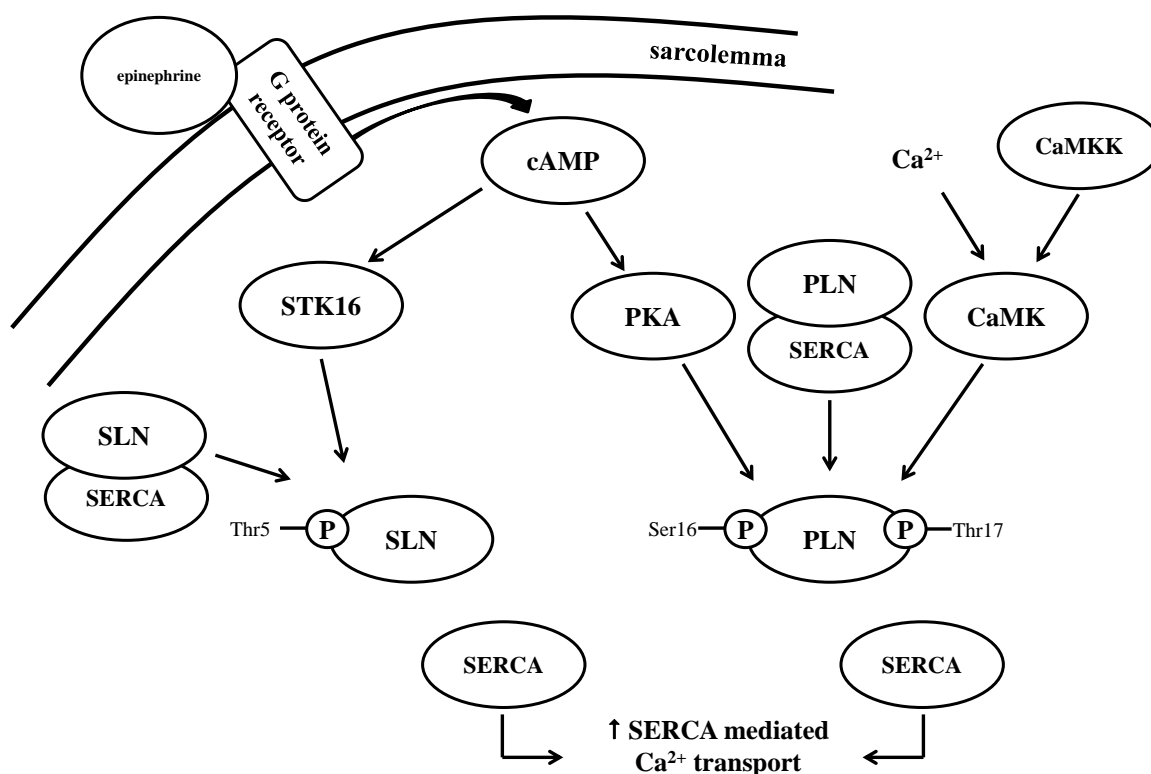
Following the release of Ca²⁺ into the cytosol, Ca²⁺ binds to high-affinity sites on SERCA, after which ATP is hydrolyzed. This results in the phosphorylation of SERCA, inducing a conformational change and a transition from high-affinity to low-affinity for Ca²⁺. The net result in the transport of Ca²⁺ from the cytosol into the SR, at a ratio of 2 Ca²⁺:1 ATP²¹. Additionally, a protein known as phospholamban (PLN) plays a pivotal role in the regulation of SERCA activity and function. In its natural unphosphorylated state, PLN binds to and inhibits SERCA2a at submaximal Ca²⁺ concentrations²² (Figure 1).

Figure 1. Graphical representation of Calcium-dependent SERCA activity. p-PLN, phosphorylated phospholamban. SERCA, sarcoplasmic reticulum calcium ATPase. (Adapted from Asahi et al.³⁸)



Upon the phosphorylation of PLN, this inhibition is relieved, which allows PLN to dissociate from SERCA, thereby enabling SERCA activity to increase at a submaximal Ca^{2+} concentration²². Phosphorylation of PLN occurs via the action of either cyclic-AMP-dependent protein kinase (PKA) or Ca^{2+} /calmodulin-dependent protein kinase (CaMK)²² at residues serine 16 ($\text{PLN}^{\text{Ser16}}$) and threonine 17 ($\text{PLN}^{\text{Thr17}}$), respectively^{39, 40} (Figure 2).

Figure 2. Illustration of proposed phospholamban and sarcolipin regulation in cardiac and skeletal muscle. Phospholamban and sarcolipin's inhibitory effect over SERCA function is alleviated following phosphorylation at specific sites by various up-stream regulators. Ca^{2+} , calcium. CamK, Calcium/calmodulin-dependent protein kinase. CaMKK, Calcium/calmodulin-dependent protein kinase kinase. cAMP, cyclic AMP. PKA, protein kinase A. PLN, phospholamban. Ser16, serine 16. SERCA, sarcoplasmic reticulum calcium ATPase. SLN, sarcolipin. STK16, serine/threonine-protein kinase 16. Thr17, threonine 17. Thr5, threonine 5.



In regards to fiber-type specific expression, PLN mRNA was shown to be expressed in both atrial and ventricular tissue as well as in soleus and EDL in mice²⁴. However, PLN is not found in mouse fast-twitch skeletal muscle^{22, 41} (Table 2), which suggests another SERCA regulator may be present in this muscle type or that SERCA1a is not regulated by endogenous proteins.

Table 2. Phospholamban and sarcolipin mRNA and protein distribution in mouse cardiac and skeletal muscle.

	PLN		SLN	
	mRNA	Protein	mRNA	Protein
Ventricle	✓ ^{24, 42}	✓ ²⁴	X	X
Atrium	✓ ^{24, 42}	✓ ²⁴	✓ ^{24, 42}	✓ ^{24, 28}
Soleus	✓ ²⁴	X	✓ ^{24, 42}	✓ ²⁸
Gastrocnemius	X	X	✓ ⁴³	✓ ²⁸
EDL	✓ ²⁴	X	✓ ⁴²	✓ ²⁸

✓, mRNA or protein is present in tissue. X, mRNA or protein is not present in tissue. **Superscript**, reference.

Sarcolipin (SLN), a protein analogous to PLN was first discovered in 1972, with recent research demonstrating that SLN exerts regulatory control over SERCA2a and SERCA1a in cardiac as well as slow- and fast-twitch muscle²². Vangheluwe et al.²⁴ have found SLN mRNA in mouse atrial tissue and soleus muscle, while recent evidence shows that SLN is expressed at the protein level in mouse atrial tissue, EDL, gastrocnemius and soleus muscles²⁸ (Table 2). Unfortunately, SLN remains a difficult protein to quantify, due to the absence of a commercially available and reliable antibody. As summarized by Tupling et al.²⁸, two different SLN antibodies have been used in previous studies to detect SLN protein levels. One antibody directed at the COOH terminus of SLN has demonstrated high levels of SLN in soleus and low levels in EDL^{44, 45}. However, a second SLN antibody targeting the NH₂ terminus showed very little to no SLN in either tissue²⁴. Furthermore, Ackermann et al.⁴⁶ mention that the SLN antibody used in their studies was ineffective for immunoblotting.

Despite the difficulty in quantifying SLN's protein levels, both PLN and SLN appear to be important in the regulation of SERCA activity and function in cardiac and skeletal

muscle. Specifically, Odermatt et al.⁴⁷ demonstrated that SLN colocalizes with SERCA1a. They also found that at low Ca^{2+} concentrations in human embryonic kidney 293 cells (HEK-293), SLN decreases maximal SERCA1a activity by ~10%, indicating a reduction in SERCA affinity for Ca^{2+} . However, at high Ca^{2+} concentrations maximal SERCA1a activity was increased by ~30%. Further evidence supporting SLN's inhibitory control over SERCA was demonstrated by Shanmugam et al.⁴⁸, where they found reduced cardiac SLN protein levels in chronic atrial fibrillation patients compared to control subjects ($53.1 \pm 6.5\%$ vs. $100.0 \pm 5.5\%$, respectively). This was associated with a concomitant increase in V_{\max} of Ca^{2+} -dependent Ca^{2+} uptake in atrial fibrillation subjects (atrial fibrillation: $204 \pm 8 \text{ nmol}\cdot\text{mg}^{-1}\cdot\text{min}^{-1}$ vs. control: $135 \pm 15 \text{ nmol}\cdot\text{mg}^{-1}\cdot\text{min}^{-1}$), along with a decrease in intracellular Ca^{2+} levels that elicited 50% of V_{\max} (atrial fibrillation: $129 \pm 9 \text{ nmol/L}$ vs. control: $159 \pm 10 \text{ nmol/L}$). These findings demonstrate that SERCA's affinity for Ca^{2+} is increased when SLN protein levels are decreased, leading to more efficient Ca^{2+} transport.

In regards to sarcolipin regulation, a protein known as STK16 (Figure 1) has been shown to relieve SLN's inhibitory control over SERCA1a in HEK-293 cells through phosphorylation at sarcolipin threonine 5 (SLN^{Thr5})⁴⁹. Specifically, when a sarcolipin threonine 5 (SLN^{T5A}) mutant was expressed, there was no change in the amount of Ca^{2+} required to elicit 50% of maximal Ca^{2+} uptake when STK16 was added, indicating that SLN's inhibitory control over SERCA was maintained. Similarly, a study by Bhupathy et al.⁵⁰ utilized adenoviral overexpression of a SLN^{T5A} mutant in cardiac myocytes, which resulted in impaired cell shortening compared to control myocytes ($3.90 \pm 0.34\%$ vs. $6.84 \pm 0.52\%$, respectively). Furthermore, overexpression of the SLN^{T5A} mutant also

resulted in increased time to 50% relaxation (SLN^{T5A}: 0.14 ± 0.01 s vs. control: 0.10 ± 0.01 s, respectively), and decreased rates of relaxation (control: -58.64 ± 8.74 $\mu\text{m/s}$ vs. control: -128.5 ± 18.54 $\mu\text{m/s}$). Finally, SLN^{T5A} myocytes demonstrated increased time for intracellular Ca²⁺ removal when compared to control myocytes (0.12 ± 0.01 s vs. 0.08 ± 0.004 s, respectively), indicating that SLN^{T5A} mutation interferes with SLN^{Thr5} phosphorylation, thereby preventing the relief of SERCA inhibition and impairing Ca²⁺ reuptake.

Acute exercise down regulates SERCA function

SERCA plays an important role in regulating muscle relaxation through the sequestration of Ca²⁺. However, published literature indicates that SERCA protein function is impaired following prolonged exercise to exhaustion (Table 3). For example, in a study by Hill et al.⁵¹, subjects performed two sets of 90 repetitions for knee flexion and extension, after which muscle biopsies were taken. They found that in human vastus lateralis muscle, Ca²⁺-uptake (which is a measure of SERCA-mediated Ca²⁺ transport) was reduced by 26% following isokinetic exercise. Data from a study by Byrd et al.⁵² shows that SERCA activity decreased by ~45% in rat gastrocnemius and vastus muscles following 45 minutes of treadmill running. Additionally, maximal Ca²⁺ uptake was reduced by 40% after 20 minutes of exercise. These results support the findings of Belcastro et al.⁵³, in which exhaustive exercise results in significantly lower SERCA activity (~21%) compared to control tissue in rat gastrocnemius. Furthermore, Duhamel et al.⁵⁴ showed that maximal SERCA activity was reduced by 32% and 27% in a low carbohydrate diet group and a high carbohydrate diet group, respectively, in human vastus lateralis tissue following cycling exercise at ~70% $\dot{V}O_{2\text{peak}}$. A search was

conducted to identify the effects of acute exercise on SERCA function in mouse tissue, however no studies were found. Even so, the described studies demonstrate that an acute bout of exercise impairs SERCA-mediated Ca^{2+} transport, which appears to directly contribute to muscle fatigue.

Table 3. Acute exercise effects on SERCA expression and function in cardiac and skeletal muscle.

Study	Tissue	Exercise intervention	Outcome
Hill et al. ⁵¹	Human vastus lateralis	2 sets of 90 reps of knee flexion (60°/sec) and extension (240°/sec)	<ul style="list-style-type: none"> • ↓ Ca^{2+}-uptake by 26%
Byrd et al. ⁵²	Rat gastrocnemius and vastus muscles	Treadmill running at 21 m/min and 10% grade for 20 min, 45 min or until exhaustion	<ul style="list-style-type: none"> • ↓ SERCA activity • ↓ maximal Ca^{2+} uptake by 40%
Belcastro et al. ⁵³	Rat gastrocnemius	Treadmill running at 25 m/min at a 10% grade until voluntary exhaustion	<ul style="list-style-type: none"> • ↓ in SERCA activity by 21%
Duhamel et al. ⁵⁴	Human vastus lateralis	Cycling at ~70% $\text{VO}_{2\text{peak}}$ until volitional fatigue (< 50 rpm)	<ul style="list-style-type: none"> • ↓ in SERCA activity by 32% (Lo CHO) and by 27% (Hi CHO) • ↓ Ca^{2+} uptake by 36% (Lo CHO) and by 24% (Hi CHO)

Exercise-training enhances SERCA expression and function

Although acute exercise down regulates SERCA protein function, it remains possible that a chronic exercise-training program may stimulate muscles to adapt to overcome this

initial decrease in SERCA function (Table 4). For example, Ferreira et al.⁵⁵ demonstrated that SERCA2a protein content in C57BL/6J soleus increased by ~20% following 8 weeks of treadmill running, 5 days per week for 60 minutes at “the highest workload that can be maintained over time without continual blood lactate accumulation”⁵⁶. For that study, this workload equated to ~60% of maximal speed achieved during a graded treadmill exercise test. Similarly, SERCA1a content also increased by ~20% in plantaris muscle. Bueno et al.⁵⁷ used a similar treadmill training protocol and found that C57BL/6J mice demonstrated a ~17% increase in both SERCA2a and SERCA1a protein levels in soleus and plantaris, respectively, compared to their sedentary counterparts. Interestingly, it was shown that SERCA2a mRNA expression significantly increased in rat gastrocnemius following both a moderate- or high-intensity training regime in a study by Kubo, et al.⁵⁸. In that study, animals trained for five consecutive days, for a 6-week period. One group performed moderate-intensity exercise consisting of running at 20 meters per minute (m/min) at 0% grade for 60 minutes; whereas the high-intensity group performed five 1-minute sprints at 75 m/min at 15% grade, separated by 1-minute bouts of recovery at 20 m/min at 15% grade. An interesting finding from that study is that high-intensity interval training resulted in similar increases in gastrocnemius SERCA2a mRNA compared to moderate-intensity exercise-training (high-intensity = 1.50 ± 0.13 ; moderate-intensity = 1.23 ± 0.12). While the studies discussed above focused on rodent models, Duhamel et al.⁵⁹ found that three consecutive days of submaximal exercise-training resulted in a 14% increase in SERCA1a protein content in human quadriceps muscle, with no change in SERCA2a protein content. Therefore, it is possible that the SERCA1a protein isoform may respond to exercise-training to a greater extent than does SERCA2a.

Table 4. Exercise-training effects on SERCA expression and function in cardiac and skeletal muscle.

Study	Tissue	Exercise-training intervention	Outcome
Ferreira et al. ⁵⁵	Mouse soleus and plantaris	Treadmill running at MLSS, up to 60 min, 5 days/week for 8 weeks	<ul style="list-style-type: none"> • ↑ soleus SERCA2a protein content • ↑ plantaris SERCA1a protein content
Bueno et al. ⁵⁷	Mouse soleus and plantaris	Treadmill running at MLSS for 60 min, 5 days/week for 8 weeks	<ul style="list-style-type: none"> • ↑ soleus SERCA2a protein content • ↑ plantaris SERCA1a protein content
Kubo et al. ⁵⁸	Rat gastrocnemius	Moderate-intensity: 20 m/min at 0% grade, for 60 min High-intensity: 5x1 min sprints (75 m/min, 15% grade), 1 min recovery (20 m/min, 15% grade); both for 5 consecutive days/week for 6 weeks	<ul style="list-style-type: none"> • ↑ SERCA2a mRNA
Duhamel et al. ⁵⁹	Human vastus lateralis	Cycling at ~60% $\dot{V}O_{2peak}$ for up to 2 hours, on three consecutive days	<ul style="list-style-type: none"> • ↑ SERCA1a protein content
Tate et al. ⁶⁰	Rat heart (LV)	Treadmill walking at 16 m/min at 5% grade, up to 60 min/day, 5 days/week, for 10 weeks	<ul style="list-style-type: none"> • ↑ rate of SR Ca^{2+} uptake
Tate et al. ⁶¹	Rat heart (LV)	Treadmill walking at 16 m/min at 5% grade, up to 60 min/day, 5 days/week for 10 weeks	<ul style="list-style-type: none"> • ↑ SERCA2a mRNA and protein content

Wisloff et al. ⁶²	Rat intraventricular septum (IVS)	Treadmill intervals: 85-90% VO _{2max} for 8 min, 2 min recovery at 50-60% VO _{2max} ; both at ~47% grade, 1.5 hours/day, 5 days/week for 8 weeks	<ul style="list-style-type: none"> • ↑ SERCA2a content by 82% in exercised control group and by 34% in myocardial infarcted group
Davidoff et al. ⁶³	Rat ventricular cardiomyocytes	Voluntary wheel running for 5 weeks (~2,400 m/day)	<ul style="list-style-type: none"> • ↑ rate of cardiomyocyte shortening and relengthening
Stolen et al. ⁶⁴	Mouse heart (LV)	Treadmill intervals: 85-90% VO _{2max} for 4 min, 2 min recovery at 50% VO _{2max} , 80 minutes/day, 5 days/week, 13 weeks	<ul style="list-style-type: none"> • ↑ SERCA2a content ~1.7-fold in diabetic group • ↓ time to 50% of muscle relengthening • ↑ rate of intracellular Ca²⁺ removal

Skeletal muscle is not the only muscle type that undergoes adaptations following exposure to a chronic exercise-training. As demonstrated by Tate et al.⁶⁰, cardiac muscle tissue is also affected by exercise-training. In their study, rats were assigned to one of three groups: sedentary mature, sedentary old and exercised old. The exercise-trained group participated in 8-10 weeks of rapid walking at 16 m/min at a grade of 5%, 5 times per weeks with exercise sessions lasting up to 60 minutes. Following the study, they determined that the exercise-training protocol increased the rate of SERCA-mediated Ca²⁺ uptake in cardiac muscle by ~53%. The same exercise protocol was utilized in a later study by Tate et al.⁶¹ and it was shown that left ventricle (LV) SERCA2a mRNA and protein levels were increased by ~110% and ~25%, respectively in the exercised old

group compared to the sedentary old group. Another study lead by Wisloff⁶² examined the influence of exercise-training on myocardial SERCA2a expression in a model of myocardial infarction (MI). The four experimental groups consisted of: sham-sedentary, sham-training, infarction-sedentary and infarction-training. The training program consisted of 8 weeks of sprint interval treadmill training at 25° incline, 5 days per week for 1.5 hours each session. This training regimen resulted in an 82% increase in SERCA2a protein content in sham-training compared to sham-sedentary and a 34% increase in infarction-training compared to infarction-sedentary. While this study utilized a procedure to induce myocardial infarction, their results demonstrate that exercise has the ability to enhance SERCA2a protein content in both healthy and infarcted hearts. Further support for the notion that exercise-training enhances SERCA2a protein content is found in a study by Davidoff et al.⁶³. In that study, rats were fed either a control or a high-sucrose diet, with subsets of each given access to exercise wheels. Following 8 weeks on a high sucrose diet, rates of cardiomyocyte shortening and relengthening were impaired compared to those on the control diet, indicating that both Ca²⁺ release and uptake were impaired and that cardiac dysfunction was present. Interestingly, 5 weeks of voluntary wheel running (for an average of ~2,400 m/day) completely reversed cardiomyocyte dysfunction and normalized Ca²⁺ transport. Another study utilizing high-intensity exercise-training was conducted by Stolen et al.⁶⁴ where mice alternated between running for 4 minutes at 85-90% VO_{2max} and running for 2 minutes at 50% VO_{2max}. Mice trained for 80 minutes/day, 5 days/week, for a total of 13 weeks. Following exercise-training, diabetes-induced muscle relengthening and intracellular Ca²⁺ removal impairments were restored to WT levels. Furthermore, exercise-training

also increased SERCA2a protein content ~1.7-fold in diabetic cardiomyocytes. Additionally, a recent study by Epp et al.⁶⁵ demonstrated for the first time that exercise-training can help prevent the development of diastolic dysfunction and impaired SERCA2a expression and function in diabetic cardiac muscle. The results from all of the studies discussed indicate that prolonged exercise-training produces protective adaptations to enhance SERCA protein content and function. However, it remains to be elucidated what mechanisms are responsible for how exercise-training regulates these changes in SERCA expression and function in cardiac and skeletal muscle.

AMPK is a major energy regulator in cardiac and skeletal muscle

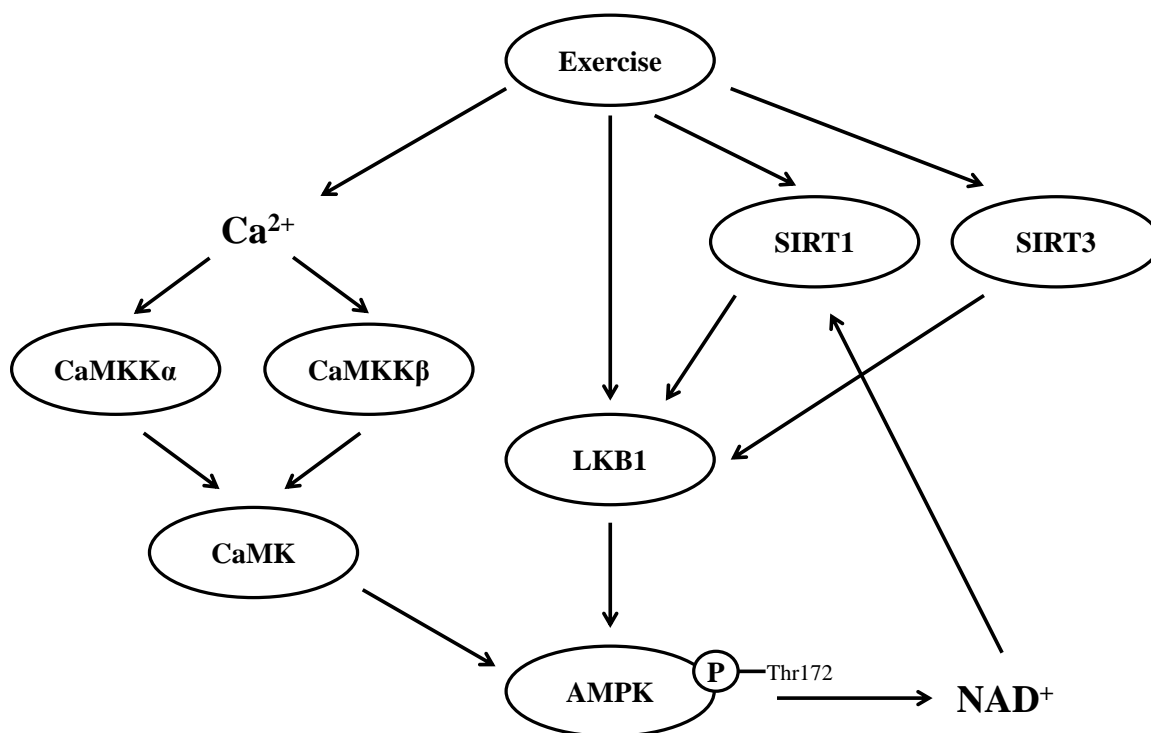
Adenosine monophosphate-activated protein kinase (AMPK) acts as an energy sensor in cardiac and skeletal muscle⁶⁶ by sensing an increase in adenosine monophosphate (AMP) following exercise or other metabolic challenges⁶⁷. This results in an activation of energy metabolism and a transition from anabolic to catabolic pathways⁶⁸. Structurally, AMPK is a heterotrimeric complex, consisting of α -, β - and γ -subunits⁶⁹⁻⁷¹ (Table 1). In a paper by Stapleton et al.²⁹ AMPK α 1 and AMPK α 2 were identified as the two major isoforms of AMPK α in cardiac and skeletal muscle tissue. Similarly, the β -subunit is divided into two subunits, namely β 1 and β 2⁷², with the β 2-subunit being expressed in higher levels in skeletal muscle³³. Finally, all three γ -subunit isoforms (γ 1, γ 2 and γ 3) appear to be found in skeletal muscle, with the γ 3-subunit being expressed at a higher level than either the γ 1- or γ 2- subunit³¹. All three subunits play an important role in AMPK's structure and function. However, the α -subunit serves as the catalytic portion of the enzyme^{30, 70, 73}, while the β -subunit has a structural role, where it acts as a

scaffolding protein to hold the α - and γ -subunits together^{74, 75}. Cheung et al.³¹ demonstrated that γ -subunit contains a site involved in binding AMP. As previously mentioned, the three subunits form a heterotrimeric complex and it is interesting to note that the α_2 subunit is present in the two most highly expressed heterotrimers in human skeletal muscle, namely the $\alpha_2\beta_2\gamma_1$ heterotrimer followed by $\alpha_2\beta_2\gamma_3$ ^{73, 76}.

Activation of AMPK is important in regulating various physiological processes (Figure 3) and there are multiple ways in which activation can occur. Activation can occur through direct phosphorylation at Thr¹⁷² (AMPK α^{Thr172})⁷⁷, which was found to be the main site of AMPK phosphorylation within the α -subunit⁷⁸ and is required for maximal AMPK activation⁷¹. Exercise results in the activation of AMPK through the conversion of AMP from ATP⁷⁷, which causes an upward shift in the AMP:ATP ratio^{70, 79}. Notably, high-intensity exercise has been shown to significantly enhance AMPK activation of the $\alpha_2\beta_2\gamma_3$ heterotrimer⁷⁶; whereas, lower intensity exercise results in moderate $\alpha_2\beta_2\gamma_1$ activation and even less $\alpha_1\beta_2\gamma_1$ activation⁸⁰. AMPK can also be activated through an allosteric change, caused by AMP binding to the γ -subunit, which causes a conformational shift that exposes the α -subunit's active site^{70, 71, 81}. Moreover, the conformational change induced by AMP helps inhibit the dephosphorylation of AMPK α^{Thr172} in the presence of phosphatases, such as protein phosphatase 2C α ^{71, 82} and, thereby, prevents the de-activation of AMPK. Allosteric changes to AMPK results in ~3 fold increase in AMPK activity^{71, 83}; whereas AMPK is activated ~1,000-fold when allosteric changes are combined with the phosphorylation at AMPK α^{Thr172} ⁷¹. This indicates that phosphorylation is the major contributor to AMPK activation and

demonstrates that the phosphorylation of the AMPK α -subunit is an integral part of this process.

Figure 3. Proposed exercise-mediated regulation of adenosine monophosphate-activated protein kinase in cardiac and skeletal muscle. Exercise is capable of increasing AMPK phosphorylation through various regulatory proteins, while p-AMPK α^{Thr172} is capable of activating SIRT1 through a positive feedback mechanism. AMPK, Adenosine monophosphate-activated protein kinase. Ca²⁺, calcium. CamK, Calcium/calmodulin-dependent protein kinase. CaMKK α , Calcium/calmodulin-dependent protein kinase kinase α . CaMKK β , Calcium/calmodulin-dependent protein kinase kinase β . LKB1, Serine/threonine kinase 11. NAD⁺, Nicotinamide adenine dinucleotide. SIRT1, Sirtuin 1. SIRT3, Sirtuin 3. Thr172, Threonine 172.



Phosphorylation of AMPK α^{Thr172} occurs as a result of the action of a few upstream kinases, with the dominant AMPK kinase (AMPKK) being LKB1^{84, 85} (Figure 3). In 2003, the group of Hawley et al.⁸⁵ showed that the AMPK activator, AICAR stimulates AMPK α^{Thr172} phosphorylation by activating LKB1, while Sakamoto et al.³⁵ demonstrated

that LKB1 activity is not altered by muscle contraction. However, a more recent study showed that LKB1 mediates AMPK α^{Thr172} phosphorylation and AMPK α_2 activity following exercise-training⁸⁶. Interestingly, recent evidence demonstrates that sirtuins 1 and 3 (SIRT1 and SIRT3, respectively) also activate the LKB1 mediated pathway through increased LKB1 phosphorylation and deacetylation⁸⁷⁻⁹⁰ and that exercise-training increases SIRT1 and SIRT3 protein content and activity in skeletal muscle^{89, 91, 92}. Furthermore, AMPK is also involved in increasing the activity of SIRT1 by inducing an increase in NAD⁺⁹³, contributing to a positive feed-back loop, whereas AMPK does not appear to be involved in SIRT3 protein expression⁹⁴. While other factors may be involved in activating AMPK, such as leptin and adiponectin⁹⁵, it appears as though their effects may be modulated via an LKB1-mediated pathway⁹⁶.

Although LKB1 is a major activator of AMPK, it has been shown that the protein Ca²⁺/calmodulin-dependent protein kinase kinase (CaMKK) can also phosphorylate AMPK α^{Thr172} in response to the activation of Ca²⁺/calmodulin signalling⁹⁷⁻⁹⁹. Even though CaMKK has different isoforms, it has been shown that CaMKK β regulates AMPK α^{Thr172} phosphorylation in HeLa cells and rat brain tissue^{97, 99}. Specifically, when normalized to their ability to activate CaMKI, CaMKK β phosphorylates AMPK α^{Thr172} 7-times more than CaMKK α ⁹⁷. However, there is a controversy regarding the role of CaMKK α and CaMKK β for regulating AMPK α in cardiac and skeletal muscle. CaMKK α and CaMKK β were not detected in mouse skeletal muscle⁹⁷, while CaMKK α was absent from cardiac tissue and CaMKK β was only slightly detectable in the heart³⁶. A more recent study has demonstrated that CaMKK α and CaMKK β appear to be expressed in rat skeletal muscle, with AMPK activity decreasing when CaMKK was

inhibited³⁷. Therefore, it is possible that CaMKK may contribute to the exercise-induced changes in p-AMPK α^{Thr172} .

As mentioned previously, two AMPK α isoforms exist, namely AMPK α_1 and AMPK α_2 , with both isoforms being co-expressed in skeletal and cardiac muscle²⁹. Studies utilizing a muscle specific AMPK α_2 kinase dead transgenic mouse model (AMPK α_2 KD) or whole-body AMPK α_2 knockout mice (AMPK α_2 KO) have shown that the AMPK α_2 subunit plays a critical role in regulating various metabolic proteins. For example, a study by Jorgensen et al.¹⁰⁰ found that AMPK α_2 KO mice displayed a ~60-70% reduction in basal and exercise-induced skeletal muscle AMPK α^{Thr172} phosphorylation compared to wild-type (WT) mice. They also found that AMPK α_2 KO mice displayed a ~20% reduction in various mitochondrial marker protein content (cytochrome c, cytochrome c oxidase, citrate synthase and 3-hydroxylacyl-CoA dehydrogenase), which may reduce the capacity for oxidative phosphorylation. A study by Mu et al.¹⁰¹ used AMPK α_2 KD mice to demonstrate that the AMPK α_2 subunit is required for contraction-stimulated AMPK α^{Thr172} phosphorylation and subsequent AMPK activation. Furthermore, contraction-stimulated glucose uptake was reduced by 30-40% in the AMPK α_2 KD mice. A more recent study by Lefort et al.¹⁰² found similar findings as Mu et al.¹⁰¹, with AMPK α_2 KD mice displaying no change in AMPK α^{Thr172} phosphorylation or AMPK α activity following muscle contraction. They found that there was a 50% reduction in contraction-stimulated glucose transport in AMPK α_2 KD mice compared to WT animals. In a study by Habets et al.¹⁰³, the presence of the AMPK α_2 KD transgene completely ablated the 1.6-fold increase in CD36-mediated long-chain fatty acid uptake and oxidation induced by AICAR. From this finding, the researchers suggested that AMPK α_2

is essential for contraction-induced increase in long-chain fatty acid uptake mediated through CD36. Furthermore, they also demonstrated that the AMPK α_2 subunit is important in downstream AMPK signaling within cardiac muscle, as evidenced by the decrease in ACC phosphorylation. Jeppesen et al.¹⁰⁴ used the same animal model to demonstrate that this impaired AMPK signaling also occurs in skeletal muscle. These findings are in contrast with Dzamko et al.¹⁰⁵, however it remains possible that differences in exercise stimulus, muscle tissue type and/or AICAR administration may account for these differences. Regardless, based on these collective findings, AMPK α_2 appears to play an important role in the AMPK signalling pathway, both at rest and in response to exercise-training.

Does AMPK exert regulatory control over SERCA?

AMPK's importance in regulating energy homeostasis within cardiac and skeletal muscle during muscle contraction and SERCA's importance in regulating metabolic rate of resting muscle lead us to ask the question of 'whether AMPK may exert regulatory effects over SERCA?'. To date, very little is known in regards to whether AMPK exerts a regulatory effect on SERCA expression and function in cardiac and skeletal muscle, both at rest and in response to exercise-training. In fact, only two papers by Dong et al.^{106, 107} are known to examine the possibility that AMPK regulates SERCA protein expression; whereas no published study has examined if AMPK mediates the exercise-training-induced changes in SERCA protein expression. Notably, Dong's studies demonstrate a relationship between these two proteins, where the partial or complete deletion of the AMPK α_2 subunit reduced SERCA3 activity and expression in mouse and

human endothelial cells¹⁰⁷. Specifically, AMPK α_2 KO display a phenotype where SERCA activity was impaired by ~25% in mouse endothelial cells, while adenoviral overexpression of a constitutively active AMPK α_2 protein restored SERCA activity in mouse aortic endothelial cells¹⁰⁷. In contrast, the use of gene silencing techniques to knock down AMPK α_2 protein content also reduced SERCA activity in mouse aortic endothelial cells¹⁰⁷. Thus, Dong et al.¹⁰⁷ concluded that SERCA3 function is regulated by AMPK expression and signalling in endothelial cells. However, what remains to be elucidated is whether this regulation carries over to skeletal and cardiac muscle. It must be noted that endothelial cells predominantly express SERCA3 and SERCA2b rather than the SERCA1a and SERCA2a isoforms found in skeletal and/or cardiac muscle. This tissue-specific distinction is of importance when interpreting the data presented by Dong et al.¹⁰⁷, because the various SERCA isoforms may be differentially regulated in each tissue.

Fiber-type recruitment patterns

A phenomenon known as the ‘size principle’ guides muscle contraction, with small motor units being recruited initially upon contraction and large motor units being recruited if additional force is required^{108, 109}. Interestingly, small motor neurons innervate slow-twitch muscle fibers and have a low firing threshold, whereas large motor neurons innervate fast-twitch muscle fibers and have a higher firing threshold¹¹⁰⁻¹¹². The gastrocnemius (gastroc) muscle utilizes the ‘size principle’ during muscle contraction because it is a mixed fiber-type muscle^{10, 113} and ultimately, this phenomenon may lead to fiber-type specific differences in the expression and function of various proteins in mixed

fiber-type muscles. Unfortunately, many studies take mixed fiber-type muscles and homogenize them as a whole and no significant differences are found in mRNA/protein content or enzyme activity pre- and post-exercise-training. However, it remains possible that analyzing fiber-type specific responses in these same muscles will lead to significant differences. The reason for this is fiber-types become mixed when homogenizing the tissue as a whole, which might mask the actual fiber-type specific change that may be occurring in different fiber types. In contrast, if the different fiber types were isolated before analysis, it is possible that large changes may be observed between the different muscle fiber-types. As an example, a study by McConell et al.¹¹⁴ looked at differences in AMPK α^{Thr172} phosphorylation following pre- and post-training exercise trials in human vastus lateralis muscle. They found that an acute bout of exercise resulted in an 11-fold increase in AMPK α^{Thr172} phosphorylation amongst untrained participants. Conversely, this increase in AMPK α^{Thr172} phosphorylation was abolished following 10 days of exercise-training. However, that study failed to look at fiber-type specific differences. A follow-up study by Lee-Young et al.¹¹⁵ used a similar exercise protocol as McConell et al.¹¹⁴ and found a ~50% increase in basal AMPK α^{Thr172} phosphorylation in type I, IIa and IIx fibers following 10 days of exercise-training when the muscle fibers were isolated from resting muscle. However, a distinct response to an acute bout of exercise was observed between fiber types, where only type IIx fibers demonstrated an exercise-induced increase in AMPK α^{Thr172} phosphorylation following exercise-training. These findings demonstrate that exercise-induced differences in AMPK α^{Thr172} phosphorylation occur in a fiber-type specific manner, which may lead to fiber-type specific adaptations for proteins downstream of AMPK.

Recent advancements in technology have made it possible to dissect individual muscle fibers from muscle cross-sections using laser capture microdissection (LCM)¹¹⁶. In fact, we believe a modified version of this technique will allow for the dissection of areas of high or low slow-twitch fiber concentration from muscle slices, thereby making it possible to determine if type I or type II fibers are differentially adapting to exercise. Using this method avoids the need to homogenize and analyze muscle as a whole and potentially missing any fiber-type specific differences that may be occurring.

Chapter 2: Study design and methods

Statement of problem

While it is currently known that the AMPK α_2 subunit plays a role in regulating control over SERCA function in endothelial cells, it remains to be seen if this interaction occurs in skeletal and cardiac muscle. Furthermore, although it is known that exercise-training enhances AMPK activity in cardiac and skeletal muscle, it is not yet known if the AMPK α_2 pathway regulates the expression and function of SERCA proteins in response to exercise-training.

Rationale

Based on the theoretical framework presented, I intend to determine if an AMPK α_2 -related biological process regulates SERCA protein expression and function in cardiac and skeletal muscle of sedentary and exercise-trained C57BL/6J mice.

Hypotheses

Four working hypotheses were tested in my proposal. Specifically, I hypothesized that:

1. SERCA protein expression and function will be reduced in cardiac and skeletal muscle isolated from the AMPK α_2 kinase dead transgenic mouse (AMPK α_2 KD), which is known to have a 46-95% reduction in AMPK α^{Thr172} phosphorylation in cardiac and skeletal muscle, as compared to wild-type (WT) mice^{101, 103, 104}.
2. Exercise-training will increase the relative level of AMPK α^{Thr172} phosphorylation and enhance SERCA protein expression and function in cardiac and skeletal muscle isolated from WT mice

3. The exercise-stimulated increase in SERCA protein expression and function will be blunted in cardiac and skeletal muscle isolated from the AMPK α_2 KD mice,
4. SERCA1a and SERCA2a isoforms will differentially adapt to exercise-training based on the specific fiber-type that is assessed.

Animal model

Animals were treated in accordance with the guidelines of the University of Manitoba Animal Protocol Management and Review Committee and the Canadian Council on Animal Care¹¹⁷. Two male AMPK α_2 kinase dead transgenic (KD) mice (~2 months old; 24g) were sent to us from Dr. Morris Birnbaum's laboratory (University of Pennsylvania) in order to establish a breeding colony of AMPK α_2 KD mice at our facility. Male AMPK α_2 KD mice were provided access to female C57BL6/J mice in order to create a breeding colony. The AMPK α_2 KD transgene is expected to be passed according to Mendelian frequency (50%). The heterozygote AMPK α_2 KD transgenic manipulation produces the overexpression of a dominant kinase dead AMPK α_2 protein isoform, resulting in the inactivation of the α_2 catalytic subunit¹⁰¹. More specifically, arginine was substituted for lysine 45 to produce cDNA encoding a kinase dead AMPK α_2 protein^{33, 101}. Certain phenotypic differences are present in the AMPK α_2 KD mouse model, including reduced voluntary wheel running activity and exercise intolerance, as demonstrated by Mu et al.¹⁰¹. Additionally, AMPK α_2 KD mice also display impaired mitochondrial respiration¹¹⁸, glucose uptake¹⁰¹ and fatty acid uptake/oxidation¹⁰³. Of note, is that basal muscle AMPK α_2 activity is diminished by ~46% in cardiomyocytes¹⁰³ and by ~70-95% in skeletal muscle^{101, 104} in this animal model. Interestingly, this reduction in AMPK

activity is limited to cardiac and skeletal muscle using a muscle creatine kinase (MCK) promoter¹⁰¹, which allows muscle specific expression of the transgene^{119, 120}. For this reason, AMPK activity remains unaffected in the kidney, pancreas, lung, spleen, brain, liver and adipose tissue in this KD mouse model¹⁰¹. Therefore, any differences seen between WT and KD mice will be due to local muscle differences instead of systemic changes in metabolism. A whole-body AMPK α_1 or AMPK α_2 knockout mouse model was considered¹²¹. However, their usefulness is limited in our study because differences for AMPK α^{Thr172} phosphorylation are seen in a wide array of tissues. As a result, any differences observed for experiments using whole body knockout could not be attributable solely to muscular adaptations, making our hypothesis more difficult to test. After breeding sufficient mice for our experiments, 32 AMPK α_2 KD mice and 32 wild-type (WT) mice (2 months of age at the start of the experimental protocol) were fed a low-fat Western diet (TestDiet product 5TJS; 12% kcal from fat, 72% kcal from carbohydrates and 16% kcal from protein).

Exercise-training

All animals were divided into 1 of 2 experimental groups. Specifically, half of the WT and half of the KD mice were housed in standard animal cages and were considered to be the sedentary group (i.e. non-exercise trained). The remaining animals were housed in cages that contained a voluntary running wheel (Coulbourn Instruments; ACT-551; Figure 4) for a maximum of 5 months and were considered to be the exercise-trained groups.

Figure 4. Mouse running wheel (Coulbourn Instruments; ACT-551).



The voluntary wheel running system is beneficial because it allows animals to run at will. In our experience with voluntary wheel running, mice may run up to an average of 9 km/day, whereas another study showed that certain C57BL/10 mice ran an average of ~7 km in a 24 hour period¹²². It has also been demonstrated by Duncan et al.¹²³ that distance run in a voluntary wheel is inversely proportional to the age of mice. Furthermore, mice appear to run further and at a higher intensity at night^{101, 124}, which is facilitated with the voluntary wheel running protocol. With this protocol, the total number of wheel counts will be collected on a computer and will be converted to total running distance. Unfortunately, KD mice have been shown to display reduced running activity by 20-30%¹⁰¹, which may result in decreased total voluntary running distance. Forced treadmill running is an alternative exercise-training modality intended to help standardize the amount of exercise each animal performs. However, treadmill running would be conducted during the day, which is when mice appear to be less active^{101, 124}. Furthermore, studies investigating the effects of treadmill running in mice have used

speeds ranging from 12-20 m/min¹²⁵⁻¹²⁹. Using the highest speed of 20 m/min would result in a total running distance of 1.2 km in one hour and the total time required to achieve the distances ran with voluntary running wheels would be substantial. Additionally, mice run at varying intensities throughout the day¹²⁴ and this behaviour would be difficult to reproduce accurately on a treadmill. Voluntary wheel running has previously been shown to modify AMPK activity *in vivo* and has previously been used for this purpose^{130, 131}. For these reasons, our study utilized voluntary running wheels in order to maximize the exercise-training induced adaptations.

Graded exercise test

Exercise-training induced changes in mouse running capacity were measured using a graded treadmill exercise test¹³² (Columbus Instruments; Exer-3/6 Treadmill; Figure 5), as modified by our lab. Hoydal et al.¹³² demonstrated a strong correlation between VO_{2max} and running speed for both mice and rats using their protocol. For baseline testing, mice ran at 7 m/min with speed being increased by 1.6 m/min until fatigue. For follow-up testing, mice warmed up at 60% of previous max speed for 2 minutes, followed by increases to 70% and 80% of previous max speed for an additional 2 minutes each. Mice then ran at 95% of previous max speed for the final 2 minutes of warm-up. From this point, the treadmill speed was increased by 0.8 m/min until the animal is fatigued. Animals were deemed fatigued when they could no longer maintain a running pace. Tests were conducted at baseline, 1, 2, 3, 4 and 5 months.

Figure 5. Mouse treadmill (Columbus Instruments; Exer-3/6 Treadmill).



Oral glucose tolerance test

An oral glucose tolerance test (OGTT) was conducted at the completion of the exercise-training protocol to determine if there were any differences between groups. Briefly, the mice were fasted for 8 h and one drop of blood was taken from a tail prick at baseline. The mice were then provided an oral administration of glucose (2 g/kg body weight) and blood was sampled again 15, 30, 60, and 120 min thereafter. Blood glucose was measured using a glucose meter (AlphaTRAK).

Echocardiography

Echocardiography was employed to identify changes in left ventricular structure and function in vivo, as previously described¹³³⁻¹³⁵. Prior to conducting echocardiograms (either the day of, or a day before), mice were weighed and 1 cm of hair was removed from the thorax region using Nair. Nair was removed using 70% ethanol, after which a layer of acoustic gel was applied. A GE Vivid 7 machine (GE Medical Systems) was used and a 13-MHz probe was placed over the gel to acquire both a parasternal long axis view and a parasternal short axis view. Heart rate (HR), ejection fraction (EF), left ventricular internal dimension in diastole (LVIDd), left ventricular posterior wall dimension (LVPWd), tissue doppler imaging (TDI), early ventricular filling velocity (E wave), atrial ventricular filling velocity (A wave), E/A ratio and deceleration time (DT) were the variables measured. Echocardiography is a valid method for examining mouse heart structure and function¹³⁶. Echocardiography was performed at the conclusion of the study by our collaborators in the Dr. Jassal research group¹³³.

Tissue removal

Upon completion of the 5-month exercise-training protocol, animals were removed from the running wheel cages approximately 2 hours before tissue collection. This tissue isolation procedure was utilized in order to minimize sedentary time in exercise-trained mice after having been exposed to an exercise wheel for 5 consecutive months. This ensured that mice could remain active as long as possible, as opposed to changing their environment for an extended period of time prior to tissue collection. The animals were anesthetized (15.0 mg ketamine: 1.0 mg xylazine · (100 g body mass)⁻¹) and

gastrocnemius (gastroc) from one leg and the heart (i.e. left ventricle) were removed from each animal. Half of this tissue was frozen immediately in liquid nitrogen and the remaining tissue was homogenized using a glass mortar and pestle (Kimble Chase Glassware; 885451-0021, 885452-0021) for further study. All homogenization was done in phenylmethylsulfonyl fluoride (PMSF) buffer, consisting of: 250 mM sucrose, 5 mM HEPES (pH 7.5), 0.2 mM PMSF and 0.2%NaN₃ in a ratio of 1:10 (*w/v*). The gastroc from the second leg was isolated and placed in a cryomold, covered with Tissue-Tek O.C.T. compound (Fisher Scientific; 14-373-65) and frozen in melting isopentane on liquid nitrogen. All tissues were stored at -80°C until further use.

Western blot analysis

Total protein content of muscle homogenates was quantified in triplicate using the bicinchoninic acid (BCA) protein assay. Twenty micrograms of sample was loaded and resolved on 7.5 - 15% SDS-polyacrylamide gels (depending on protein size), followed by transfer onto polyvinylidene difluoride membranes (PVDF; Bio-Rad Laboratories). Blots were blocked in either 5% milk or 5% BSA in tris-buffered saline tween (TBST), depending on the protein of interest, for one hour at room temperature. After blocking, blots were immuno-labeled with anti-SERCA1a (Cell Signaling Technology; #4219), anti-SERCA2a (Cell Signaling Technolgy; #4388), anti-AMPK α (Cell Signaling Technology; #2532), anti-phosphorylated-AMPK α ^{Thr172} (Cell Signaling Technology; #4188), anti-PLN (Santa Cruz Biotechnology, Inc.; sc-21923), anti-phosphorylated-PLN Thr17 (Santa Cruz Biotechnology, Inc.; sc-17024-R), anti-phosphorylated-PLN Ser16 (Santa Cruz Biotechnology, Inc.; sc-12963), anti-phosphorylated-ACC (Cell Signaling

Technology; #3661) and anti-cytochrome C oxidase (COX IV; Cell Signaling Technology; #4844) primary antibodies overnight at 4°C. After incubation in primary antibody, blots were washed 3 times with TBST for 10 minutes each, followed by incubation in secondary anti-rabbit antibody (Cell Signaling Technology; #7074) or anti-goat antibody (Santa Cruz Biotechnology, Inc.; sc-2020) for 2 hours at room temperature. Blots were then washed another 3 times in TBST for 10 minutes each. Membranes were then incubated in ECL reagent (Thermo Scientific; 32106 or Amersham; RPN2232) and visualized with the Fluor-S-Max MultiImager (Bio-Rad Laboratories). Blots were then be stripped and re-imaged for β -tubulin (Cell Signaling Technology; #2128), using the same techniques listed above. A loading control (LC) was loaded in each gel in order to standardize protein levels. A wild-type left ventricle sample was used as a loading control for left ventricle samples, while a wild-type gastrocnemius sample was used as a loading control for gastrocnemius samples. To quantify blots, the intensity of the protein of interest was normalized to the loading control, while β -tubulin intensity was also normalized to the loading control. Finally, the normalized intensity of the protein of interest was divided by the normalized β -tubulin intensity to produce a ratio. This process was carried out for all samples.

RNA isolation from left ventricle tissue

Approximately 100-150 mg of tissue was homogenized in a tube with 2 ml of TRIzol reagent (Life Technologies; 15596-026), after which 200 μ l of choloform was added to each sample. Samples were then agitated by hand for 15 seconds, followed by incubation at room temperature for 3 minutes. Tubes were then centrifuged at 12,000g for 15

minutes at 4°C. The aqueous phase was then transferred to a fresh tube and 500 µl of isopropanol was added to each sample. Tubes were then shaken by hand and incubated at room temperature for 10 minutes, followed by another shake and then centrifuged at 12,000g for 10 minutes at 4°C. After centrifugation, supernatant was discarded and 1 ml of 75% ethanol was used to re-suspend the pellet and then sample was centrifuged at 7,500g for 10 minutes at 4°C. Supernatant was once again discarded and the pellet was air dried for 10 minutes. The pellet was then re-suspended in ~50-70 µl of RNase and DNase free water and then incubated for 10 minutes at 60°C.

Left ventricle qPCR

Prior to carrying out qPCR, primers were checked for specificity by running the amplified product in an agarose gel. The primers were only used when the amplified product corresponded to the predicted amplicon length with the presence of a single visible band. Afterwards, the primers were diluted in DNase/RNase free water to a final concentration of 10 µM. For DNase preparation (Invitrogen; 18068-015), each reaction required: 1 µL 10x DNase buffer, 1 µl DNase I, 200 ng of RNA and DEPC-treated water to 10 µl. Incubate each reaction at room temperature for 15 min. Stop each enzymatic reaction by adding 1 µl of 25 mM EDTA and incubate at 65°C for 10 minutes. Once DNase step has been completed, pipette each reaction into a well of a PCR plate and add (to each well): 25 µl of 2x SYBR Green RT-PCR reaction mix (Bio-Rad Laboratories; 170-8893), 0.75 µl forward primer, 0.75 µl reverse primer, 10 µl DNase-treated RNA sample, 1 µl iScript reverse transcriptase for one-step RT-PCR (Bio-Rad Laboratories; 170-8893) and 12.5 µl of nuclease-free water. The reaction protocol was setup so that

cDNA synthesis occurred at 50°C for 10 minutes, followed by reverse transcriptase inactivation at 95°C for 5 minutes. Afterwards, PCR cycling and detection was carried out at 95°C for 10 seconds and 60°C for 30 seconds for 45 cycles. Melt curve analysis was then completed for 80 cycles at 95°C for 1 minute, then 55°C for 1 minute and finally between 55°C and 95°C for 10 seconds (increasing by 0.5°C per cycle). All steps were completed using the Bio-Rad iCycler iQ PCR Thermal Cycler (Bio-Rad Laboratories).

The following genes were targeted in left ventricle qPCR using primers specific for SERCA2a, PLN, RyR2, and GAPDH (Table 5). GAPDH was used as a control to account for any potential variations in the amount of RNA input and the efficiency of reverse transcription.

Table 5. Forward and reverse primers for left ventricle qPCR (*n.b. All primers span introns*).

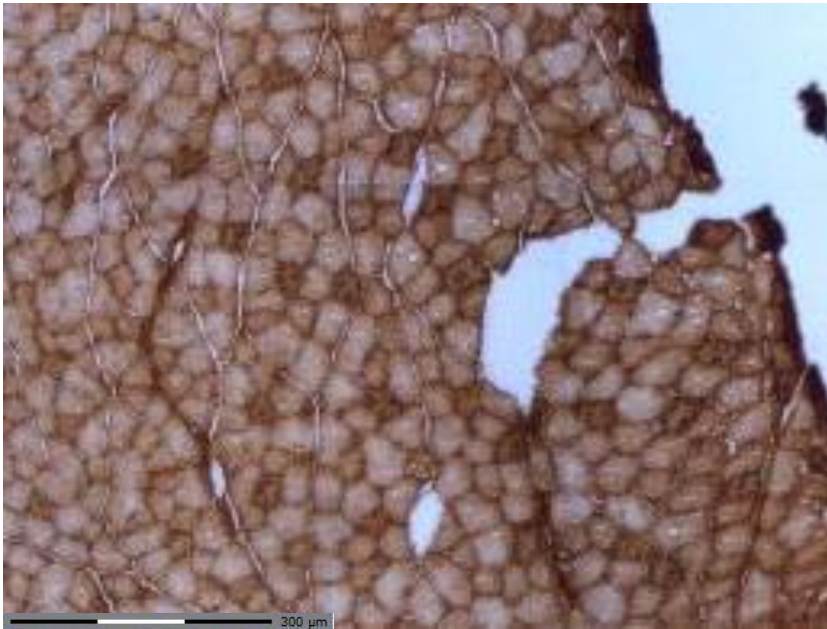
Gene	Forward primer (5'-3')	Reverse primer (5'-3')
SERCA2a	TGGAGAACGCTCACACAAAG	CTCAATCACAAGTTCCAGCA
PLN	CTTTTGCCTTCCTGGCATAA	AGGTTCTGGAGATTCTGACG
RyR2	GACCAACTCCTAGATTTC	GTCCTCTGATTGTTAAGTC
GAPDH	TGCACCACCAACTGCTTAGC	GGCATGGACTGTGGTCATGAG

Immunohistochemistry

Immunohistochemistry was performed in order to identify type I muscle fibres in the gastroc that was stored in O.C.T. compound (Figure 6). More specifically, frozen gastrocnemius tissue was sectioned into 12 µm-thick cross-sections in the transverse plane using a Cryostat machine (Leica Microsystems) at -20°C. Following sectioning,

slides were fixed in 4% paraformaldehyde for 20 minutes on glass slides. Slides were washed 3 times for 15 minutes each in 0.1 M phosphate buffered saline (PBS; 0.1 M phosphate buffer + 0.9% NaCl), followed by incubation in 0.1 M PBS + 10% normal donkey serum for 1 hour at room temperature. Sections were then incubated in primary anti-myosin heavy chain 1 antibody (Sigma; M-8421) at a 1:1,000 dilution in 0.1 M PBS + 1% normal donkey serum overnight at room temperature. After 3 washes for 10 minutes in 0.1 M PBS, slides were incubated in secondary donkey anti-mouse antibody (Jackson Labs; 715-065-150) at a 1:500 dilution in 0.1 M PBS + 1% normal donkey serum for one hour at room temperature. Slides were washed another 3 times for 10 minutes in 0.1 M PBS and then tissues were treated with Vectastain ABC (Vector Laboratories; PK-4000) for 1 hour at room temperature. Another 2 washes for 10 minutes in 0.1 M PBS and 1 wash for 10 minutes in 0.1 M phosphate buffer (PhB) were performed, followed by a 2-10 minute incubation in ImmPACT DAB peroxidase substrate (Vector Laboratories; SK-4105). Finally, slides were washed 3 times for 10 minutes in 0.1 PhB, dried and then mounted. Type I muscle fibers were stained dark brown, distinguishing them from type II muscle fibers which will be very light in colour (Figure 6).

Figure 6. Slow, skeletal myosin (Sigma-Aldrich; M8421) immunostained mouse gastrocnemius cross-section. Dark staining, type I skeletal muscle fiber. Light staining, type II skeletal muscle fiber.



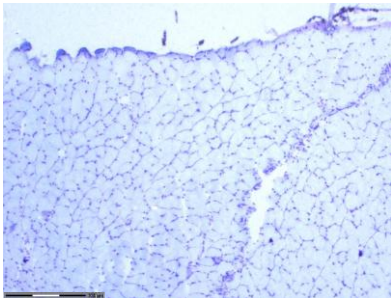
Laser capture microdissection (LCM)

Following staining, LCM was performed using the Zeiss PALM MicroBeam laser capture microdissection system (Carl Zeiss Canada Ltd.). Areas of $\sim 7,500 \mu\text{m}^2$ containing a high percentage of type I muscle fibers (Figure 7) were dissected from each slice and collected in the adhesive caps of PCR tubes (Carl Zeiss Canada Ltd.; 415190-9201-000). Following LCM, samples were incubated in a mixture of RNeasy lysis buffer (Qiagen; 74004) and β -mercaptoethanol for 30 minutes. For simplicity, we will refer to this LCM-enriched type I fiber population as “LCM-TypeI”. The same procedure was carried out for type II muscle fibers, which will be referred to as “LCM-TypeII” throughout this document. Following the LCM of type I and type II muscle fibers from a single slide, we then took the next slide from the same tissue and lysed the whole slice.

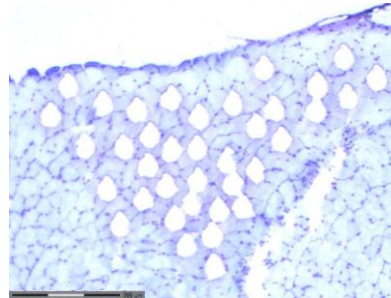
We will refer to this LCM whole tissue sample as “LCM-Whole”. All samples were stored at -80°C until further use.

Figure 7. Gastrocnemius cross-section pre- and post-LCM. Slides were stained with cresyl violet stain to highlight cross-section structure.

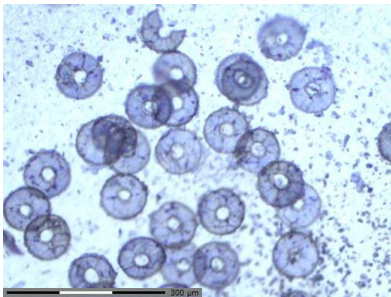
A. Gastrocnemius cross-section pre-LCM



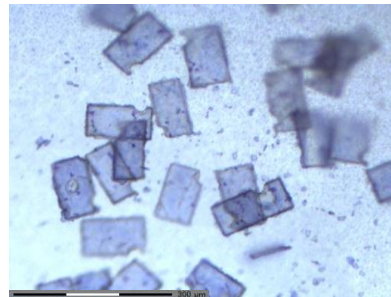
B. Gastrocnemius cross-section post-LCM



C. Areas of high slow-twitch fibre concentration



D. Areas of high fast-twitch fibre concentration



RNA isolation from microdissected muscle samples

RNA was isolated from LCM samples using the RNeasy Micro Kit (Qiagen; 74004), with modifications, following the total RNA isolation from microdissected cryosections protocol. Microdissected samples (type I or type II fibers) were pooled together and topped up to $300\ \mu\text{L}$ of buffer RLT. Twenty ng of carrier RNA were then be added to the sample, followed by $293\ \mu\text{L}$ RNase free H_2O + $7\ \mu\text{L}$ proteinase k. The samples were

incubated at 55°C for 10 minutes, after which 300 µL of ethanol was added to the solution. Samples were then put into a column and centrifuged, followed by the addition of 350 µL of RW1 buffer. After another spin, any traces of genomic DNA were removed using deoxyribonuclease (DNase) I (80 µL of a 1:7 dilution in RDD buffer) and then another wash with RW1 buffer. Another spin was performed, after which 500 µL of RPE buffer was applied to the sample. The sample was spun again, after which 500 µL of 80% ethanol was added and then RNA will be collected in a new collection tube using RNase free water. The same protocol was used for whole gastroc samples, except without carrier RNA. Following RNA isolation, RNA concentration, protein contamination and RNA integrity of all samples were assessed using the 2100 Bioanalyzer, 2100 Bioanalyzer RNA Pico 6000 kit and 2100 Expert Software (Agilent Tehnologies).

qPCR from microdissected muscle samples

The SuperScript VILO cDNA Synthesis Kit (Invitrogen; 11754-050) was used to perform reverse transcription. The same quantity of RNA (~8,148 ng) was used for all samples, with the total sample volume being made up to 14 µl with nuclease-free water. Reverse transcription reactions were carried out in a Master Cycler Gradient Thermal Cycler (Eppendorf). Prior to real-time polymerase chain reactions (qPCR), synthesized cDNA was preamplified with the TaqMan PreAmp Master Mix Kit (Applied Biosystems; 4391128). Fourteen preamplification cycles were used in order to produce a larger volume of cDNA to test a greater number of genes. Incubation of the preamplification

reactions was performed using the Master Cycler Gradient thermal cycler (Eppendorf), with all preamplified cDNA being made to a final volume of 1 ml.

qPCR reactions were performed in triplicate on 96-well qPCR plates. Each well contained: 1.00 μ l TaqMan Gene Expression Assay, 4.00 μ l nuclease-free water, 10 μ l iTaq Universal Probes Supermix (Bio-Rad Laboratories; 172-5130) and 5 μ l preamplified cDNA. Multiple plates were compared, with whole muscle cDNA serving as a calibrator sample. A water lane was set-up on all plates in order to rule out any contamination of plates or reagents. The reaction protocol was setup as follows, using the Bio-Rad iCycler iQ PCR Thermal Cycler (Bio-Rad Laboratories):

- Polymerase activation and DNA denaturation: 1 minute at 95°C
- PCR cycling and detection (40 cycles): 15 seconds at 95°C and 30 seconds at 60°C

The following genes were targeted in laser captured gastrocnemius qPCR using TaqMan gene expression assays for MHC β , PGC-1 α , SERCA1, SERCA2 and β -tubulin (Table 6). β -tubulin was used as a control to account for any potential variations in the amount of RNA input.

Table 6. TaqMan gene expression assays.

Gene	Assay ID
MHC β	Mm01319006_g1
PGC-1 α	Mm01208835_m1
SERCA1	Mm01275320_m1
SERCA2	Mm01201431_m1
β -tubulin	Mm00726185_s1

SERCA activity assay

Kinetic properties of calcium-dependent SERCA activity were measured using a spectrophotometric assay¹³⁷, as modified by Tupling et al.¹³⁸ and Duhamel et al.¹³⁹ for use on a plate reader (SPECTRAmax; Molecular Devices). Samples were thawed, with three samples being measured on a plate. Depending on protein concentration and tissue type, 8 (gastroc samples) to 25 (left ventricle) μg of protein was mixed with 4.25 mL of assay buffer. Calcium-dependent activity was then measured by varying the amount of calcium (10-25 μL of 1 mM CaCl_2) loaded in an eppendorf tube that contained 250 μL of cocktail. The assay buffer contained 4.25 ml ATPase buffer, 15 μL lactate dehydrogenase, 15 μL pyruvate kinase and 8.8 μL ionophore. In order to obtain basal ATPase activity, 2 μL of the SERCA inhibitor CPA¹⁴⁰ was used in one sample, which, when subtracted from total Ca^{2+} -stimulated ATPase activity, enabled the calculation of Ca^{2+} -stimulated SERCA activity. After plotting the graph of enzyme activity versus Ca^{2+} concentration, maximal enzyme activity (V_{max}), Ca_{50} and the Hill coefficient were calculated. V_{max} was defined the peak SERCA activity; whereas, Ca_{50} was defined as the concentration of Ca^{2+} that elicits 50% of V_{max} when graphed using a sigmoidal fit of the data, as calculated by Graph Pad Prism (version 5.04). The Hill coefficient was defined as the slope of the relationship between $[\text{Ca}^{2+}]_f$ and SERCA activity and is obtained through nonlinear regression using the portion of the SERCA activity curve that corresponds to 10-90% V_{max} ^{59, 141}.

Statistical analyses

All data were analyzed using a 2-way ANOVA with two between group comparisons (Factor 1: genetic background and Factor 2: exercise-training). When significant differences ($P < 0.05$) were observed within the ANOVA, a Newman-Keuls post hoc was utilized to identify differences between specific means. Data is presented as mean \pm SE.

Chapter 3: Results

General characteristics of animals

Physiological parameters of WT and KD mice (sedentary and exercise-trained) are presented in Table 7. Wild-type animals that had access to voluntary running wheels ran an average of $4 \pm 1 \text{ km}\cdot\text{day}^{-1}$ and KD mice ran an average of $5 \pm 1 \text{ km}\cdot\text{day}^{-1}$ throughout the 5 month protocol. At the time of tissue collection there was no difference in body mass between groups. Similarly, there were no differences in heart mass, heart mass to body mass ratio or the OGTT area under the curve.

Table 7. General characteristics of C57BL/6J mice used in this study at time of tissue collection.

	WT+Sed	WT+Ex	KD+Sed	KD+Ex
Body mass (g)	31 ± 2	34 ± 3	31 ± 2	31 ± 2
Heart mass (mg)	88 ± 3	98 ± 5	88 ± 6	94 ± 6
Heart mass : body mass ratio (mg/g)	2.9 ± 0.1	3.0 ± 0.2	2.8 ± 0.1	3.0 ± 0.1
Oral glucose tolerance test (area under the curve)	2011 ± 83	1988 ± 189	1962 ± 82	1767 ± 92

Values are means ± SE ($n = 8$ mice per group). **WT+Sed**, wild-type mice housed in standard cages (sedentary condition). **WT+Ex**, wild-type mice housed in cages with voluntary exercise wheels (exercised condition). **KD+Sed**, AMPK α 2 kinase dead mice housed in standard cages (sedentary condition). **KD+Ex**, AMPK α 2 kinase dead mice housed in cages with voluntary exercise wheels (exercised condition).

Graded exercise treadmill test

To determine whether exercise-training resulted in changes in running capacity, a graded exercise treadmill test was performed at the end of the study protocol (Table 8). A main effect of genotype was observed for maximum speed achieved during the graded exercise treadmill test, where WT > KD ($P < 0.05$). Furthermore, a main effect of exercise was also observed, where Sed < Ex ($P < 0.01$).

Table 8. Five month graded exercise treadmill test.

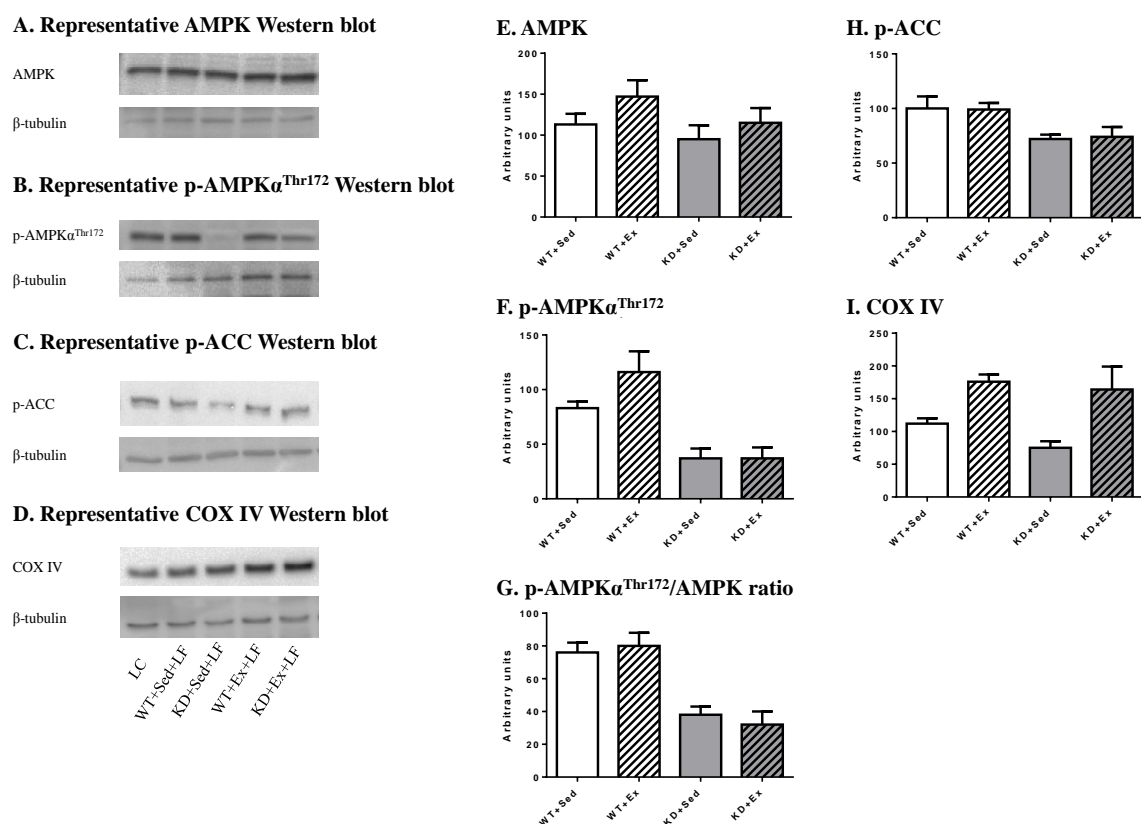
	WT+Sed	WT+Ex	KD+Sed	KD+Ex
Maximum speed achieved (m/min)	18 ± 1	25 ± 2	14 ± 1	21 ± 2

Values are means ± SE ($n = 8$ mice per group). **WT+Sed**, wild-type mice housed in standard cages (sedentary condition). **WT+Ex**, wild-type mice housed in cages with voluntary exercise wheels (exercised condition). **KD+Sed**, AMPK α 2 kinase dead mice housed in standard cages (sedentary condition). **KD+Ex**, AMPK α 2 kinase dead mice housed in cages with voluntary exercise wheels (exercised condition). Main effect of genotype, where WT > KD ($P < 0.05$). A main effect of exercise was observed, where Sed < Ex ($P < 0.01$).

Left ventricle metabolic marker protein abundance

Protein expression was assessed using Western blotting techniques in order to determine if any changes occurred as a result of genotype or exercise-training. In left ventricle samples (Figure 8), total AMPK protein levels were not affected by genotype or exercise. Alternatively, there was a main effect of genotype on p-AMPK α^{Thr172} , p-AMPK α^{Thr172} /AMPK ratio and p-ACC, where WT > KD ($P < 0.01$). In contrast, no effect of genotype was observed for COX IV. While there was no effect of exercise on p-AMPK α^{Thr172} , p-AMPK α^{Thr172} /AMPK ratio and p-ACC, a main effect of exercise was observed for COX IV protein abundance, where Sed < Ex ($P < 0.005$).

Figure 8. Representative Western blots and graphs depicting left ventricular protein expression of AMPK, p-AMPK α^{Thr172} , p-AMPK α^{Thr172} /AMPK ratio, p-ACC and COX IV from sedentary and exercise-trained animals. Graphs indicated the mean \pm SE ($n = 5$ mice per group). (A) Representative AMPK Western blot, (B) Representative p-AMPK α^{Thr172} Western blot, (C) Representative p-ACC Western blot, (D) Representative COX IV Western blot, (E) AMPK, (F) p-AMPK α^{Thr172} , (G) p-AMPK α^{Thr172} /AMPK ratio, (H) p-ACC and (I) COX IV. A main effect of genotype was observed for p-AMPK α^{Thr172} , p-AMPK α^{Thr172} /AMPK ratio and p-ACC, where WT > KD ($P < 0.01$). A main effect of exercise was observed for COX IV, where Sed < Ex ($P < 0.005$). **WT+Sed**, wild-type mice housed in standard cages (sedentary condition). **WT+Ex**, wild-type mice housed in cages with voluntary exercise wheels (exercised condition). **KD+Sed**, AMPK $\alpha 2$ kinase dead mice housed in standard cages (sedentary condition). **KD+Ex**, AMPK $\alpha 2$ kinase dead mice housed in cages with voluntary exercise wheels (exercised condition).

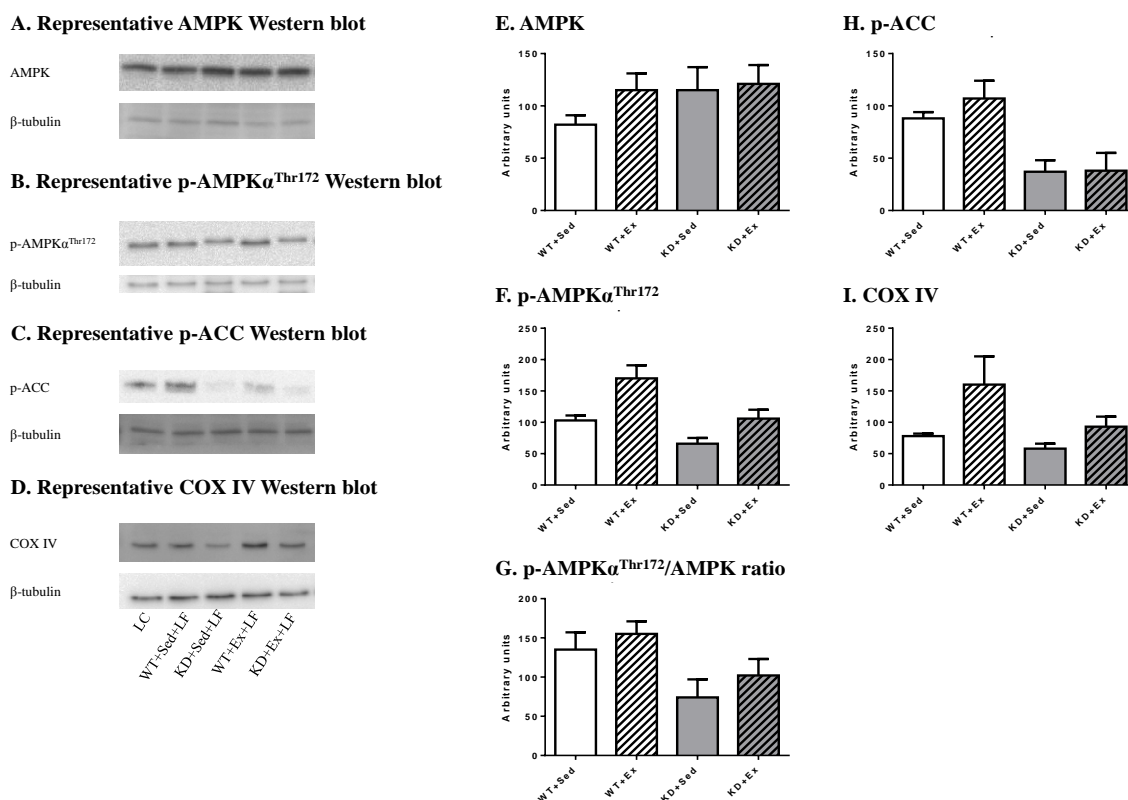


Gastrocnemius metabolic marker protein abundance

Similar to left ventricle samples, total AMPK protein abundance in gastroc samples (Figure 9) was not affected by genotype or exercise. However, a main effect of genotype

was observed for p-AMPK $^{\text{Thr172}}$, p-ACC and COX IV, where WT > KD ($P < 0.05$). There was also a main effect of exercise observed for p-AMPK $^{\text{Thr172}}$ and COX IV, where Sed < Ex ($P < 0.05$). In contrast, p-ACC remained unchanged following exercise-training.

Figure 9. Representative Western blots and graphs depicting gastrocnemius protein expression of AMPK, p-AMPK $^{\text{Thr172}}$, p-AMPK $^{\text{Thr172}}$ /AMPK ratio, p-ACC and COX IV from sedentary and exercise-trained animals. Graphs indicated the mean \pm SE ($n = 5$ mice per group). (A) Representative AMPK Western blot, (B) Representative p-AMPK $^{\text{Thr172}}$ Western blot, (C) Representative p-ACC Western blot, (D) Representative COX IV Western blot, (E) AMPK, (F) p-AMPK $^{\text{Thr172}}$, (G) p-AMPK $^{\text{Thr172}}$ /AMPK ratio, (H) p-ACC and (I) COX IV. A main effect of genotype was observed for p-AMPK $^{\text{Thr172}}$, p-AMPK $^{\text{Thr172}}$ /AMPK ratio, p-ACC and COX IV, where WT > KD ($P < 0.05$). A main effect of exercise was observed for p-AMPK $^{\text{Thr172}}$ and COX IV, where Sed < Ex ($P < 0.05$). **WT+Sed**, wild-type mice housed in standard cages (sedentary condition). **WT+Ex**, wild-type mice housed in cages with voluntary exercise wheels (exercised condition). **KD+Sed**, AMPK α 2 kinase dead mice housed in standard cages (sedentary condition). **KD+Ex**, AMPK α 2 kinase dead mice housed in cages with voluntary exercise wheels (exercised condition).

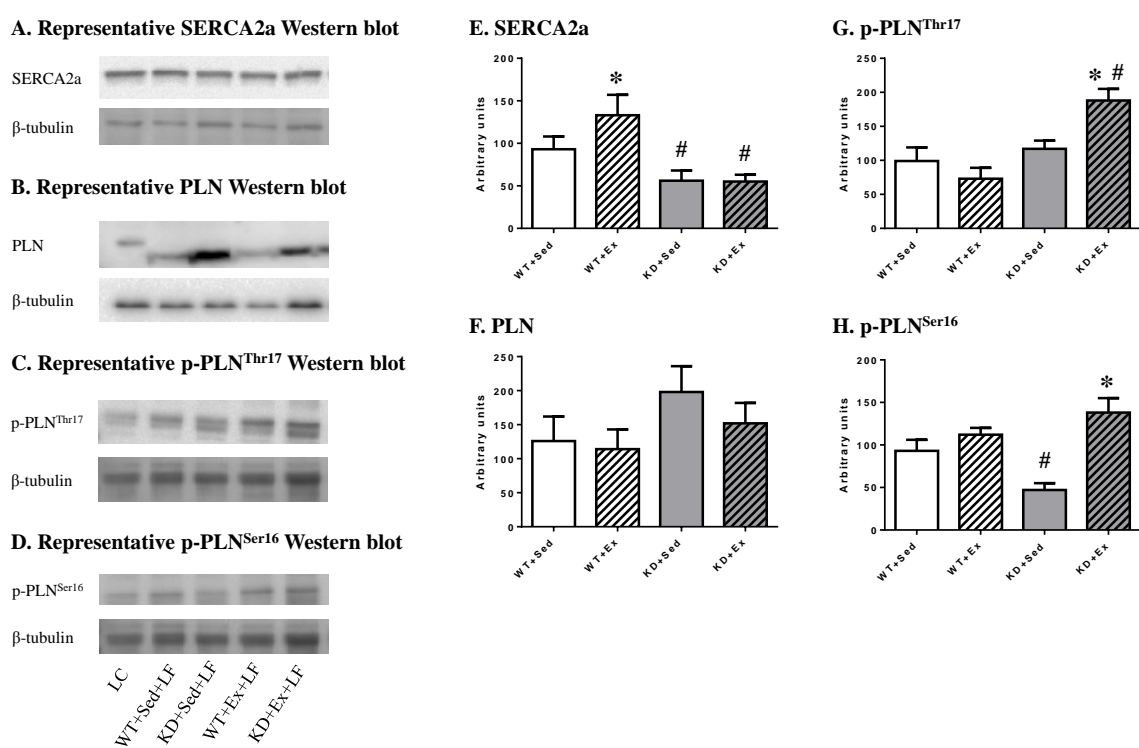


Left ventricle SERCA2a, PLN, p-PLN^{Thr17} and p-PLN^{Ser16} protein levels

In left ventricle samples (Figure 10), there was a decrease of ~40% in SERCA2a protein abundance in sedentary KD mice compared to sedentary WT mice ($P < 0.05$). Notably, exercise-training increased SERCA2a protein content by ~43% in WT mice, as compared to WT sedentary mice ($P < 0.05$). In contrast, exercise-training did not alter the content of SERCA2a protein in LV samples isolated from KD mice. In fact, SERCA2a protein content was ~59% lower in exercise-trained KD mice, as compared to WT exercise-trained mice ($P < 0.05$).

There was a main effect of genotype observed for PLN, where WT < KD ($P < 0.05$) and a main effect of exercise observed for PLN, where Ex < Sed ($P < 0.05$). No difference in p-PLN^{Thr17} was observed between WT+SED and KD+SED mice. Additionally, exercise did not alter p-PLN^{Thr17} protein levels in WT mice. Interestingly, p-PLN^{Thr17} was ~61% and ~158% higher in exercise-trained KD mice, as compared to KD+Sed mice and WT+Ex mice ($P < 0.05$). A different response was observed for p-PLN^{Ser16} phosphorylation. In fact, p-PLN^{Ser16} phosphorylation was reduced by ~49% in KD+Sed mice, as compared to their WT counterparts ($P < 0.05$). Furthermore, although exercise-training did not alter p-PLN^{Ser16} phosphorylation in WT mice, exercise did increase p-PLN^{Ser16} phosphorylation by ~194% in exercise-trained KD mice ($P < 0.05$). However, the relative levels of p-PLN^{Ser16} phosphorylation was similar between exercise-trained WT and exercise-trained KD mice.

Figure 10. Representative Western blots and graphs depicting left ventricular protein expression of SERCA2a, PLN, p-PLN^{Thr17} and p-PLN^{Ser16} from sedentary and exercise-trained animals. Graphs indicated the mean \pm SE ($n = 5$ mice per group). (A) Representative SERCA2a Western blot, (B) Representative PLN Western blot, (C) Representative p-PLN^{Thr17} Western blot, (D) Representative p-PLN^{Ser16} Western blot, (E) SERCA2a, (F) PLN, (G) p-PLN^{Thr17} and (H) p-PLN^{Ser16}. A main effect of genotype was observed for PLN, where WT < KD ($P < 0.05$). A main effect of exercise was observed for PLN, where Sed > Ex ($P < 0.05$). *, different from Sed of same genotype ($P < 0.05$). #, different from WT from same training condition ($P < 0.05$). **WT+Sed**, wild-type mice housed in standard cages (sedentary condition). **WT+Ex**, wild-type mice housed in cages with voluntary exercise wheels (exercised condition). **KD+Sed**, AMPK α 2 kinase dead mice housed in standard cages (sedentary condition). **KD+Ex**, AMPK α 2 kinase dead mice housed in cages with voluntary exercise wheels (exercised condition).



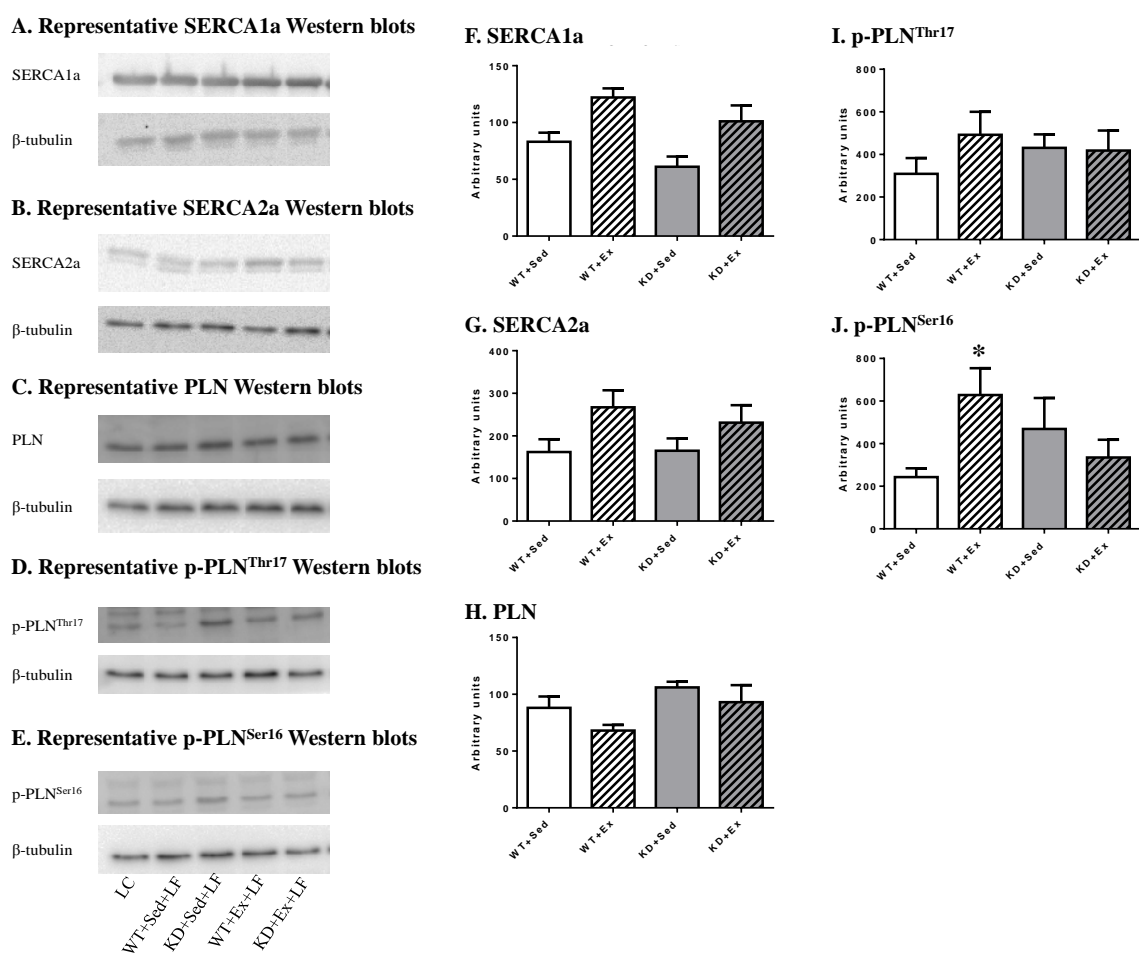
Gastrocnemius SERCA1a, SERCA2a, PLN, p-PLN^{Thr17} and p-PLN^{Ser16} protein levels

Western blotting was also used to assess changes in protein content and phosphorylation in gastroc muscle (Figure 11). A main effect of genotype and exercise-training was observed for SERCA1a protein content, where WT > KD ($P < 0.05$) and Sed

< Ex ($P < 0.01$), respectively. While presence of the KD transgene had no effect on SERCA2a protein levels, a main effect of exercise-training was observed for SERCA2a, where Sed < Ex ($P < 0.05$).

Similar to observations made in cardiac muscle, there was a main effect of genotype observed for PLN, where WT < KD ($P < 0.05$) and a main effect of exercise observed for PLN, where Ex < Sed ($P < 0.05$). In contrast to the observations made in LV tissue for p-PLN^{Thr17} phosphorylation levels, the gastroc data indicate that no differences between groups were observed for genotype or exercise-training status. No differences between WT+Sed and KD+Sed were observed for p-PLN^{Ser16} phosphorylation in gastroc sample. However, exercise-training increased p-PLN^{Ser16} phosphorylation by ~158% in WT mice compared to their sedentary counterparts ($P < 0.05$). In contrast, exercise-training did not alter p-PLN^{Ser16} phosphorylation in KD mice.

Figure 11. Representative Western blots and graphs depicting gastrocnemius protein expression of SERCA1a, SERCA2a, PLN, p-PLN^{Thr17} and p-PLN^{Ser16} from sedentary and exercise-trained animals. Graphs indicated the mean \pm SE ($n = 5$ mice per group). (A) Representative SERCA1a Western blot, (B) Representative SERCA2a Western blot, (C) Representative PLN Western blot, (D) Representative p-PLN^{Thr17} Western blot, (E) Representative p-PLN^{Ser16} Western blot, (F) SERCA1a, (G) SERCA2a, (H) PLN, (I) p-PLN^{Thr17} and (J) p-PLN^{Ser16}. A main effect of genotype was observed for SERCA1a, where WT > KD ($P < 0.05$) and for PLN, where WT < KD ($P < 0.05$). A main effect of exercise was observed for SERCA1a and SERCA2a, where Sed < Ex ($P < 0.05$) and for PLN, where Sed > Ex ($P < 0.05$). *, different from Sed of same genotype ($P < 0.05$). **WT+Sed**, wild-type mice housed in standard cages (sedentary condition). **WT+Ex**, wild-type mice housed in cages with voluntary exercise wheels (exercised condition). **KD+Sed**, AMPK α 2 kinase dead mice housed in standard cages (sedentary condition). **KD+Ex**, AMPK α 2 kinase dead mice housed in cages with voluntary exercise wheels (exercised condition).

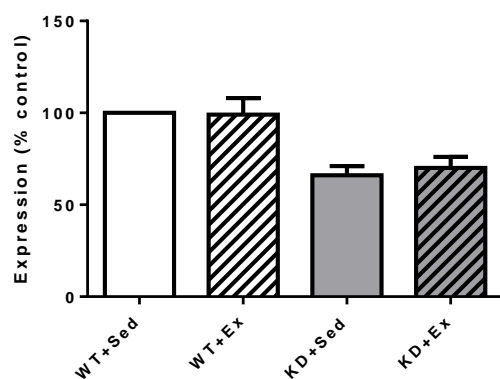


Left ventricle mRNA expression

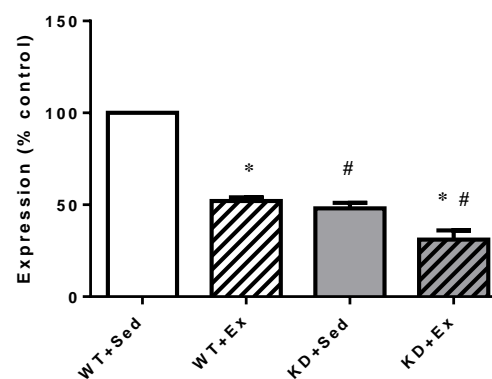
Levels of mRNA expression in left ventricular tissue were assessed using qPCR (Figure 12). A main effect of genotype was observed for SERCA2a mRNA expression, where WT > KD ($P < 0.05$). However, exercise-training had no effect on SERCA2a mRNA expression. Interestingly, PLN mRNA was reduced by 52% in sedentary KD mice, as compared to WT+Sed mice ($P < 0.05$). Notably, exercise-training down-regulated PLN expression by ~48% in WT mice, as compared to WT+Sed mice ($P < 0.05$). Exercise-training also reduced PLN expression by an additional ~35% in KD mice, as compared to KD+Sed mice ($P < 0.05$). Finally, it was notable that KD+Ex mice also had a ~40% reduction in PLN expression as compared to WT+Ex mice ($P < 0.05$). In regards to RyR2 mRNA expression, sedentary KD mice had 66% less RyR2 mRNA in comparison to WT+Sed mice ($P < 0.05$). Notably, exercise-training also reduced RyR2 mRNA expression by ~79%, as compared to WT+Sed mice ($P < 0.05$). In contrast, exercise-training increase RyR2 expression by ~91% and ~210%, as compared to KD+Sed mice and WT+Ex mice, respectively ($P < 0.05$).

Figure 12. Quantitative PCR data characterizing left ventricle mRNA expression of SERCA2a, PLN and RyR2 from sedentary and exercise-trained animals. Graphs indicated the mean \pm SE ($n = 5$ mice per group). (A) SERCA2a, (B) PLN and (C) RyR2. A main effect of genotype was observed for SERCA2a, where WT > KD ($P < 0.05$). *, different from Sed of same genotype ($P < 0.05$). #, different from WT from same training condition ($P < 0.05$). **WT+Sed**, wild-type mice housed in standard cages (sedentary condition). **WT+Ex**, wild-type mice housed in cages with voluntary exercise wheels (exercised condition). **KD+Sed**, AMPK α 2 kinase dead mice housed in standard cages (sedentary condition). **KD+Ex**, AMPK α 2 kinase dead mice housed in cages with voluntary exercise wheels (exercised condition).

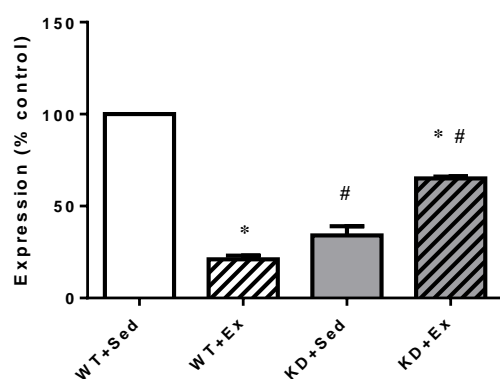
A. SERCA2a



B. PLN



C. RyR2



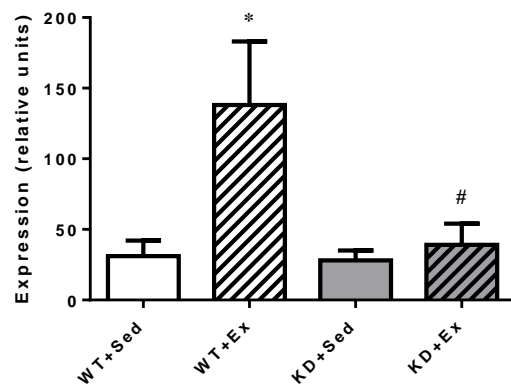
Laser captured gastrocnemius mRNA expression

Although there was no main effect of genotype in whole gastrocnemius tissue for MHC-1 β expression (Figure 13), exercise-training stimulated a different response between fiber types. Specifically, exercise-training increased MHC-1 β mRNA by 345%

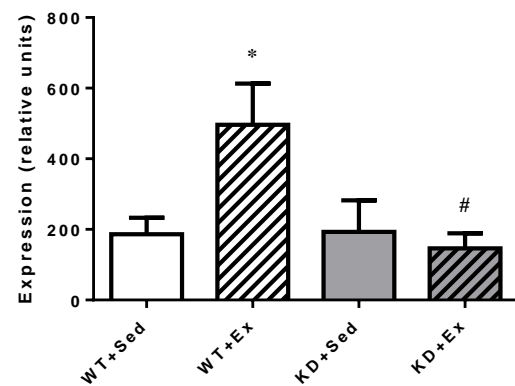
in LCM-Whole tissue samples isolated from WT mice, as compared to WT sedentary mice ($P < 0.05$). However, exercise-training did not alter the expression of MHC-1 β in LCM-Whole tissue samples isolated from KD mice. In fact, the observed interaction effect indicated that MHC-1 β expression was ~72% lower in LCM-Whole tissue isolated from KD+Ex, as compared to WT+Ex mice ($P < 0.05$). A similar interaction effect was observed for MHC-1 β expression for LCM-TypeI tissue. Specifically, exercise-training increased MHC-1 β mRNA by ~167% in WT mice, as compared to WT sedentary mice ($P < 0.05$). However, exercise-training was without effect in LCM-TypeI tissue samples isolated from KD mice. Furthermore, MHC-1 β expression was ~71% lower in LCM-TypeI tissue isolated from KD+Ex, as compared to WT+Ex mice ($P < 0.05$). When comparisons were made for LCM-TypeII tissue samples, no statistical changes in MHC-1 β expression were observed between groups. It is worth noting that the relative expression level of MHC-1 β was 40-140 fold lower in LCM-TypeII tissue, as compared to LCM-TypeI tissue.

Figure 13. Quantitative PCR data characterizing mRNA expression of MHC-1 β from laser captured gastrocnemius of sedentary and exercise-trained animals. Graphs indicated the mean \pm SE ($n = 5$ mice per group). (A) LCM-Whole, (B) LCM-TypeI and (C) LCM-TypeII. *, different from Sed of same genotype ($P < 0.05$). #, different from WT from same training condition ($P < 0.05$). **WT+Sed**, wild-type mice housed in standard cages (sedentary condition). **WT+Ex**, wild-type mice housed in cages with voluntary exercise wheels (exercised condition). **KD+Sed**, AMPK α 2 kinase dead mice housed in standard cages (sedentary condition). **KD+Ex**, AMPK α 2 kinase dead mice housed in cages with voluntary exercise wheels (exercised condition).

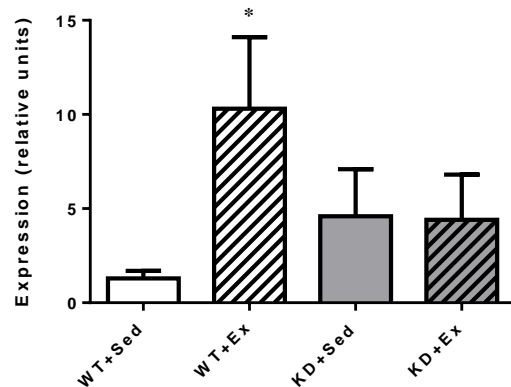
A. LCM-Whole



B. LCM-TypeI



C. LCM-TypeII



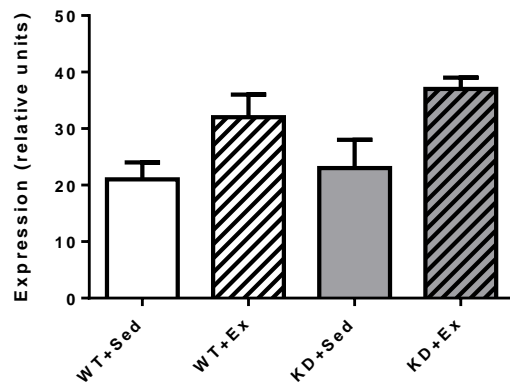
In whole gastrocnemius tissue (Figure 14), there was no effect of genotype on PGC-1 α mRNA expression. However, a main effect of exercise-training was observed for PGC-1 α mRNA in LCM-Whole tissue, where Sed < Ex ($P < 0.05$). A different response was observed for LCM-TypeI tissue, where KD+Sed mice had an 88% higher expression of

PGC-1 α mRNA, as compared to WT+Sed mice ($P < 0.05$). Notably, exercise-training increased PGC-1 α mRNA by ~131% in WT mice, as compared to their sedentary counterparts ($P < 0.05$). However, there was no effect of exercise-training amongst KD mice. In fact, PGC-1 α mRNA expression was not different when comparisons were made between WT+Ex and KD+Ex mice. Finally, although there was no effect of genotype on PGC-1 α mRNA expression, a main effect of exercise observed for PGC-1 α mRNA expression measured in LCM-TypeII tissue, where Sed < Ex ($P < 0.05$).

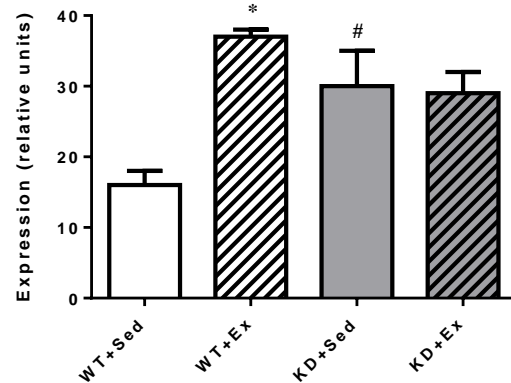
Figure 14. Quantitative PCR data characterizing mRNA expression of PGC-1 α from laser captured gastrocnemius of sedentary and exercise-trained animals.

Graphs indicated the mean \pm SE ($n = 5$ mice per group). (A) LCM-Whole, (B) LCM-TypeI and (C) LCM-TypeII. A main effect of exercise was observed for PGC-1 α whole gastrocnemius and PGC-1 α fast-twitch fibers, where Sed < Ex ($P < 0.05$). *, different from Sed of same genotype ($P < 0.05$). #, different from WT from same training condition ($P < 0.05$). **WT+Sed**, wild-type mice housed in standard cages (sedentary condition). **WT+Ex**, wild-type mice housed in cages with voluntary exercise wheels (exercised condition). **KD+Sed**, AMPK α 2 kinase dead mice housed in standard cages (sedentary condition). **KD+Ex**, AMPK α 2 kinase dead mice housed in cages with voluntary exercise wheels (exercised condition).

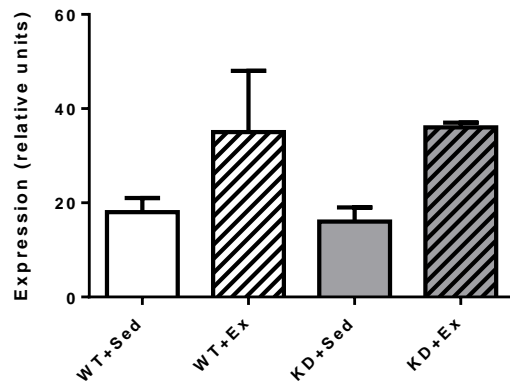
A. LCM-Whole



B. LCM-TypeI



C. LCM-TypeII

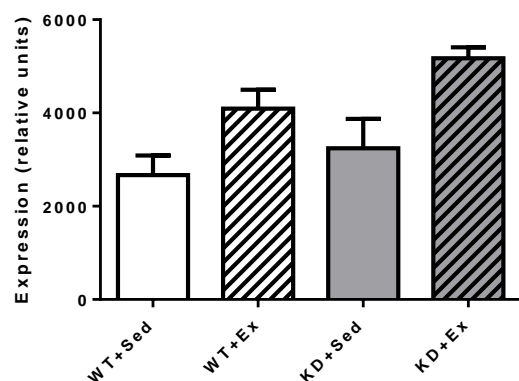


There was no effect of genotype on SERCA1a mRNA expression in LCM-Whole tissue samples (Figure 15). However, a main effect of exercise-training was observed for

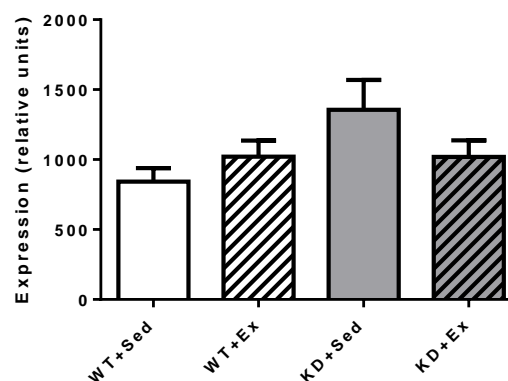
SERCA1a mRNA expression in LCM-Whole tissue, where Sed < Ex ($P < 0.05$). In contrast, SERCA1a mRNA expression was not altered by genotypic or exercise-training in LCM-TypeI tissue. However, the pattern of change for SERCA1a mRNA in LCM-TypeII tissue was similar to that observed for LCM-Whole tissue, where genotype had no effect but a main effect of exercise was observed (i.e. Sed < Ex; $P < 0.05$).

Figure 15. Quantitative PCR data characterizing mRNA expression of SERCA1a from laser captured gastrocnemius of sedentary and exercise-trained animals. Graphs indicated the mean \pm SE ($n = 5$ mice per group). (A) LCM-Whole, (B) LCM-TypeI and (C) LCM-TypeII. A main effect of exercise was observed for SERCA1a whole gastrocnemius and SERCA1a fast-twitch fibers, where Sed < Ex ($P < 0.05$). **WT+Sed**, wild-type mice housed in standard cages (sedentary condition). **WT+Ex**, wild-type mice housed in cages with voluntary exercise wheels (exercised condition). **KD+Sed**, AMPK α 2 kinase dead mice housed in standard cages (sedentary condition). **KD+Ex**, AMPK α 2 kinase dead mice housed in cages with voluntary exercise wheels (exercised condition).

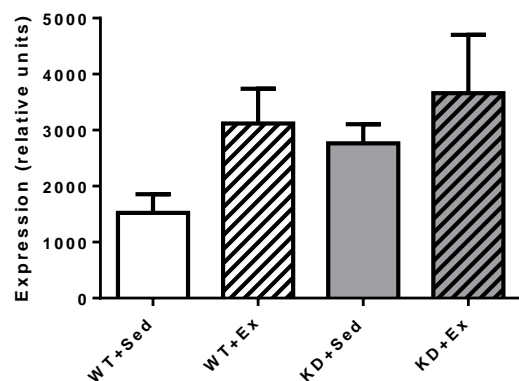
A. LCM-Whole



B. LCM-TypeI



C. LCM-TypeII

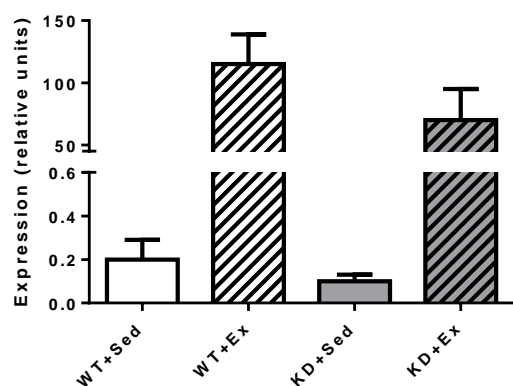


Despite there being no effect of genotype on SERCA2a mRNA expression in LCM-Whole tissue samples (Figure 16), a main effect of exercise-training was observed for SERCA2 mRNA expression, where Sed < Ex ($P < 0.05$). In contrast, an interaction effect was observed in LCM-TypeI tissue. Specifically, SERCA2a mRNA expression

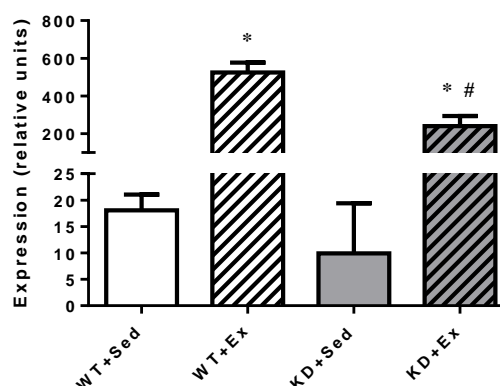
was not different when comparisons were made between WT+Sed and KD+Sed mice. However, SERCA2a mRNA increased by 19-fold in exercise-trained WT mice, as compared to their sedentary counterparts ($P < 0.01$). This exercise-stimulated response was blunted in KD mice, where exercise-training stimulated a 9-fold increase for SERCA2a mRNA in LCM-TypeI tissue ($P < 0.01$). In fact, SERCA2a mRNA expression in LCM-TypeI tissue was ~54% lower amongst KD+Ex mice, as compared to WT+Ex mice ($P < 0.01$). Finally, the pattern of change for SERCA2a mRNA in LCM-TypeII tissue was similar to that observed for LCM-Whole tissue, where genotype had no effect but a main effect of exercise was observed (i.e. Sed < Ex; $P < 0.05$).

Figure 16. Quantitative PCR data characterizing mRNA expression of SERCA2a from laser captured gastrocnemius of sedentary and exercise-trained animals. Graphs indicated the mean \pm SE ($n = 5$ mice per group). (A) LCM-Whole, (B) LCM-TypeI and (C) LCM-TypeII. A main effect of exercise was observed for SERCA2a whole gastrocnemius and SERCA2a fast-twitch fibers, where Sed < Ex ($P < 0.05$). *, different from Sed of same genotype ($P < 0.01$). #, different from WT from same training condition ($P < 0.01$). **WT+Sed**, wild-type mice housed in standard cages (sedentary condition). **WT+Ex**, wild-type mice housed in cages with voluntary exercise wheels (exercised condition). **KD+Sed**, AMPK α 2 kinase dead mice housed in standard cages (sedentary condition). **KD+Ex**, AMPK α 2 kinase dead mice housed in cages with voluntary exercise wheels (exercised condition).

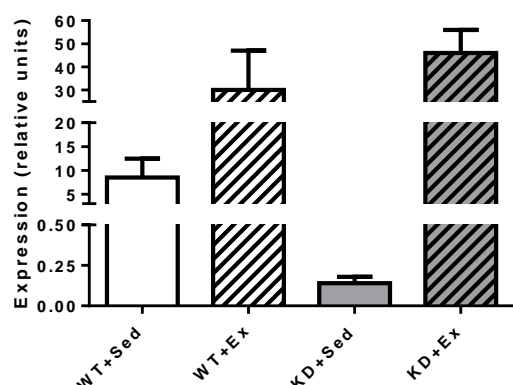
A. LCM-Whole



B. LCM-TypeI



C. LCM-TypeII

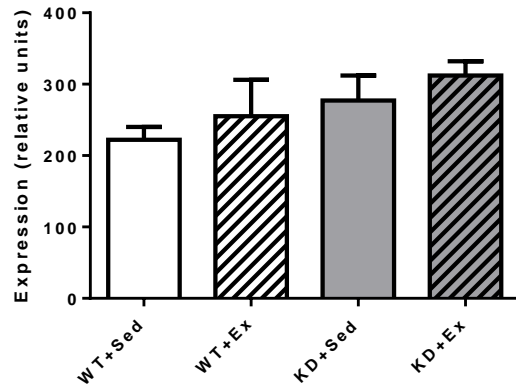


For RyR1 mRNA expression (Figure 17), there was no effect of genotype or exercise-training observed in LCM-Whole or LCM-TypeI tissue samples. However, a main effect of genotype was observed for RyR1 mRNA expression in LCM-TypeII tissue, where WT

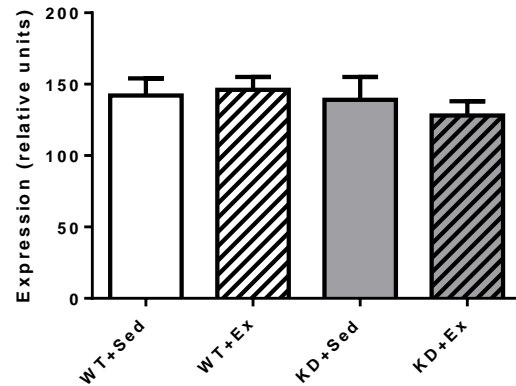
< KD ($P < 0.05$). Exercise-training was without effect on RyR1 mRNA expression in LCM-TypeII tissue.

Figure 17. Quantitative PCR data characterizing mRNA expression of RyR1 from laser captured gastrocnemius of sedentary and exercise-trained animals. Graphs indicated the mean \pm SE ($n = 5$ mice per group). (A) LCM-Whole, (B) LCM-TypeI and (C) LCM-TypeII. A main effect of genotype was observed for RyR1 fast-twitch fibers, where WT < KD ($P < 0.05$). **WT+Sed**, wild-type mice housed in standard cages (sedentary condition). **WT+Ex**, wild-type mice housed in cages with voluntary exercise wheels (exercised condition). **KD+Sed**, AMPK α 2 kinase dead mice housed in standard cages (sedentary condition). **KD+Ex**, AMPK α 2 kinase dead mice housed in cages with voluntary exercise wheels (exercised condition).

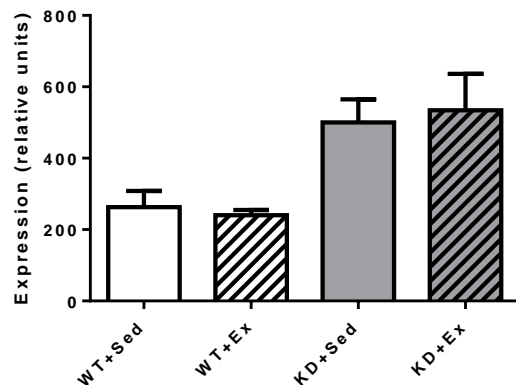
A. LCM-Whole



B. LCM-TypeI



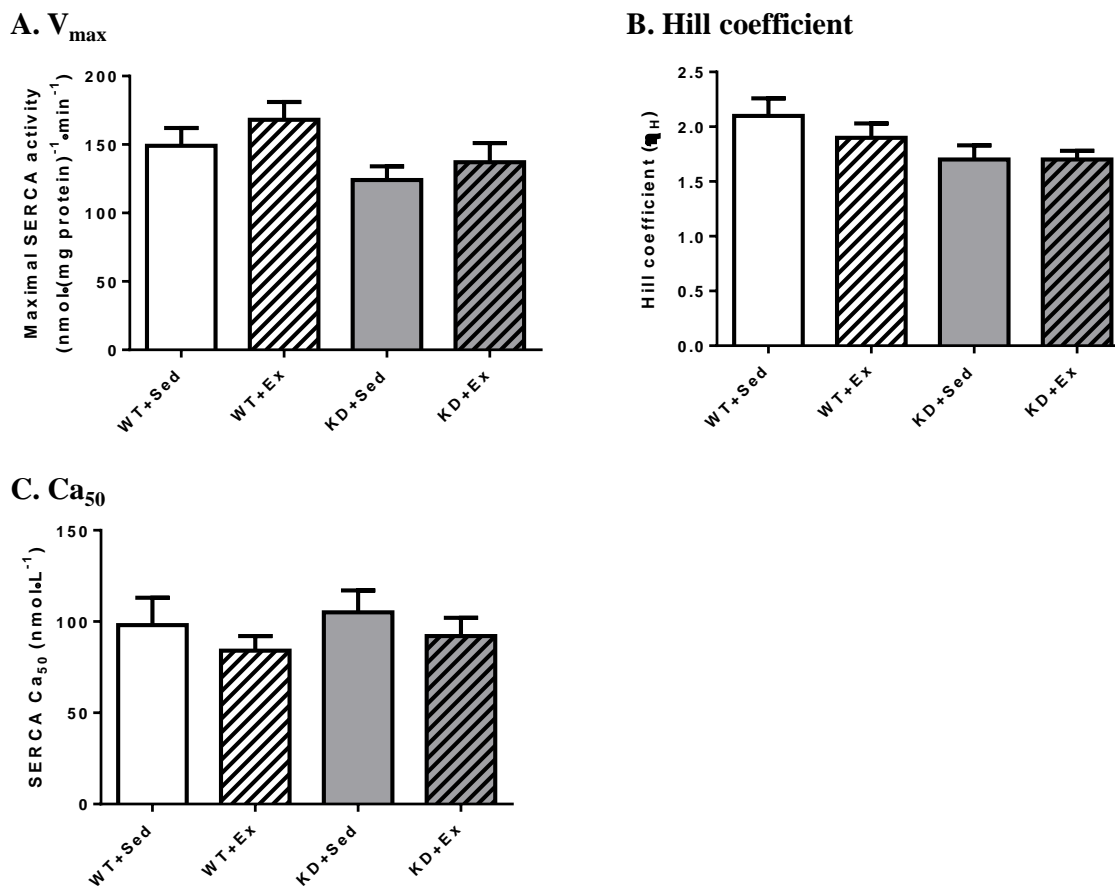
C. LCM-TypeII



Calcium-dependent SERCA activity in left ventricle and gastrocnemius samples

To assess the kinetic properties of calcium-dependent SERCA activity, a spectrophotometric assay was conducted. For left ventricle samples (Figure 18), a main effect of genotype was observed for V_{\max} and Hill coefficient, where WT > KD ($P < 0.05$). No effect of exercise-training was observed for either parameter in LV tissue. Similarly, no differences were observed for Ca_{50} between any of the groups.

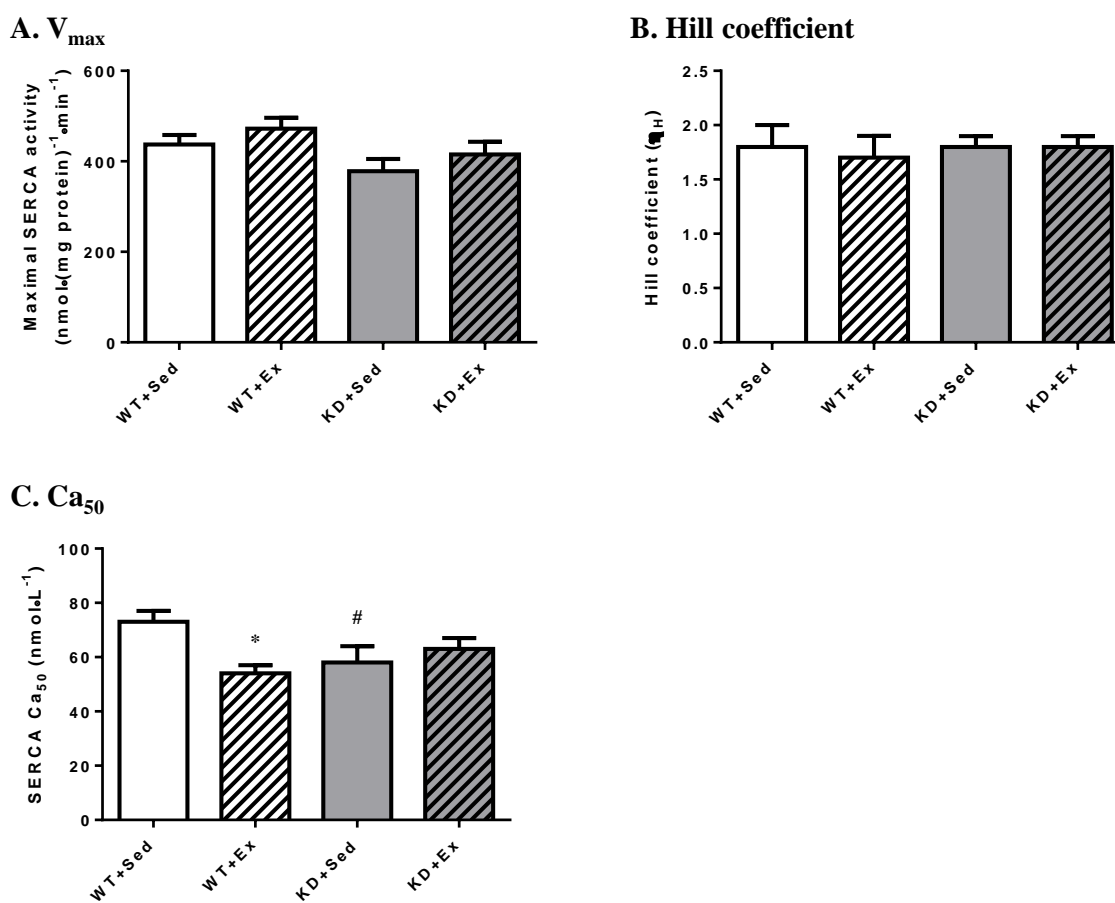
Figure 18. Calcium-dependent SERCA activity from left ventricle samples isolated from sedentary and exercise-trained animals. Graphs indicate the mean \pm SE ($n = 8$ mice per group). (A) Maximal SERCA activity (V_{\max}), (B) Hill coefficient and (C) Ca_{50} . Main effect of genotype for V_{\max} and Hill coefficient, where WT > KD ($P < 0.05$). **WT+Sed**, wild-type mice housed in standard cages (sedentary condition). **WT+Ex**, wild-type mice housed in cages with voluntary exercise wheels (exercised condition). **KD+Sed**, AMPK α 2 kinase dead mice housed in standard cages (sedentary condition). **KD+Ex**, AMPK α 2 kinase dead mice housed in cages with voluntary exercise wheels (exercised condition).



For gastroc samples (Figure 19), a main effect of genotype was observed for V_{\max} , where WT > KD ($P < 0.05$). No effect of exercise was observed for V_{\max} . Additionally, there was no effect of genotype or exercise-training on the Hill coefficient. In contrast, an interaction effect ($P < 0.05$) was observed for Ca_{50} , where Ca_{50} was reduced by ~21% amongst KD+Sed mice, as compared to WT+Sed mice ($P < 0.05$). Exercise-training also

reduced Ca_{50} by ~26% amongst WT mice ($73 \pm 4 \text{ nmol}\cdot\text{L}^{-1}$), as compared to WT+Sed mice ($54 \pm 3 \text{ nmol}\cdot\text{L}^{-1}$). However, exercise-training did not alter Ca_{50} amongst KD mice. Finally, Ca_{50} was not different when comparisons were made between WT+Ex and KD+Ex mice.

Figure 19. Calcium-dependent SERCA activity from gastrocnemius samples isolated from sedentary and exercise-trained animals. Graphs indicate the mean \pm SE ($n = 8$ mice per group). (A) Maximal SERCA activity (V_{\max}), (B) Hill coefficient and (C) Ca_{50} . Main effect of genotype on V_{\max} , where WT > KD ($P < 0.05$). *, different from Sed of same genotype ($P < 0.05$). #, different from WT from same training condition ($P < 0.05$). **WT+Sed**, wild-type mice housed in standard cages (sedentary condition). **WT+Ex**, wild-type mice housed in cages with voluntary exercise wheels (exercised condition). **KD+Sed**, AMPK α 2 kinase dead mice housed in standard cages (sedentary condition). **KD+Ex**, AMPK α 2 kinase dead mice housed in cages with voluntary exercise wheels (exercised condition).



Echocardiography

To determine whether changes in cardiac structure and function occurred, *in vivo* echocardiography was performed (Table 9). While no effect of genotype was observed for heart rate, a main effect of exercise-training was observed, where Sed > Ex ($P < 0.05$). Additionally, no effects of genotype or exercise-training were observed for ejection fraction. In contrast, an interaction effect was observed for left ventricular internal diastolic dimension (LVIDd). Specifically, LVIDd increased by ~13% in sedentary KD mice, as compared to sedentary WT mice ($P < 0.05$). Exercise-training also stimulated an increase of ~13% for LVIDd amongst WT+Ex mice, as compared to WT+Sed mice ($P < 0.05$). However, there was no effect of exercise-training amongst KD mice. Additionally, there was no difference in LVIDd between exercise-trained WT and exercise-trained KD mice. Left ventricular posterior wall dimension (LVPWd), tissue Doppler imaging (TDI) of left ventricular posterior wall, E wave, A wave and E/A ratio did not change based on genotype or exercise-training. An interaction effect ($P < 0.05$) was observed for deceleration time (DT), where the DT for KD+Sed mice was ~43% higher than the values observed for sedentary WT mice. Although exercise-training did not alter DT in WT mice, exercise-training did result in a 29% faster DT amongst KD+Ex mice, as compared to KD+Sed mice ($P < 0.05$). Finally, DT was not different when comparisons were made between WT+Ex and KD+Ex mice.

Table 9. Echocardiography parameters at 20 weeks.

	WT+Sed	WT+Ex	KD+Sed	KD+Ex
Heart rate (beats/min)	686 ± 11	659 ± 16	701 ± 12	658 ± 18
Ejection fraction (%)	82 ± 1	82 ± 2	79 ± 1	82 ± 1
Left ventricular internal diastolic dimension (LVIDd; mm)	2.4 ± 0.04	2.7 ± 0.09	* 2.7 ± 0.05	# 2.7 ± 0.05
Left ventricular posterior wall dimension (LVPWd; mm)	0.9 ± 0.01	0.9 ± 0.02	0.9 ± 0.02	0.9 ± 0.02
TDI of left ventricular posterior wall (cm/sec)	1.7 ± 0.1	1.6 ± 0.1	1.7 ± 0.1	1.7 ± 0.1
Early ventricular filling velocity (E wave; mm/sec)	613 ± 47	651 ± 48	664 ± 45	574 ± 29
Atrial ventricular filling velocity (A wave; mm/sec)	387 ± 42	434 ± 47	379 ± 49	356 ± 45
E/A ratio	1.5 ± 0.08	1.5 ± 0.10	1.7 ± 0.11	1.8 ± 0.18
Deceleration time (DT; ms)	24.4 ± 1.8	26.9 ± 3.3	34.9 ± 3.2	# 21.6 ± 1.1 *

Values are means ± SE ($n = 8$ mice per group). **WT+Sed**, wild-type mice housed in standard cages (sedentary condition). **WT+Ex**, wild-type mice housed in cages with voluntary exercise wheels (exercised condition). **KD+Sed**, AMPK α 2 kinase dead mice housed in standard cages (sedentary condition). **KD+Ex**, AMPK α 2 kinase dead mice housed in cages with voluntary exercise wheels (exercised condition). A main effect of exercise-training was observed for heart rate, where Sed > Ex. ($P < 0.05$). *, different from Sed of same genotype ($P < 0.05$). #, different from WT from same training condition ($P < 0.05$).

Chapter 4: Discussion

A recent paper by Dong et al.¹⁰⁷ demonstrated that AMPK α_2 signaling is involved in the regulation of SERCA3 function in endothelial cells. However, it remains to be elucidated whether AMPK is involved in the regulation of SERCA1a and SERCA2a in skeletal and cardiac muscle. Therefore, the primary purpose of this study was to determine the role that AMPK α_2 may play in regulating SERCA expression and function within cardiac and skeletal muscle tissue. Furthermore, it has previously been demonstrated that exercise-training enhances AMPK activity^{142, 143}, while also up-regulating SERCA1a and SERCA2a expression and function in cardiac⁶⁰⁻⁶³ and skeletal muscle^{55, 57-59}. With this in mind, a secondary aim of this study was to determine whether exercise-induced changes in SERCA1a and SERCA2a expression and function in cardiac and skeletal muscle are mediated through an AMPK α_2 -mediated process. Finally, a previous study by Lee-Young et al.¹¹⁵ has indicated that exercise-training up-regulates AMPK α^{Thr172} phosphorylation in a fiber-type specific manner. Therefore, the final objective of this study was to determine if the genetic manipulation of AMPK α_2 or exercise-training would stimulate fiber-type specific changes in SERCA1a or SERCA2a expression in skeletal muscle.

AMPK α_2 KD mice are characterized by a down-regulation of AMPK signaling

In order to test our hypotheses, we made the decision to utilize a KD mouse model in our study. As expected, we observed a main effect of genotype where the p-AMPK α^{Thr172} /AMPK ratio was reduced by 45-50% in both cardiac and skeletal muscle. These findings indicate that the KD transgenic model was effective for reducing the

relative level of AMPK activation in both cardiac and skeletal muscle, which is in agreement with previous studies using the same animal model^{101, 103, 104}. Additionally, the observed changes in total p-ACC in KD mice, as compared to WT mice, support previously published data¹⁰³. However, it must be acknowledged that Habets et al.¹⁰³ published data indicating that p-ACC protein levels were reduced to an even greater extent in KD mice than the levels reported in this study.

AMPK α_2 KD transgene and exercise-training affect exercise capacity

Another method that was utilized to determine the efficacy of our animal model for testing our hypotheses was to have the mice perform a graded exercise test, as previously described by Hoydal et al.¹³² and modified by our lab. Our data clearly indicate that genotype influenced the maximum speed achieved during the graded exercise test, where KD mice did not achieve as high of a speed as their WT counterparts. We interpret these observations as an indication that animals that are characterized by impaired AMPK α_2 signaling have reduced aerobic capacity or an attenuated ability to adapt to progressive increases in exercise intensity during an acute bout of exercise. Previous reports in the literature support this idea and have demonstrated that incremental exercise progressively activates AMPK^{Thr172} phosphorylation¹⁴², and more specifically AMPK α_2 activity *in vivo*¹⁴⁴. Notably, other reports that have utilized animal models characterized with impaired AMPK signaling indicate that exercise tolerance is lower in animals with decreased AMPK signaling. Specifically, Fujii et al.¹⁴⁵ used an animal model similar to ours and observed ~63% decrease in total workload as measured by graded exercise treadmill test in KD mice compared to WT mice. Another study by O'Neill et al.¹²⁶ had

AMPK $\beta_1\beta_2$ knockout mice perform a graded exercise treadmill test and demonstrated that AMPK $\beta_1\beta_2$ knockout mice had ~57% reduction in maximal running speed.

With respect to the effect of exercise-training, our graded exercise test data for WT mice agree with data published by Hoydal et al.¹³² and demonstrate that the voluntary wheel running model of exercise-training increases graded exercise test performance. Our data also indicate that KD mice significantly improved their graded exercise test performance in response to 5 months of exercise-training. It is likely that the enhanced performance amongst KD mice may be explained, at least in part, by the fact that cardiac and skeletal muscle COX IV protein levels were elevated following exercise-training in KD mice. Specifically, exercise-training up-regulated COX IV protein levels by ~57% and ~119% in left ventricle tissue isolated from WT and KD mice, respectively, as compared to their sedentary counterparts. Exercise-training also up-regulated COX IV protein levels by ~105% and ~60% in skeletal muscle isolated from WT and KD mice. These data support previous literature indicating that exercise-training up-regulates COX IV by ~60% in skeletal muscle¹⁴⁶. Based on the fact that COX IV protein levels were enhanced following exercise-training in KD mice, it appears that exercise-training activates multiple pathways in order to up-regulate the expression of proteins involved in the regulation of oxidative phosphorylation. Alternatively, it is possible that the residual AMPK^{Thr172} phosphorylation¹⁰⁴ observed in KD mice was sufficient to enable the training-induced increases in COX IV and, thereby, contribute to the enhanced graded exercise test performance.

Regulation of SERCA2a in cardiac tissue

This study supports previous observations that SERCA2a protein abundance appears to be influenced by an AMPK α_2 -mediated signaling process¹⁴⁷. Specifically, our data indicate that SERCA2a protein content was ~40% lower in left ventricle tissue isolated from sedentary KD mice, as compared to sedentary WT mice. Moreover, this study is the first to demonstrate that exercise-training influences SERCA protein content in an AMPK α_2 -related manner. It was observed in this study that exercise-trained KD mice had a ~59% lower amount of SERCA2a protein content than their exercise-trained WT counterparts. The general changes observed for SERCA2a protein abundance are supported by similar changes in mRNA. For example, qPCR data indicate that SERCA2a mRNA levels were down-regulated by 34% in sedentary KD mice, as compared to WT sedentary mice, and by ~30% in exercise-trained KD mice, as compared to exercise-trained WT mice. It was also notable that a main effect of genotype was observed for V_{\max} , where maximal SERCA2a activity was ~17% higher amongst WT mice, as compared to KD mice. This reduction in maximal SERCA activity was similar in magnitude to that reported previously in endothelial cells¹⁰⁷. Specifically, Dong et al.¹⁰⁷ reported that maximal SERCA3 activity was impaired by ~25% in endothelial cells isolated from AMPK α_2 knock-out mice. Even so, the current study is the first to report that a transgenic animal model characterized by a 50% lower amount of AMPK α_2 signaling is also characterized by reduced SERCA2a protein abundance in cardiac tissue from exercise-trained mice. Additionally, our data from sedentary mice is in agreement with previously published data that have utilized the same and other experimental models that are characterized by impaired AMPK activity¹⁴⁷⁻¹⁴⁹. For example, the AMPK α_2 KD

model was used by Turdi et al.¹⁴⁷ and they found a reduction in cardiac SERCA2a protein abundance. Furthermore, diabetic animals tend to have low levels of p-AMPK^{Thr172}^{148, 149} while also being characterized by reduced SERCA2a mRNA expression, protein abundance and enzyme activity in cardiac tissue^{64, 148, 150-153}. Collectively, these changes in AMPK signaling and SERCA2a proteins are thought to contribute to the development of diastolic dysfunction in the diabetic heart (i.e. as indicated by a slower myocardial relaxation rate)^{64, 149, 150, 152, 153}.

Our data indicate that exercise-training enhanced myocardial SERCA2a protein content by ~43% in WT mice. These data support previously published reports indicating that exercise-training up-regulates SERCA2a protein content in rats^{61, 65} and WT mice¹⁵⁴. However, we must acknowledge that these exercise-stimulated changes in protein content amongst WT mice were not supported by similar changes in myocardial SERCA2a mRNA expression in the current study. Tate et al.⁶¹ have previously reported that myocardial SERCA2a mRNA expression is up-regulated by ~110% following a treadmill-based exercise-training protocol. It is possible that the difference in training models could account for the discrepancies. Specifically, our study employed voluntary wheel running, which enables mice to select the intensity and duration for which they run. In contrast, Tate et al.⁶¹ used a 10 week treadmill-based training protocol, where mice ran up to 60 minutes at 16 m·min⁻¹ at a 5% grade, 5 days·week⁻¹. It is also possible that this discrepancy could be explained by the tissue sampling protocol that was utilized in each study. Specifically, animals in the current study were removed from the running wheel cages approximately 2 hours before tissue collection; whereas, Tate et al.⁶¹ collected tissue 24 hours after the last exercise bout. Finally, it is possible that the

exercise-training reduced the post-translational rate of SERCA2a protein turnover, which may explain why protein content was enhanced even though mRNA expression appeared to be unchanged.

A novel observation reported for the first time was the observation that exercise-training did not influence myocardial SERCA2a protein content in KD mice. We interpret this data as an indication that the transgenic knockdown of AMPK α_2 signaling prevents the exercise-stimulated adaptations in myocardial SERCA2a protein content. Published literature has previously demonstrated that the AMPK α_2 subunit is important in the regulation of expression and function of various proteins. Specifically, Jorgensen et al.¹⁰⁰ identified the importance of AMPK α_2 in regulating hexokinase II, glucose-transporter-4 (GLUT4), cytochrome c, cytochrome c oxidase, citrate synthase and 3-hydroxyacyl-CoA dehydrogenase protein levels. However, their data showed differences between sedentary AMPK α_2 knockout mice and exercise-trained AMPK α_2 knockout mice. Thus, the lack of AMPK α_2 did not eliminate exercise-induced changes in protein abundance in the study by Jorgensen et al.¹⁰⁰. In contrast, Mu et al.¹⁰¹ demonstrated that contraction-stimulated glucose uptake was reduced by 30-40% in skeletal muscle of KD mice compared to WT mice. They also demonstrated that the likely cause for this reduced glucose uptake was due to inhibition of GLUT4 translocation to the cell surface. Finally, a study by Lefort et al.¹⁰² found that KD mice display decreased p-ACC compared to WT mice, however muscle contraction still caused an increase in p-ACC in KD mice. Collectively, these data indicate that the AMPK α_2 subunit plays an important role in the expression and regulation of a multitude of proteins.

Regulation of SERCA1a and SERCA2a in skeletal muscle

We also examined the regulation of SERCA protein isoforms in skeletal muscle tissue. Notably, we report for the first time that sedentary KD mice displayed ~27% lower SERCA1a in gastroc muscle tissue, as compared to sedentary WT mice. However, an effect of genotype was not observed for SERCA2a in gastroc muscle tissue isolated from KD mice. Even so, maximal SERCA activity (V_{\max}) was reduced by ~12-14% in sedentary and exercise-trained KD mice, as compared to their WT counterparts. It is important to indicate that the Ca^{2+} -dependent SERCA activity assay employed in this study cannot be used to assess the activity of specific SERCA protein isoforms. Thus, we cannot determine if changes in SERCA1a or SERCA2a protein content contributed to the observed changes in V_{\max} . The observed changes in SERCA1a protein content in gastrocnemius muscle were not explained by similar changes in SERCA1a mRNA. Although it is unclear why this discrepancy exists, a study by Racz et al.¹⁵⁵ recently demonstrated that diabetes does not alter SERCA1a mRNA expression or protein levels in skeletal muscle. Although the current study did not utilize the same diabetic model, it is important to indicate the transgenic model utilized in the current study and the streptozotocin diabetic model utilized by Racz et al.¹⁵⁵ are both characterized by reductions in p-AMPK^{Thr172}^{156, 157}. Even so, it must be acknowledged that Racz et al.¹⁵⁵ examined the regulation of SERCA1a in soleus muscle and not the gastrocnemius, which was utilized in the current study. Furthermore, in the study by Peters et al.¹⁵⁸ it was observed that SERCA1a mRNA expression was decreased in fast-twitch skeletal muscle in a rat model of congestive heart failure (which is a model that is characterized by reduced protein levels and activity of the different AMPK subunits¹⁵⁹).

It was of particular interest that exercise-training enhanced SERCA1a protein abundance in skeletal muscle isolated from both WT (~47% increase) and KD (~66% increase) mice, as compared to their sedentary counterparts. It was also notable that exercise-training also enhanced SERCA2a protein content in skeletal muscle. These findings add to the literature that has previously demonstrated that exercise-training increases SERCA1a protein content in skeletal muscle^{32, 55, 59}. However, the observed changes in SERCA1a and SERCA2a protein content due to exercise were not accompanied by similar changes in maximal SERCA activity (V_{\max}). Exercise-training did enhance Ca_{50} by ~26% amongst WT mice, as compared to WT+Sed mice. However, this exercise-stimulated change was not observed amongst KD animals, which can most likely be explained by the fact that Ca_{50} was ~21% lower amongst KD+Sed mice, as compared to WT+Sed mice. The exercise-stimulated increases in SERCA1a and SERCA2a protein expression were accompanied by a 53-59% up-regulation of SERCA1a and SERCA2a mRNA in WT and KD mice, respectively. This observation amongst WT mice contrasts the findings published by Kubo et al.⁵⁸, which indicated that SERCA1a mRNA expression was unchanged in response to a 6 week treadmill-based exercise-training protocol (where mice ran at $20 \text{ m}\cdot\text{min}^{-1}$ for 60 minutes a day which equates to $1.2 \text{ km}\cdot\text{day}^{-1}$). It is possible that the different modes of exercise-training may explain this discrepancy.

Fiber-type specific differences in various protein content

A study by Lee-Young et al.¹¹⁵ found that AMPK activation occurs in a fiber-type specific manner, with type IIx muscle fibers demonstrating a higher level of

AMPK α^{Thr172} phosphorylation following a single bout of exercise, both before and after 10 days of exercise-training. That report was the main reason why the current study sought to determine whether SERCA1a and SERCA2a isoforms are differentially regulated in a fiber-type specific manner. In order to test hypothesis 4, the laser capture microdissection technique was utilized to enrich areas of high and low type I fiber content based on the expression pattern of MHC-1 β . It is important to indicate that the differences in non-normalized levels of MHC-1 β mRNA measured in the different LCM tissue types (i.e. Whole, TypeI and TypeII) confirmed our selection of high concentration areas of slow-twitch and fast-twitch muscle fibers. These enriched samples were then lysed to collect mRNA and analyzed using qPCR. This laser capture method has been employed in previous studies to examine mitochondrial adaptations in different muscle fibers¹⁶⁰, electron transport system abnormalities¹⁶¹ and changes in fiber-type distribution in obese and diabetic animals¹⁶². A more recent study (published after this project was started) has utilized LCM to identify fiber-type specific changes in mRNA of various proteins, including SERCA1a and SERCA2a as a result of atrophy¹⁶³. In fact, Vanderburg et al¹⁶³ demonstrated that lack of activity increased SERCA1 mRNA expression while SERCA2a mRNA expression decreased in gastrocnemius slow-twitch muscle fibers. Alternatively, SERCA1 mRNA levels remained unchanged despite an increase in SERCA2a mRNA in fast-twitch muscle fibers. Even so, to our knowledge, the current study is the first to utilize the LCM technique to examine changes in mRNA expression of various proteins following exercise-training.

It was notable that exercise-training stimulated a 3-fold increase in MHC-1 β mRNA expression in LCM-Whole tissue isolated from WT mice, as compared to sedentary WT

mice. Similar changes for MHC-1 β mRNA levels were observed in LCM-TypeI as well as LCM-TypeII tissue samples. This data supports previous observations made by Klitgaard et al.¹⁶⁴, where they reported a greater increase of MHC-1 β protein levels in vastus lateralis muscle in subject who regularly exercised (i.e. walking, cycling and jogging). Our novel data also indicate that exercise-training did not alter MHC-1 β mRNA expression in the LCM-Whole or enriched LCM-TypeI or LCM-TypeII tissue isolated from KD mice. We interpret these observations as an indication that the AMPK α_2 subunit may play a role in exercise-induced changes of MHC-1 β mRNA in skeletal muscle.

Exercise-training also up-regulated PGC-1 α expression in LCM-Whole and LCM-TypeII tissue. This exercise-stimulated effect was also observed for LCM-TypeI tissue isolated from WT mice, but not KD mice. We believe this discrepancy can be explained by the higher levels of PGC-1 α expression in LCM-TypeI tissue isolated from KD+Sed mice. As summarized by Winder et al.¹⁶⁵, muscle contraction has been shown to increase PGC-1 α mRNA expression and protein abundance. Specifically, Baar et al.¹⁶⁶ demonstrated that both PGC-1 α mRNA and protein increased in skeletal muscle following completion of a swimming protocol. Furthermore, a study by Terada & Tabata¹⁶⁷ showed an increase in PGC-1 α protein content in soleus, plantaris and gastrocnemius following the completion of a running exercise protocol. Pilegaard et al.¹⁶⁸ also demonstrated an increase in skeletal muscle PGC-1 α mRNA expression after exposure to a prolonged exercise protocol.

A novel observation generated using the LCM technique was the identification of a main effect of exercise-training for SERCA1a mRNA expression in LCM-Whole and

TypeII tissue, but not amongst LCM-TypeI tissue. This observation was also supported by a similar main effect of exercise-training for SERCA2a mRNA expression in LCM-Whole and TypeII tissue. Based on these observations, it appears that factors other than the AMPK α_2 subunit alone may regulate SERCA1a or SERCA2a mRNA expression in LCM-Whole and type II skeletal muscle fibers.

It was also observed that SERCA2a mRNA expression was up-regulated by exercise-training amongst LCM-TypeI tissue isolated from WT mice. However, although exercise-training also enhanced the expression of SERCA2a mRNA in LCM-TypeI tissue isolated from KD mice, the exercise-stimulated response was blunted by 54%. We interpret this observation as evidence indicating that the AMPK α_2 subunit influences the regulation of SERCA2a in type I skeletal muscle fibers following exercise-training. We must acknowledge that these observations do not match the results published by Kubo et al.⁵⁸, which indicated that exercise-training does not alter SERCA1a mRNA expression in gastroc tissue. However, Kubo et al.⁵⁸ did report that SERCA2a mRNA levels increased by ~124% in gastrocnemius tissue. It is likely these discrepancies may be explained by difference in experimental protocols, where the use of the LCM technique to enrich type I and type II muscle fibers in the current study is one example. In fact, it is important to point out that in response to exercise, SERCA2a mRNA expression was up-regulated by ~2.5-fold in LCM-TypeII tissue isolated from WT mice, but by 270-fold in LCM-TypeI fibers. Thus, it appears that the magnitude of change observed for SERCA2a mRNA was significantly higher amongst type I fibers, as compared to type II fibers. This exercise-stimulated fiber-type specific difference in expression may be explained, at least theoretically, based on the size principle, which indicates that type I fibers are recruited

initially upon contraction to remain active until they become fatigued. It is also notable that the presence of the AMPK α_2 kinase dead transgene negatively influenced the regulation of SERCA2a mRNA in type I skeletal muscle fibers, but not type II muscle fibers following exercise-training. It is unclear to us why this fiber type specific difference was observed; however, it may have been influenced by the observed up-regulation of MHC-1 β amongst both LCM-TypeI and TypeII fiber samples. In fact, an up-regulation of SERCA2a mRNA would be consistent with an exercise-induced transition from fast-to-slow twitch fiber types.

Regulation of PLN

The kinetic properties of SERCA proteins can be acutely regulated by at least two endogenous regulator proteins, namely SLN and PLN. Unfortunately, a reliable antibody for SLN is not yet commercially available. Moreover, SLN is not expressed in the left ventricle²⁴. It was demonstrated in our study that PLN protein levels were increased in KD mice compared to WT mice, in both cardiac and skeletal muscle. Our data support previous studies that have shown that PLN protein content is negatively regulated in animal models that are characterized by reduced AMPK activity^{65, 152, 153, 169}. For example, it is known that PLN protein content is up-regulated in diabetic animal models, which further inhibits SERCA-mediated Ca²⁺-transport at submaximal Ca²⁺-concentrations^{152, 153, 169}. While total PLN protein content increased in KD mice, it must be mentioned that myocardial PLN mRNA expression was reduced by 52% and ~40% in KD+Sed and KD+Ex mice, respectively, as compared to their WT counterparts. We interpret these data as an indication that there may be a reduced rate of post-translational

PLN protein turnover. Additionally, a main effect of exercise was observed for PLN, where PLN protein levels in exercise-trained mice were lower compared to their sedentary counterparts in both cardiac and skeletal muscle. This exercise-induced reduction in cardiac PLN protein abundance can be explained by decreases in PLN mRNA expression in WT+Ex and KD+Ex mice, as compared to WT+Sed and KD+Sed mice, respectively. It must be acknowledged that our data demonstrating an effect of exercise-training on PLN protein content is not in agreement with Rose et al.¹⁷⁰. Although we cannot explain this discrepancy, it is possible that differences in exercise-training protocols may account for different observations.

Although total PLN content is an important regulator of SERCA2a protein function in the heart, the relative phosphorylation status of p-PLN^{Thr17} and p-PLN^{Ser16} is known to relieve the inhibition that PLN exerts on SERCA activity at submaximal Ca²⁺-concentrations²². Therefore, we examined the phosphorylation status of p-PLN^{Thr17} and p-PLN^{Ser16}. It is notable that p-PLN^{Ser16} protein content was decreased in sedentary KD mice compared to sedentary WT mice, while there was no change in p-PLN^{Thr17} protein content. The changes in p-PLN^{Ser16} are in agreement with Zhong et al.¹⁴⁹, however they also observed a decrease in p-PLN^{Thr17} protein levels. Differences in findings may be due to the use of a STZ-induced diabetic animal model in the study by Zhong et al.¹⁴⁹. Furthermore, exercise-training did not alter p-PLN^{Thr17} or p-PLN^{Ser16} in WT mice. However, this data is in contrast to data presented by Kemi et al.¹⁵⁴, where it was demonstrated that exercise-training enhances p-PLN^{Thr17} by ~50% but does not alter p-PLN^{Ser16} status in WT mice. It is possible that this discrepancy can be explained by the different exercise-training models employed by Kemi et al.¹⁵⁴, as compared to the

voluntary wheel running model utilized in this study. Additionally, our data indicates that exercise-training increased p-PLN^{Thr17} and p-PLN^{Ser16} by ~61% and ~194%, respectively, in KD mice as compared to their sedentary counterparts; whereas there was no effect of exercise-training in WT mice. This increase in p-PLN^{Thr17} and p-PLN^{Ser16} may be a compensatory response in an effort to prevent any negative outcomes that may occur due to an increase in total PLN protein levels. Moreover, it was evident that KD+Sed mice were characterized by a ~49% lower level of p-PLN^{Ser16}, as compared to WT+Sed mice. Thus, it is possible that the AMPK α_2 has a role in regulating the exercise-stimulated changes in PLN phosphorylation. Support for this notion is provided by the observation that exercise-training enhances p-PLN^{Ser16} in the high-fat fed, low dose streptozotocin-injected diabetic rat (which is an inducible model of type 2 diabetes) and also in the db/db mouse (which is a genetic model of type 2 diabetes)⁶⁴. However, it should be noted that Ca₅₀ was not altered in the left ventricle samples isolated from any experimental group in the current study. Therefore, it is unclear if the observed changes in PLN phosphorylation would be of physiological relevance. Even so, it was observed that the Hill coefficient, which is a measure of SERCA2a Ca²⁺-binding-affinity, was significantly higher amongst WT mice, as compared to KD mice. This change would be expected to enhance SERCA2a activity at sub-maximal Ca²⁺-concentrations amongst WT, as compared to KD mice.

We also examined the relative phosphorylation levels of PLN in skeletal muscle. Specifically, the only effect observed was in exercise-trained WT mice had ~158% higher p-PLN^{Ser16} protein levels, as compared to sedentary WT mice. The lack of change in p-PLN^{Thr17} matches the findings of Rose et al.¹⁷⁰ where exercise-training had no effect on

p-PLN^{Thr17} in skeletal muscle. It is notable that Rose et al.¹⁷¹ also demonstrated in a different study that a single bout of exercise can enhance the phosphorylation status of p-PLN^{Thr17} in human quadriceps muscle, but that this acute effect of exercise is lost following 3 weeks of exercise-training¹⁷⁰. Interestingly, Ca₅₀ was enhanced by ~26% amongst WT+Ex mice, as compared to WT+Sed mice. Moreover, Ca₅₀ was enhanced by ~21% amongst KD+Sed mice, as compared to WT+Sed mice. This observation generally tracks the changes observed for p-PLN^{Ser16}.

AMPK α_2 KD mice are characterized by a prolonged cardiac deceleration time

Our study utilized echocardiography and tissue Doppler imaging (TDI) to monitor changes in cardiac structure and function between WT and KD mice or as a result of exercise-training. Notably, LVIDd was ~13% larger amongst sedentary KD mice compared to sedentary WT mice. Epp et al.⁶⁵ recently demonstrated that the high-fat fed, low dose streptozotocin-injected diabetic rat is also characterized by an enlargement of LVIDd. Similar changes in LVIDd have also been reported for high sucrose fed diabetic rats¹⁷² and streptozotocin-induced type 1 diabetic rats^{173, 174}. However, it must be acknowledged that diabetes had no effect on LVIDd in the db/db mouse (which is a genetic model of type 2 diabetes)¹⁷⁵. Echocardiography data also indicate that LVIDd increased by ~13% following exercise-training amongst WT mice, as compared to sedentary WT mice. It has previously been shown that exercise-training does not alter LVIDd in exercise-trained humans (people participated in up to 50 minutes of running/jogging at 70% of heart rate reserve up to 5 days·week⁻¹ for an average of 7.3 months)¹⁷⁶ or mice (exercise 5 days·week⁻¹ for 8 weeks alternating between a maximum speed of 41 m·min⁻¹ (sprint) and a minimum speed of 16 m·min⁻¹ (recovery))¹⁷⁷. It is

possible that the 5-month exercise-training period employed in the current study was of sufficient duration to induce the observed changes, whereas shorter protocol did not. Even so, it must be acknowledged that no other structural parameters indicated that cardiac hypertrophy had occurred (e.g. changes in heart:body weight ratios, thickening of the posterior wall thickness, etc).

Tissue Doppler imaging was also employed in this study. Notably, deceleration time was prolonged by ~43% in sedentary KD mice, as compared to sedentary WT mice. Exercise-training enhanced the deceleration time by ~38% amongst KD mice so values were similar to those observed in WT+Sed and WT+Ex mice. This observation suggests that diastolic function may be impaired in sedentary KD mice. However, caution must be utilized when interpreting the change in deceleration time because no changes in other parameters that may indicate the development of diastolic dysfunction were observed (e.g. E/A ratios were unchanged in any experimental group). It should also be mentioned that this observed change in DT amongst KD mice does not support the observations made by Nielsen et al.¹⁷⁸, which indicated that deceleration time is enhanced in the type I diabetic heart.

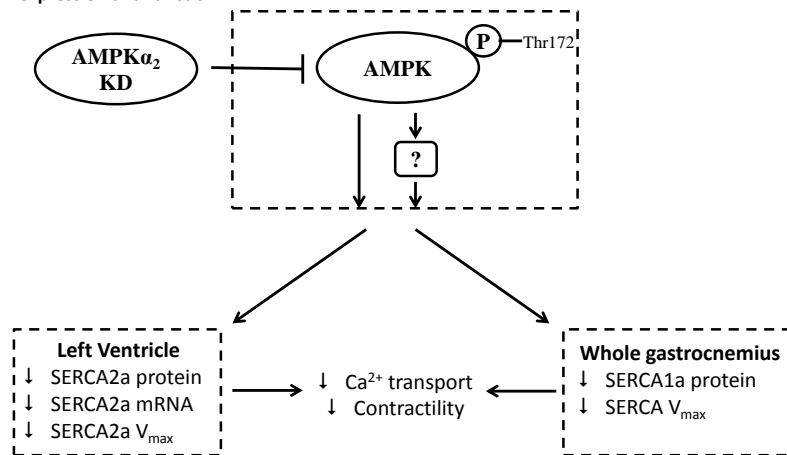
The link between AMPK and SERCA

Together, our data supports previous literature that identifies a potential link between AMPK and SERCA^{107, 147}. More specifically, it appears as though a decrease in AMPK α_2 activity negatively influences SERCA expression and function in cardiac and skeletal muscle. Additionally, this relationship between AMPK α_2 and SERCA appears to occur in sedentary mice and in exercise-trained mice. Figure 20 was developed as a way to summarize my data and to provide an overview of how the parameters that we

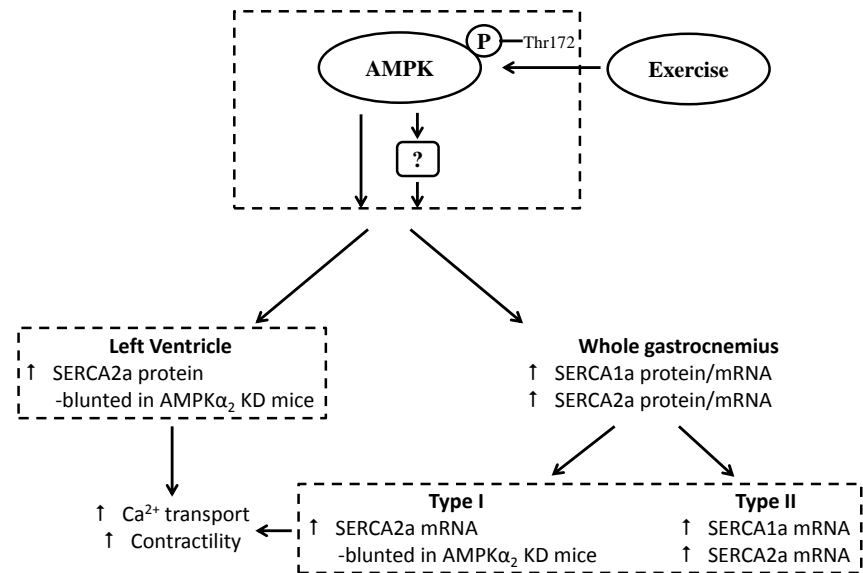
manipulated in the experiment and outcome measures are related. Other experimental models that are characterized by reduced AMPK activity include diabetes^{157, 179}, aging¹⁴⁷ and heart failure¹⁵⁹. Furthermore, it has been demonstrated that diabetes⁶⁴, aging¹⁴⁷ and heart failure¹⁸⁰⁻¹⁸² models are characterized by impaired SERCA expression and function. My observation that a transgenic animal model characterized by reduced AMPK^{Thr12} phosphorylation, namely the KD mouse, provides data indicating that an AMPK-mediated mechanism may be directly contributing to the observed reduction in SERCA protein content. With this data in mind, it is possible that impaired AMPK signaling contributes to the down-regulation of SERCA protein content and the pathophysiology of diabetes, aging and heart failure. Furthermore, the data presented in this thesis suggest that AMPK phosphorylation may be a target that can be exploited to enhance SERCA expression and function in models characterized by reduced AMPK activity.

Figure 20. The link between AMPK α_2 and SERCA expression and function in cardiac and skeletal muscle. (A) AMPK α_2 KD transgene and its downstream effects on SERCA expression and function and (B) Exercise and its downstream effects on SERCA expression. **AMPK**, adenosine monophosphate activated protein kinase. **AMPK α_2 KD**, AMPK α_2 kinase dead mice. **SERCA**, sarcoplasmic reticulum calcium ATPase.

A. AMPK α_2 KD transgene and its downstream effects on SERCA expression and function.



B. Exercise and its downstream effects on SERCA expression.



Limitations

While we interpret our data as an indication that AMPK α_2 plays a role in regulating SERCA expression and function in cardiac and skeletal muscle, it would be negligent to ignore the various limitations that exist within our animal model and experimental methods. For example, one limitation with this study is that the researcher was not blinded to the genotype or exercise-training status of the mice performing the graded exercise tests. It is possible that the researcher provided greater levels of encouragement to exercise-trained mice knowing that they should be performing to a higher level than sedentary animals. Additionally, knowing which animals were WT or KD may have caused similar issues for encouragement and determining when animals were fatigued. However, this limitation is mitigated by the observation that COX IV protein levels were higher amongst exercise-trained, as compared to sedentary mice, as well as amongst WT, as compared to KD mice. These changes in COX IV protein content indicate that a greater adaptation for exercise tolerance was obtained by the expected groups. Thus, despite the researcher being aware of which animals were WT or transgenic and which were sedentary or exercise-trained, our Western blotting results provide support that the differences observed in the graded exercise test were based on physiological parameters.

A second limitation in this study is that we did not identify extreme responders with respect to exercise and p-AMPK α^{Thr172} . It remains possible that mice who ran further distances may demonstrate greater changes in p-AMPK α^{Thr172} and SERCA expression and function. Alternatively, it is possible that mice that ran the shortest distances did not adapt in a similar manner. Likewise, we did not consider the effects of exercise intensity in our experiments. Therefore, it is possible that animals that ran similar total distances

but did so by running at slower or faster speeds may have responded differently. Finally, we collected tissue after 5 months of exercise training and did not consider the effects of shorter training protocols or the acute effects of a single bout of exercise.

Another limitation exists within the use of laser capture microdissection. This method was somewhat limited in its ability to select slow- and fast-twitch muscle fibers. For this study, we used stained slices to identify areas with a high concentration of either type I or type II muscle fibers. Unfortunately, this approach does not allow the specific selection of single type I or type II fibers alone. As a result, we were forced to isolate an enriched area of mostly type I or mostly type II fibers within each LCM sample. Our results would be more specific if we would have used immunohistochemistry to identify type IIa, type IIx and type IIb muscle fibers rather than simply using the approach that employed to stain type I fibers based on MHC-1 β isoform content. Even with this limitation, our LCM mRNA expression data indicate that the approach we used to isolate MHC-1 β expression was 200-fold lower in LCM-TypeII tissue, as compared to LCM-TypeI tissue samples. Thus, we believe this data supports our decision to characterize fiber-type specific changes between type I and type II skeletal muscle samples.

A fourth limitation within this study is that our KD animal model does not result in complete inactivation of AMPK. In our study, AMPK phosphorylation was reduced by ~55% in cardiac muscle and by ~36% in skeletal muscle. Thus, the residual p-AMPK activity would be expected to stimulate some AMPK α_2 -dependent signaling pathways. For example, we provide data indicating that p-ACC, which is a downstream target of p-AMPK, was not completely inhibited. However, muscle-specific AMPK α_1 and AMPK α_2 knockout mice are not yet commercially available. Additionally, whole-body AMPK α_1

and AMPK α_2 knockout animals would be alter the physiological functions of a variety of tissues other than cardiac and skeletal muscle. Therefore, we decided to use the AMPK α_2 kinase dead mouse model because it provided us with the best option for examining our hypotheses. Additionally, many of our results have demonstrated that the KD mouse model is sufficient to demonstrate the importance of the AMPK α_2 subunit for regulating protein content in cardiac and skeletal muscle.

Another limitation for this study is the use of Western blotting techniques. While Western blots are useful in identifying changes in protein levels, it is a semi-quantitative technique. Any differences found are relative to the samples used as opposed to knowing exact amount of the desired protein in each sample. Quantitative measures do exist (i.e. ELISA, protein-based multiplex technique), however these methods were not conducted.

Conclusion

Our novel study shows that the AMPK α_2 subunit plays a role in SERCA expression and function in cardiac and skeletal muscle. Specifically, SERCA2a protein content was lower in both sedentary and exercise-trained KD mice compared to their WT counterparts. These changes in SERCA2a protein content are supported by similar reductions in SERCA2a mRNA expression in KD mice when compared to WT mice. Furthermore, KD mice demonstrated a reduction in maximal SERCA2a enzyme activity in cardiac muscle. While these differences in SERCA2a protein were not observed in skeletal muscle, KD mice did demonstrate reduced SERCA1a protein abundance and a decrease in maximal SERCA activity in skeletal muscle when compared to WT mice. Interestingly, decreases in cardiac and skeletal muscle SERCA activity can be explained

in part by increases in total PLN protein abundance in KD mice compared to WT mice. Taken together, these findings support our hypothesis that AMPK α_2 kinase dead transgenic mice will have reduced SERCA protein expression and function in both cardiac and skeletal muscle.

Exercise-training did not have an effect on p-AMPK α^{Thr172} protein levels in left ventricle tissue, however in gastrocnemius muscle exercise-training resulted in an increase of p-AMPK α^{Thr172} . Despite the lack of increase in cardiac p-AMPK α^{Thr172} , exercise-trained WT mice did display an increase in SERCA2a protein content, however no changes were observed in maximal SERCA2a activity or SERCA2a mRNA expression. An increase in SERCA1a and SERCA2a protein content in gastrocnemius was observed in response to exercise-training, which can be explained by exercise-induced increases in SERCA1a and SERCA2a mRNA expression. These changes in SERCA protein abundance and mRNA expression were not accompanied by exercise-induced changes in SERCA V_{max} . These findings therefore partially support our second hypothesis that exercise-training will increase the relative level of AMPK α^{Thr172} phosphorylation and enhance SERCA protein expression and function in cardiac and skeletal muscle isolated from WT mice.

Notably, the exercise-induced increase in left ventricle SERCA2a protein content seen in WT mice was blunted in KD mice. Furthermore, while exercise-training increased SERCA1a protein content in gastrocnemius from both WT and KD mice, exercise-trained KD mice demonstrated reduced SERCA1a protein levels compared to exercise-trained WT mice. Unfortunately, these differences in SERCA2a and SERCA1a protein content cannot be explained by concomitant changes in mRNA. Therefore, our data partially

support our third hypothesis that the exercise-stimulated increase in SERCA protein expression and function will be blunted in cardiac and skeletal muscle from isolated from KD mice.

Data from our laser captured mRNA experiments presents novel data with respect to skeletal muscle SERCA1a and SERCA2a mRNA expression. It was demonstrated that exercise-training increased SERCA1a mRNA in fast-twitch muscle fibers; however, similar changes were not observed in slow-twitch fibers. Furthermore, our data show that SERCA2a mRNA expression increased in both slow-twitch and fast-twitch muscle fibers. Therefore, our findings support our final hypothesis that SERCA1a and SERCA2a isoforms will differentially adapt to exercise-training based on the specific fiber-type assessed.

What remains to be elucidated is the exact mechanism that links AMPK and SERCA. Interestingly, the literature indicates that the activation of the SERCA2 promoter is regulated by SP1¹⁸³ and it has been shown that an AMPK mediated pathway can regulate SP1 phosphorylation^{184, 185}. Furthermore, there is evidence in the literature indicating that SIRT1 signaling prevents the reduced cardiac SERCA2 promoter activity that occurs when cardiomyocytes are exposed to high glucose conditions¹⁸⁶. Since SIRT1 and AMPK signaling are known to cross talk, it remains possible that AMPK α_2 activity may play a role in the regulation of SERCA promoter activity through a SP1-mediated or another yet to be identified mechanism.

In summary, the novel data presented in this study demonstrate the importance of AMPK α_2 phosphorylation in the regulation of SERCA expression and function, either directly or via SERCA mediators (i.e. PLN). Furthermore, it appears as though exercise-

training influences SERCA expression differentially in different fiber-types. Collectively, these data describe a novel AMPK-dependent mechanism that appears to regulate SERCA protein content and function in cardiac and skeletal muscle. It is possible that this AMPK-mediated mechanism may help explain the pathophysiology of conditions that are characterized by impaired AMPK activity and impaired calcium-cycling (such as diabetes, aging, heart disease or physical inactivity). Furthermore, this data suggests that AMPK signaling may be targeted by physical activity or novel therapies to enhance SERCA protein content and function in cardiac and skeletal muscle.

References

- (1) Fill M, Copello JA. Ryanodine receptor calcium release channels. *Physiol Rev* 2002 October;82(4):893-922.
- (2) Lamb GD. Excitation-contraction coupling in skeletal muscle: comparisons with cardiac muscle. *Clin Exp Pharmacol Physiol* 2000 March;27(3):216-24.
- (3) Hochachka PW. *Muscles as Molecular and Metabolic Machines*. Informa Healthcare; 1994.
- (4) Kushnir A, Marks AR. The ryanodine receptor in cardiac physiology and disease. *Adv Pharmacol* 2010;59:1-30.:1-30.
- (5) Middlekauff HR. Making the case for skeletal myopathy as the major limitation of exercise capacity in heart failure. *Circ Heart Fail* 2010 July 1;3(4):537-46.
- (6) Geeves MA. The dynamics of actin and myosin association and the crossbridge model of muscle contraction. *Biochem J* 1991 February 15;274(Pt 1):1-14.
- (7) Sahlin K, Tonkonogi M, Soderlund K. Energy supply and muscle fatigue in humans. *Acta Physiol Scand* 1998 March;162(3):261-6.
- (8) Rolfe DF, Brown GC. Cellular energy utilization and molecular origin of standard metabolic rate in mammals. *Physiol Rev* 1997 July;77(3):731-58.
- (9) Schiaffino S, Reggiani C. Fiber types in mammalian skeletal muscles. *Physiol Rev* 2011 October;91(4):1447-531.
- (10) Augusto V, Padovani CR, Campos GER. Skeletal muscle fiber types in C57BL6J mice. *Braz J morphol Sci* 2004 May 12;21(2):89-94.
- (11) Barany M. ATPase activity of myosin correlated with speed of muscle shortening. *J Gen Physiol* 1967 July;50(6):Suppl-218.
- (12) Fitts RH. Cellular mechanisms of muscle fatigue. *Physiol Rev* 1994 January;74(1):49-94.
- (13) Hoppeler H. Exercise-induced ultrastructural changes in skeletal muscle. *Int J Sports Med* 1986 August;7(4):187-204.
- (14) Peter JB, Barnard RJ, Edgerton VR, Gillespie CA, Stempel KE. Metabolic profiles of three fiber types of skeletal muscle in guinea pigs and rabbits. *Biochemistry* 1972 July 4;11(14):2627-33.

- (15) Little JP, Safdar A, Wilkin GP, Tarnopolsky MA, Gibala MJ. A practical model of low-volume high-intensity interval training induces mitochondrial biogenesis in human skeletal muscle: potential mechanisms. *J Physiol* 2010 March 15;588(Pt 6):1011-22.
- (16) Sacchetto R, Margreth A, Pelosi M, Carafoli E. Colocalization of the dihydropyridine receptor, the plasma-membrane calcium ATPase isoform 1 and the sodium/calcium exchanger to the junctional-membrane domain of transverse tubules of rabbit skeletal muscle. *Eur J Biochem* 1996 April 15;237(2):483-8.
- (17) Yoshida Y, Imai S. Structure and function of inositol 1,4,5-trisphosphate receptor. *Jpn J Pharmacol* 1997 June;74(2):125-37.
- (18) Bers DM. Cardiac excitation-contraction coupling. *Nature* 2002 January 10;415(6868):198-205.
- (19) Norris SM, Bombardier E, Smith IC, Vigna C, Tupling AR. ATP consumption by sarcoplasmic reticulum Ca²⁺ pumps accounts for 50% of resting metabolic rate in mouse fast and slow twitch skeletal muscle. *Am J Physiol Cell Physiol* 2010 March;298(3):C521-C529.
- (20) Brandl CJ, Green NM, Korczak B, MacLennan DH. Two Ca²⁺ ATPase genes: homologies and mechanistic implications of deduced amino acid sequences. *Cell* 1986 February 28;44(4):597-607.
- (21) Periasamy M, Kalyanasundaram A. SERCA pump isoforms: their role in calcium transport and disease. *Muscle Nerve* 2007 April;35(4):430-42.
- (22) Hovnanian A. SERCA pumps and human diseases. *Subcell Biochem* 2007;45:337-63.:337-63.
- (23) Awede B, Berquin A, Wuytack F, Lebacq J. Adaptation of mouse skeletal muscle to a novel functional overload test: changes in myosin heavy chains and SERCA and physiological consequences. *Eur J Appl Physiol Occup Physiol* 1999 November;80(6):519-26.
- (24) Vangheluwe P, Schuermans M, Zador E, Waelkens E, Raeymaekers L, Wuytack F. Sarcolipin and phospholamban mRNA and protein expression in cardiac and skeletal muscle of different species. *Biochem J* 2005 July 1;389(Pt 1):151-9.
- (25) Mahdavi V, Periasamy M, Nadal-Ginard B. Molecular characterization of two myosin heavy chain genes expressed in the adult heart. *Nature* 1982 June 24;297(5868):659-64.
- (26) Mahdavi V, Chambers AP, Nadal-Ginard B. Cardiac alpha- and beta-myosin heavy chain genes are organized in tandem. *Proc Natl Acad Sci U S A* 1984 May;81(9):2626-30.

- (27) Pette D, Staron RS. Myosin isoforms, muscle fiber types, and transitions. *Microsc Res Tech* 2000 September 15;50(6):500-9.
- (28) Tupling AR, Bombardier E, Gupta SC et al. Enhanced Ca²⁺ transport and muscle relaxation in skeletal muscle from sarcolipin-null mice. *Am J Physiol Cell Physiol* 2011 October;301(4):C841-C849.
- (29) Stapleton D, Mitchelhill KI, Gao G et al. Mammalian AMP-activated protein kinase subfamily. *J Biol Chem* 1996 January 12;271(2):611-4.
- (30) Viollet B, Horman S, Leclerc J et al. AMPK inhibition in health and disease. *Crit Rev Biochem Mol Biol* 2010 August;45(4):276-95.
- (31) Cheung PC, Salt IP, Davies SP, Hardie DG, Carling D. Characterization of AMP-activated protein kinase gamma-subunit isoforms and their role in AMP binding. *Biochem J* 2000 March 15;346 Pt 3:659-69.:659-69.
- (32) Putman CT, Martins KJ, Gallo ME et al. Alpha-catalytic subunits of 5'AMP-activated protein kinase display fiber-specific expression and are upregulated by chronic low-frequency stimulation in rat muscle. *Am J Physiol Regul Integr Comp Physiol* 2007 September;293(3):R1325-R1334.
- (33) Thornton C, Snowden MA, Carling D. Identification of a novel AMP-activated protein kinase beta subunit isoform that is highly expressed in skeletal muscle. *J Biol Chem* 1998 May 15;273(20):12443-50.
- (34) Soltys CL, Kovacic S, Dyck JR. Activation of cardiac AMP-activated protein kinase by LKB1 expression or chemical hypoxia is blunted by increased Akt activity. *Am J Physiol Heart Circ Physiol* 2006 June;290(6):H2472-H2479.
- (35) Sakamoto K, Goransson O, Hardie DG, Alessi DR. Activity of LKB1 and AMPK-related kinases in skeletal muscle: effects of contraction, phenformin, and AICAR. *Am J Physiol Endocrinol Metab* 2004 August;287(2):E310-E317.
- (36) Anderson KA, Means RL, Huang QH et al. Components of a calmodulin-dependent protein kinase cascade. Molecular cloning, functional characterization and cellular localization of Ca²⁺/calmodulin-dependent protein kinase kinase beta. *J Biol Chem* 1998 November 27;273(48):31880-9.
- (37) Abbott MJ, Edelman AM, Turcotte LP. CaMKK is an upstream signal of AMP-activated protein kinase in regulation of substrate metabolism in contracting skeletal muscle. *Am J Physiol Regul Integr Comp Physiol* 2009 December;297(6):R1724-R1732.
- (38) Asahi M, Kurzydowski K, Tada M, MacLennan DH. Sarcolipin inhibits polymerization of phospholamban to induce superinhibition of sarco(endo)plasmic reticulum Ca²⁺-ATPases (SERCAs). *J Biol Chem* 2002 July 26;277(30):26725-8.

- (39) Simmerman HK, Collins JH, Theibert JL, Wegener AD, Jones LR. Sequence analysis of phospholamban. Identification of phosphorylation sites and two major structural domains. *J Biol Chem* 1986 October 5;261(28):13333-41.
- (40) Fujii J, Ueno A, Kitano K, Tanaka S, Kadoma M, Tada M. Complete complementary DNA-derived amino acid sequence of canine cardiac phospholamban. *J Clin Invest* 1987 January;79(1):301-4.
- (41) Liu Y, Kranias EG, Schneider MF. Regulation of Ca²⁺ handling by phosphorylation status in mouse fast- and slow-twitch skeletal muscle fibers. *Am J Physiol* 1997 December;273(6 Pt 1):C1915-C1924.
- (42) Minamisawa S, Wang Y, Chen J, Ishikawa Y, Chien KR, Matsuoka R. Atrial chamber-specific expression of sarcolipin is regulated during development and hypertrophic remodeling. *J Biol Chem* 2003 March 14;278(11):9570-5.
- (43) Marotta M, Ruiz-Roig C, Sarria Y et al. Muscle genome-wide expression profiling during disease evolution in mdx mice. *Physiol Genomics* 2009 April 10;37(2):119-32.
- (44) Babu GJ, Bhupathy P, Carnes CA, Billman GE, Periasamy M. Differential expression of sarcolipin protein during muscle development and cardiac pathophysiology. *J Mol Cell Cardiol* 2007 August;43(2):215-22.
- (45) Ottenheijm CA, Fong C, Vangheluwe P et al. Sarcoplasmic reticulum calcium uptake and speed of relaxation are depressed in nebulin-free skeletal muscle. *FASEB J* 2008 August;22(8):2912-9.
- (46) Ackermann MA, Ziman AP, Strong J et al. Integrity of the network sarcoplasmic reticulum in skeletal muscle requires small ankyrin 1. *J Cell Sci* 2011 November 1;124(Pt 21):3619-30.
- (47) Odermatt A, Becker S, Khanna VK et al. Sarcolipin regulates the activity of SERCA1, the fast-twitch skeletal muscle sarcoplasmic reticulum Ca²⁺-ATPase. *J Biol Chem* 1998 May 15;273(20):12360-9.
- (48) Shanmugam M, Molina CE, Gao S, Severac-Bastide R, Fischmeister R, Babu GJ. Decreased sarcolipin protein expression and enhanced sarco(endo)plasmic reticulum Ca²⁺ uptake in human atrial fibrillation. *Biochem Biophys Res Commun* 2011 June 24;410(1):97-101.
- (49) Gramolini AO, Trivieri MG, Oudit GY et al. Cardiac-specific overexpression of sarcolipin in phospholamban null mice impairs myocyte function that is restored by phosphorylation. *Proc Natl Acad Sci U S A* 2006 February 14;103(7):2446-51.

- (50) Bhupathy P, Babu GJ, Ito M, Periasamy M. Threonine-5 at the N-terminus can modulate sarcolipin function in cardiac myocytes. *J Mol Cell Cardiol* 2009 November;47(5):723-9.
- (51) Hill CA, Thompson MW, Ruell PA, Thom JM, White MJ. Sarcoplasmic reticulum function and muscle contractile character following fatiguing exercise in humans. *J Physiol* 2001 March 15;531(Pt 3):871-8.
- (52) Byrd SK, Bode AK, Klug GA. Effects of exercise of varying duration on sarcoplasmic reticulum function. *J Appl Physiol* 1989 March;66(3):1383-9.
- (53) Belcastro AN, Rossiter M, Low MP, Sopper MM. Calcium activation of sarcoplasmic reticulum ATPase following strenuous activity. *Can J Physiol Pharmacol* 1981 December;59(12):1214-8.
- (54) Duhamel TA, Perco JG, Green HJ. Manipulation of dietary carbohydrates after prolonged effort modifies muscle sarcoplasmic reticulum responses in exercising males. *Am J Physiol Regul Integr Comp Physiol* 2006 October;291(4):R1100-R1110.
- (55) Ferreira JC, Bacurau AV, Bueno CR, Jr. et al. Aerobic exercise training improves Ca²⁺ handling and redox status of skeletal muscle in mice. *Exp Biol Med (Maywood)* 2010 April;235(4):497-505.
- (56) Ferreira JC, Rolim NP, Bartholomeu JB, Gobatto CA, Kokubun E, Brum PC. Maximal lactate steady state in running mice: effect of exercise training. *Clin Exp Pharmacol Physiol* 2007 August;34(8):760-5.
- (57) Bueno CR, Jr., Ferreira JC, Pereira MG, Bacurau AV, Brum PC. Aerobic exercise training improves skeletal muscle function and Ca²⁺ handling-related protein expression in sympathetic hyperactivity-induced heart failure. *J Appl Physiol* 2010 September;109(3):702-9.
- (58) Kubo H, Libonati JR, Kendrick ZV, Paolone A, Gaughan JP, Houser SR. Differential effects of exercise training on skeletal muscle SERCA gene expression. *Med Sci Sports Exerc* 2003 January;35(1):27-31.
- (59) Duhamel TA, Stewart RD, Tupling AR, Ouyang J, Green HJ. Muscle sarcoplasmic reticulum calcium regulation in humans during consecutive days of exercise and recovery. *J Appl Physiol* 2007 October;103(4):1212-20.
- (60) Tate CA, Taffet GE, Hudson EK, Blaylock SL, McBride RP, Michael LH. Enhanced calcium uptake of cardiac sarcoplasmic reticulum in exercise-trained old rats. *Am J Physiol* 1990 February;258(2 Pt 2):H431-H435.
- (61) Tate CA, Helgason T, Hyek MF et al. SERCA2a and mitochondrial cytochrome oxidase expression are increased in hearts of exercise-trained old rats. *Am J Physiol* 1996 July;271(1 Pt 2):H68-H72.

- (62) Wisloff U, Loennechen JP, Currie S, Smith GL, Ellingsen O. Aerobic exercise reduces cardiomyocyte hypertrophy and increases contractility, Ca²⁺ sensitivity and SERCA-2 in rat after myocardial infarction. *Cardiovasc Res* 2002 April;54(1):162-74.
- (63) Davidoff AJ, Mason MM, Davidson MB et al. Sucrose-induced cardiomyocyte dysfunction is both preventable and reversible with clinically relevant treatments. *Am J Physiol Endocrinol Metab* 2004 May;286(5):E718-E724.
- (64) Stolen TO, Hoydal MA, Kemi OJ et al. Interval training normalizes cardiomyocyte function, diastolic Ca²⁺ control, and SR Ca²⁺ release synchronicity in a mouse model of diabetic cardiomyopathy. *Circ Res* 2009 September 11;105(6):527-36.
- (65) Epp RA, Susser SE, Morissette MP, Kehler DS, Jassal DS, Duhamel TA. Exercise training prevents the development of cardiac dysfunction in the low-dose streptozotocin diabetic rats fed a high-fat diet. *Can J Physiol Pharmacol* 2013 January;91(1):80-9.
- (66) Shirwany NA, Zou MH. AMPK in cardiovascular health and disease. *Acta Pharmacol Sin* 2010 September;31(9):1075-84.
- (67) Li C, Keaney JF, Jr. AMP-activated protein kinase: a stress-responsive kinase with implications for cardiovascular disease. *Curr Opin Pharmacol* 2010 April;10(2):111-5.
- (68) Steinberg GR, Kemp BE. AMPK in Health and Disease. *Physiol Rev* 2009 July;89(3):1025-78.
- (69) Canto C, Auwerx J. AMP-activated protein kinase and its downstream transcriptional pathways. *Cell Mol Life Sci* 2010 October;67(20):3407-23.
- (70) Hardie DG. AMP-activated/SNF1 protein kinases: conserved guardians of cellular energy. *Nat Rev Mol Cell Biol* 2007 October;8(10):774-85.
- (71) Suter M, Riek U, Tuerk R, Schlattner U, Wallimann T, Neumann D. Dissecting the role of 5'-AMP for allosteric stimulation, activation, and deactivation of AMP-activated protein kinase. *J Biol Chem* 2006 October 27;281(43):32207-16.
- (72) Hardie DG, Scott JW, Pan DA, Hudson ER. Management of cellular energy by the AMP-activated protein kinase system. *FEBS Lett* 2003 July 3;546(1):113-20.
- (73) Wojtaszewski JF, Birk JB, Frosig C, Holten M, Pilegaard H, Dela F. 5'AMP activated protein kinase expression in human skeletal muscle: effects of strength training and type 2 diabetes. *J Physiol* 2005 April 15;564(Pt 2):563-73.

- (74) Woods A, Cheung PC, Smith FC et al. Characterization of AMP-activated protein kinase beta and gamma subunits. Assembly of the heterotrimeric complex in vitro. *J Biol Chem* 1996 April 26;271(17):10282-90.
- (75) Iseli TJ, Walter M, van Denderen BJ et al. AMP-activated protein kinase beta subunit tethers alpha and gamma subunits via its C-terminal sequence (186-270). *J Biol Chem* 2005 April 8;280(14):13395-400.
- (76) Birk JB, Wojtaszewski JF. Predominant alpha2/beta2/gamma3 AMPK activation during exercise in human skeletal muscle. *J Physiol* 2006 December 15;577(Pt 3):1021-32.
- (77) Chen ZP, Stephens TJ, Murthy S et al. Effect of exercise intensity on skeletal muscle AMPK signaling in humans. *Diabetes* 2003 September;52(9):2205-12.
- (78) Hawley SA, Davison M, Woods A et al. Characterization of the AMP-activated protein kinase from rat liver and identification of threonine 172 as the major site at which it phosphorylates AMP-activated protein kinase. *J Biol Chem* 1996 November 1;271(44):27879-87.
- (79) Kahn BB, Alquier T, Carling D, Hardie DG. AMP-activated protein kinase: ancient energy gauge provides clues to modern understanding of metabolism. *Cell Metab* 2005 January;1(1):15-25.
- (80) Treebak JT, Glund S, Deshmukh A et al. AMPK-mediated AS160 phosphorylation in skeletal muscle is dependent on AMPK catalytic and regulatory subunits. *Diabetes* 2006 July;55(7):2051-8.
- (81) Carling D, Clarke PR, Zammit VA, Hardie DG. Purification and characterization of the AMP-activated protein kinase. Copurification of acetyl-CoA carboxylase kinase and 3-hydroxy-3-methylglutaryl-CoA reductase kinase activities. *Eur J Biochem* 1989 December 8;186(1-2):129-36.
- (82) Sanders MJ, Grondin PO, Hegarty BD, Snowden MA, Carling D. Investigating the mechanism for AMP activation of the AMP-activated protein kinase cascade. *Biochem J* 2007 April 1;403(1):139-48.
- (83) Sullivan JE, Carey F, Carling D, Beri RK. Characterisation of 5'-AMP-activated protein kinase in human liver using specific peptide substrates and the effects of 5'-AMP analogues on enzyme activity. *Biochem Biophys Res Commun* 1994 May 16;200(3):1551-6.
- (84) Shaw RJ, Kosmatka M, Bardeesy N et al. The tumor suppressor LKB1 kinase directly activates AMP-activated kinase and regulates apoptosis in response to energy stress. *Proc Natl Acad Sci U S A* 2004 March 9;101(10):3329-35.

- (85) Hawley SA, Boudeau J, Reid JL et al. Complexes between the LKB1 tumor suppressor, STRAD alpha/beta and MO25 alpha/beta are upstream kinases in the AMP-activated protein kinase cascade. *J Biol* 2003;2(4):28.
- (86) Sakamoto K, McCarthy A, Smith D et al. Deficiency of LKB1 in skeletal muscle prevents AMPK activation and glucose uptake during contraction. *EMBO J* 2005 May 18;24(10):1810-20.
- (87) Hou X, Xu S, Maitland-Toolan KA et al. SIRT1 regulates hepatocyte lipid metabolism through activating AMP-activated protein kinase. *J Biol Chem* 2008 July 18;283(29):20015-26.
- (88) Lan F, Cacicedo JM, Ruderman N, Ido Y. SIRT1 modulation of the acetylation status, cytosolic localization, and activity of LKB1. Possible role in AMP-activated protein kinase activation. *J Biol Chem* 2008 October 10;283(41):27628-35.
- (89) Palacios OM, Carmona JJ, Michan S et al. Diet and exercise signals regulate SIRT3 and activate AMPK and PGC-1alpha in skeletal muscle. *Aging (Albany NY)* 2009 August 15;1(9):771-83.
- (90) Pillai VB, Sundaresan NR, Kim G et al. Exogenous NAD blocks cardiac hypertrophic response via activation of the SIRT3-LKB1-AMP-activated kinase pathway. *J Biol Chem* 2010 January 29;285(5):3133-44.
- (91) Ferrara N, Rinaldi B, Corbi G et al. Exercise training promotes SIRT1 activity in aged rats. *Rejuvenation Res* 2008 February;11(1):139-50.
- (92) Suwa M, Nakano H, Radak Z, Kumagai S. Endurance exercise increases the SIRT1 and peroxisome proliferator-activated receptor gamma coactivator-1alpha protein expressions in rat skeletal muscle. *Metabolism* 2008 July;57(7):986-98.
- (93) Canto C, Gerhart-Hines Z, Feige JN et al. AMPK regulates energy expenditure by modulating NAD+ metabolism and SIRT1 activity. *Nature* 2009 April 23;458(7241):1056-60.
- (94) Gurd BJ, Holloway GP, Yoshida Y, Bonen A. In mammalian muscle, SIRT3 is present in mitochondria and not in the nucleus; and SIRT3 is upregulated by chronic muscle contraction in an adenosine monophosphate-activated protein kinase-independent manner. *Metabolism* 2012 May;61(5):733-41.
- (95) Hardie DG. New roles for the LKB1-->AMPK pathway. *Curr Opin Cell Biol* 2005 April;17(2):167-73.

- (96) Zhou L, Deepa SS, Etzler JC et al. Adiponectin activates AMP-activated protein kinase in muscle cells via APPL1/LKB1-dependent and phospholipase C/Ca²⁺/Ca²⁺/calmodulin-dependent protein kinase kinase-dependent pathways. *J Biol Chem* 2009 August 14;284(33):22426-35.
- (97) Hawley SA, Pan DA, Mustard KJ et al. Calmodulin-dependent protein kinase kinase-beta is an alternative upstream kinase for AMP-activated protein kinase. *Cell Metab* 2005 July;2(1):9-19.
- (98) Hurley RL, Anderson KA, Franzone JM, Kemp BE, Means AR, Witters LA. The Ca²⁺/calmodulin-dependent protein kinase kinases are AMP-activated protein kinase kinases. *J Biol Chem* 2005 August 12;280(32):29060-6.
- (99) Woods A, Dickerson K, Heath R et al. Ca²⁺/calmodulin-dependent protein kinase kinase-beta acts upstream of AMP-activated protein kinase in mammalian cells. *Cell Metab* 2005 July;2(1):21-33.
- (100) Jorgensen SB, Treebak JT, Viollet B et al. Role of AMPKalpha2 in basal, training-, and AICAR-induced GLUT4, hexokinase II, and mitochondrial protein expression in mouse muscle. *Am J Physiol Endocrinol Metab* 2007 January;292(1):E331-E339.
- (101) Mu J, Brozinick JT, Jr., Valladares O, Bucan M, Birnbaum MJ. A role for AMP-activated protein kinase in contraction- and hypoxia-regulated glucose transport in skeletal muscle. *Mol Cell* 2001 May;7(5):1085-94.
- (102) Lefort N, St-Amand E, Morasse S, Cote CH, Marette A. The alpha-subunit of AMPK is essential for submaximal contraction-mediated glucose transport in skeletal muscle in vitro. *Am J Physiol Endocrinol Metab* 2008 December;295(6):E1447-E1454.
- (103) Habets DD, Coumans WA, El HM et al. Crucial role for LKB1 to AMPKalpha2 axis in the regulation of CD36-mediated long-chain fatty acid uptake into cardiomyocytes. *Biochim Biophys Acta* 2009 March;1791(3):212-9.
- (104) Jeppesen J, Albers PH, Rose AJ et al. Contraction-induced skeletal muscle FAT/CD36 trafficking and FA uptake is AMPK independent. *J Lipid Res* 2011 April;52(4):699-711.
- (105) Dzamko N, Schertzer JD, Ryall JG et al. AMPK-independent pathways regulate skeletal muscle fatty acid oxidation. *J Physiol* 2008 December 1;586(Pt 23):5819-31.
- (106) Dong Y, Zhang M, Wang S et al. Activation of AMP-activated protein kinase inhibits oxidized LDL-triggered endoplasmic reticulum stress in vivo. *Diabetes* 2010 June;59(6):1386-96.

- (107) Dong Y, Zhang M, Liang B et al. Reduction of AMP-activated protein kinase alpha2 increases endoplasmic reticulum stress and atherosclerosis in vivo. *Circulation* 2010 February 16;121(6):792-803.
- (108) Henneman E, Somjen G, Carpenter DO. Functional significance of cell size in spinal motoneurons. *J Neurophysiol* 1965 May;28:560-80.:560-80.
- (109) Gordon T, Thomas CK, Munson JB, Stein RB. The resilience of the size principle in the organization of motor unit properties in normal and reinnervated adult skeletal muscles. *Can J Physiol Pharmacol* 2004 August;82(8-9):645-61.
- (110) Burke RE. Group Ia synaptic input to fast and slow twitch motor units of cat triceps surae. *J Physiol* 1968 June;196(3):605-30.
- (111) Burke RE. Firing patterns of gastrocnemius motor units in the decerebrate cat. *J Physiol* 1968 June;196(3):631-54.
- (112) Garnett R, Stephens JA. Changes in the recruitment threshold of motor units produced by cutaneous stimulation in man. *J Physiol* 1981 February;311:463-73.:463-73.
- (113) Burkholder TJ, Fingado B, Baron S, Lieber RL. Relationship between muscle fiber types and sizes and muscle architectural properties in the mouse hindlimb. *J Morphol* 1994 August;221(2):177-90.
- (114) McConell GK, Lee-Young RS, Chen ZP et al. Short-term exercise training in humans reduces AMPK signalling during prolonged exercise independent of muscle glycogen. *J Physiol* 2005 October 15;568(Pt 2):665-76.
- (115) Lee-Young RS, Canny BJ, Myers DE, McConell GK. AMPK activation is fiber type specific in human skeletal muscle: effects of exercise and short-term exercise training. *J Appl Physiol* 2009 July;107(1):283-9.
- (116) Wanagat JF, Cao ZF, Pathare PF, Aiken JM. Mitochondrial DNA deletion mutations colocalize with segmental electron transport system abnormalities, muscle fiber atrophy, fiber splitting, and oxidative damage in sarcopenia.(0892-6638 (Print)).
- (117) Canadian Council on Animal Care. Canadian Council on Animal Care Guidelines. 2012.
Ref Type: Online Source
- (118) Larsen S, Kristensen JM, Stride N, Wojtaszewski JF, Helge JW, Dela F. Skeletal muscle mitochondrial respiration in AMPKalpha2 kinase-dead mice. *Acta Physiol (Oxf)* 2012 June;205(2):314-20.

- (119) Larochelle N, Lochmuller H, Zhao J et al. Efficient muscle-specific transgene expression after adenovirus-mediated gene transfer in mice using a 1.35 kb muscle creatine kinase promoter/enhancer. *Gene Ther* 1997 May;4(5):465-72.
- (120) Bruning JC, Michael MD, Winnay JN et al. A muscle-specific insulin receptor knockout exhibits features of the metabolic syndrome of NIDDM without altering glucose tolerance. *Mol Cell* 1998 November;2(5):559-69.
- (121) Jorgensen SB, Viollet B, Andreelli F et al. Knockout of the alpha2 but not alpha1 5'-AMP-activated protein kinase isoform abolishes 5-aminoimidazole-4-carboxamide-1-beta-4-ribofuranosidebut not contraction-induced glucose uptake in skeletal muscle. *J Biol Chem* 2004 January 9;279(2):1070-9.
- (122) Festing MF, Greenwood R. Home-cage wheel activity recording in mice. *Lab Anim* 1976 April;10(2):81-5.
- (123) Duncan MJ, Smith JT, Franklin KM et al. Effects of aging and genotype on circadian rhythms, sleep, and clock gene expression in APPxPS1 knock-in mice, a model for Alzheimer's disease. *Exp Neurol* 2012 August;236(2):249-58.
- (124) Hasan S, van der Veen DR, Winsky-Sommerer R, Dijk DJ, Archer SN. Altered sleep and behavioral activity phenotypes in PER3-deficient mice. *Am J Physiol Regul Integr Comp Physiol* 2011 December;301(6):R1821-R1830.
- (125) Maarbjerg SJ, Jorgensen SB, Rose AJ et al. Genetic impairment of AMPKalpha2 signaling does not reduce muscle glucose uptake during treadmill exercise in mice. *Am J Physiol Endocrinol Metab* 2009 October;297(4):E924-E934.
- (126) O'Neill HM, Maarbjerg SJ, Crane JD et al. AMP-activated protein kinase (AMPK) beta1beta2 muscle null mice reveal an essential role for AMPK in maintaining mitochondrial content and glucose uptake during exercise. *Proc Natl Acad Sci U S A* 2011 September;108(38):16092-7.
- (127) Aoi W, Naito Y, Hang LP et al. Regular exercise prevents high-sucrose diet-induced fatty liver via improvement of hepatic lipid metabolism. *Biochem Biophys Res Commun* 2011 September 23;413(2):330-5.
- (128) Berglund ED, Lustig DG, Baheza RA et al. Hepatic glucagon action is essential for exercise-induced reversal of mouse fatty liver. *Diabetes* 2011 November;60(11):2720-9.
- (129) Fu L, Liu X, Niu Y, Yuan H, Zhang N, Lavi E. Effects of high-fat diet and regular aerobic exercise on global gene expression in skeletal muscle of C57BL/6 mice. *Metabolism* 2012 February;61(2):146-52.

- (130) Leick LF, Wojtaszewski JF FAU - Johansen S, Johansen ST FAU - Kiilerich K et al. PGC-1alpha is not mandatory for exercise- and training-induced adaptive gene responses in mouse skeletal muscle.(0193-1849 (Print)).
- (131) Thomson DM FAU, Porter BB FAU, Tall JH FAU, Kim HJ FAU, Barrow JR FAU, Winder WW. Skeletal muscle and heart LKB1 deficiency causes decreased voluntary running and reduced muscle mitochondrial marker enzyme expression in mice.(0193-1849 (Print)).
- (132) Hoydal MA, Wisloff U, Kemi OJ, Ellingsen O. Running speed and maximal oxygen uptake in rats and mice: practical implications for exercise training. *Eur J Cardiovasc Prev Rehabil* 2007 December;14(6):753-60.
- (133) Jassal DS, Han SY, Hans C et al. Utility of tissue Doppler and strain rate imaging in the early detection of trastuzumab and anthracycline mediated cardiomyopathy. *J Am Soc Echocardiogr* 2009 April;22(4):418-24.
- (134) Jassal DS, Othman RA, Ahmadi R et al. The role of Tissue Doppler imaging in the noninvasive detection of chronic rejection after heterotopic cardiac transplantation in rats. *Echocardiography* 2009 January;26(1):37-43.
- (135) Syed F, Diwan A, Hahn HS. Murine echocardiography: a practical approach for phenotyping genetically manipulated and surgically modeled mice. *J Am Soc Echocardiogr* 2005 September;18(9):982-90.
- (136) Scherrer-Crosbie M, Thibault HB. Echocardiography in translational research: of mice and men. *J Am Soc Echocardiogr* 2008 October;21(10):1083-92.
- (137) Simonides WS, van HC. An assay for sarcoplasmic reticulum Ca²⁺-ATPase activity in muscle homogenates. *Anal Biochem* 1990 December;191(2):321-31.
- (138) Tupling R, Green H, Senisterra G, Lepock J, McKee N. Effects of 4-h ischemia and 1-h reperfusion on rat muscle sarcoplasmic reticulum function. *Am J Physiol Endocrinol Metab* 2001 October;281(4):E867-E877.
- (139) Duhamel TA, Green HJ, Stewart RD, Foley KP, Smith IC, Ouyang J. Muscle metabolic, SR Ca²⁺ -cycling responses to prolonged cycling, with and without glucose supplementation. *J Appl Physiol* 2007 December;103(6):1986-98.
- (140) Seidler NW, Jona I, Vegh M, Martonosi A. Cyclopiazonic acid is a specific inhibitor of the Ca²⁺-ATPase of sarcoplasmic reticulum. *J Biol Chem* 1989 October 25;264(30):17816-23.
- (141) Green HJ, Burnett M, Duhamel TA et al. Abnormal sarcoplasmic reticulum Ca²⁺-sequestering properties in skeletal muscle in chronic obstructive pulmonary disease. *Am J Physiol Cell Physiol* 2008 August;295(2):C350-C357.

- (142) Rasmussen BB, Winder WW. Effect of exercise intensity on skeletal muscle malonyl-CoA and acetyl-CoA carboxylase. *J Appl Physiol* 1997 October;83(4):1104-9.
- (143) Rasmussen BB, Hancock CR, Winder WW. Postexercise recovery of skeletal muscle malonyl-CoA, acetyl-CoA carboxylase, and AMP-activated protein kinase. *J Appl Physiol* 1998 November;85(5):1629-34.
- (144) Fujii N, Hayashi T, Hirshman MF et al. Exercise induces isoform-specific increase in 5'AMP-activated protein kinase activity in human skeletal muscle. *Biochem Biophys Res Commun* 2000 July 14;273(3):1150-5.
- (145) Fujii N, Seifert MM, Kane EM et al. Role of AMP-activated protein kinase in exercise capacity, whole body glucose homeostasis, and glucose transport in skeletal muscle -insight from analysis of a transgenic mouse model-. *Diabetes Res Clin Pract* 2007 September;77 Suppl 1:S92-S98.
- (146) Green HJ, Duhamel TA, Foley KP, Ouyang J, Smith IC, Stewart RD. Glucose supplements increase human muscle in vitro Na⁺-K⁺-ATPase activity during prolonged exercise. *Am J Physiol Regul Integr Comp Physiol* 2007 July;293(1):R354-R362.
- (147) Turdi S, Fan X, Li J et al. AMP-activated protein kinase deficiency exacerbates aging-induced myocardial contractile dysfunction. *Aging Cell* 2010 August;9(4):592-606.
- (148) Sriwijitkamol A, Coletta DK, Wajcberg E et al. Effect of acute exercise on AMPK signaling in skeletal muscle of subjects with type 2 diabetes: a time-course and dose-response study. *Diabetes* 2007 March;56(3):836-48.
- (149) Richter EA, Ruderman NB. AMPK and the biochemistry of exercise: implications for human health and disease. *Biochem J* 2009 March 1;418(2):261-75.
- (150) Lebeche D, Davidoff AJ, Hajjar RJ. Interplay between impaired calcium regulation and insulin signaling abnormalities in diabetic cardiomyopathy. *Nat Clin Pract Cardiovasc Med* 2008 November;5(11):715-24.
- (151) Belke DD, Swanson EA, Dillmann WH. Decreased sarcoplasmic reticulum activity and contractility in diabetic db/db mouse heart. *Diabetes* 2004 December;53(12):3201-8.
- (152) Kim HW, Ch YS, Lee HR, Park SY, Kim YH. Diabetic alterations in cardiac sarcoplasmic reticulum Ca²⁺-ATPase and phospholamban protein expression. *Life Sci* 2001 December 14;70(4):367-79.

- (153) Zhong Y, Ahmed S, Grupp IL, Matlib MA. Altered SR protein expression associated with contractile dysfunction in diabetic rat hearts. *Am J Physiol Heart Circ Physiol* 2001 September;281(3):H1137-H1147.
- (154) Kemi OJ, Ellingsen O, Ceci M et al. Aerobic interval training enhances cardiomyocyte contractility and Ca²⁺ cycling by phosphorylation of CaMKII and Thr-17 of phospholamban. *J Mol Cell Cardiol* 2007 September;43(3):354-61.
- (155) Racz G, Szabo A, Ver A, Zador E. The slow sarco/endoplasmic reticulum Ca²⁺-ATPase declines independently of slow myosin in soleus muscle of diabetic rats. *Acta Biochim Pol* 2009;56(3):487-93.
- (156) Li Q, Li J, Ren J. UCF-101 mitigates streptozotocin-induced cardiomyocyte dysfunction: role of AMPK. *Am J Physiol Endocrinol Metab* 2009 October;297(4):E965-E973.
- (157) Guo Z, Xia Z, Yuen VG, McNeill JH. Cardiac expression of adiponectin and its receptors in streptozotocin-induced diabetic rats. *Metabolism* 2007 October;56(10):1363-71.
- (158) Peters DG, Mitchell HL, McCune SA, Park S, Williams JH, Kandarian SC. Skeletal muscle sarcoplasmic reticulum Ca(2+)-ATPase gene expression in congestive heart failure. *Circ Res* 1997 November;81(5):703-10.
- (159) Kim M, Shen M, Ngoy S, Karamanlidis G, Liao R, Tian R. AMPK isoform expression in the normal and failing hearts. *J Mol Cell Cardiol* 2012 May;52(5):1066-73.
- (160) Cao Z, Wanagat J, McKiernan SH, Aiken JM. Mitochondrial DNA deletion mutations are concomitant with ragged red regions of individual, aged muscle fibers: analysis by laser-capture microdissection. *Nucleic Acids Res* 2001 November 1;29(21):4502-8.
- (161) Wanagat J, Cao Z, Pathare P, Aiken JM. Mitochondrial DNA deletion mutations colocalize with segmental electron transport system abnormalities, muscle fiber atrophy, fiber splitting, and oxidative damage in sarcopenia. *FASEB J* 2001 February;15(2):322-32.
- (162) Adachi T, Kikuchi N, Yasuda K et al. Fibre type distribution and gene expression levels of both succinate dehydrogenase and peroxisome proliferator-activated receptor-gamma coactivator-1alpha of fibres in the soleus muscle of Zucker diabetic fatty rats. *Exp Physiol* 2007 March;92(2):449-55.
- (163) Vanderburg CR, Clarke MS. Laser capture microdissection of metachromatically stained skeletal muscle allows quantification of fiber type specific gene expression. *Mol Cell Biochem* 2013 March;375(1-2):159-70.

- (164) Klitgaard H, Bergman O, Betto R et al. Co-existence of myosin heavy chain I and IIa isoforms in human skeletal muscle fibres with endurance training. *Pflugers Arch* 1990 June;416(4):470-2.
- (165) Winder WW, Taylor EB, Thomson DM. Role of AMP-activated protein kinase in the molecular adaptation to endurance exercise. *Med Sci Sports Exerc* 2006 November;38(11):1945-9.
- (166) Baar K, Wende AR, Jones TE et al. Adaptations of skeletal muscle to exercise: rapid increase in the transcriptional coactivator PGC-1. *FASEB J* 2002 December;16(14):1879-86.
- (167) Terada S, Tabata I. Effects of acute bouts of running and swimming exercise on PGC-1 α protein expression in rat epitrochlearis and soleus muscle. *Am J Physiol Endocrinol Metab* 2004 February;286(2):E208-E216.
- (168) Pilegaard H, Saltin B, Neufer PD. Exercise induces transient transcriptional activation of the PGC-1 α gene in human skeletal muscle. *J Physiol* 2003 February 1;546(Pt 3):851-8.
- (169) Le Douairon LS, Gratas-Delamarche A, Malarde L et al. Combined insulin treatment and intense exercise training improved basal cardiac function and Ca²⁺-cycling proteins expression in type 1 diabetic rats. *Appl Physiol Nutr Metab* 2012 February;37(1):53-62.
- (170) Rose AJ, Frosig C, Kiens B, Wojtaszewski JF, Richter EA. Effect of endurance exercise training on Ca²⁺ calmodulin-dependent protein kinase II expression and signalling in skeletal muscle of humans. *J Physiol* 2007 September 1;583(Pt 2):785-95.
- (171) Rose AJ, Kiens B, Richter EA. Ca²⁺-calmodulin-dependent protein kinase expression and signalling in skeletal muscle during exercise. *J Physiol* 2006 August 1;574(Pt 3):889-903.
- (172) Vasanji Z, Dhalla NS, Netticadan T. Increased inhibition of SERCA2 by phospholamban in the type I diabetic heart. *Mol Cell Biochem* 2004 June;261(1-2):245-9.
- (173) Shao CH, Wehrens XH, Wyatt TA et al. Exercise training during diabetes attenuates cardiac ryanodine receptor dysregulation. *J Appl Physiol* 2009 April;106(4):1280-92.
- (174) Tappia PS, Thliveris J, Xu YJ, Aroutiounova N, Dhalla NS. Effects of amino acid supplementation on myocardial cell damage and cardiac function in diabetes. *Exp Clin Cardiol* 2011;16(3):e17-e22.

- (175) Semeniuk LM, Kryski AJ, Severson DL. Echocardiographic assessment of cardiac function in diabetic db/db and transgenic db/db-hGLUT4 mice. *Am J Physiol Heart Circ Physiol* 2002 September;283(3):H976-H982.
- (176) Wolfe LA, Martin RP, Watson DD, Lasley RD, Bruns DE. Chronic exercise and left ventricular structure and function in healthy human subjects. *J Appl Physiol* 1985 February;58(2):409-15.
- (177) Riggs CE, Jr., Michaelides MA, Parpa KM, Smith-Blair NJ. The effects of aerobic interval training on the left ventricular morphology and function of VLCAD-deficient mice. *Eur J Appl Physiol* 2010 November;110(5):915-23.
- (178) Nielsen LB, Bartels ED, Bollano E. Overexpression of apolipoprotein B in the heart impedes cardiac triglyceride accumulation and development of cardiac dysfunction in diabetic mice. *J Biol Chem* 2002 July 26;277(30):27014-20.
- (179) Davidson E, Coppey L, Lu B et al. The roles of streptozotocin neurotoxicity and neutral endopeptidase in murine experimental diabetic neuropathy. *Exp Diabetes Res* 2009;2009:431980. Epub;2010 Feb 3.:431980.
- (180) Schwinger RH, Munch G, Bolck B, Karczewski P, Krause EG, Erdmann E. Reduced Ca(2+)-sensitivity of SERCA 2a in failing human myocardium due to reduced serin-16 phospholamban phosphorylation. *J Mol Cell Cardiol* 1999 March;31(3):479-91.
- (181) Mercadier JJ, Lompre AM, Duc P et al. Altered sarcoplasmic reticulum Ca2(+)-ATPase gene expression in the human ventricle during end-stage heart failure. *J Clin Invest* 1990 January;85(1):305-9.
- (182) Arai M, Alpert NR, MacLennan DH, Barton P, Periasamy M. Alterations in sarcoplasmic reticulum gene expression in human heart failure. A possible mechanism for alterations in systolic and diastolic properties of the failing myocardium. *Circ Res* 1993 February;72(2):463-9.
- (183) Brady M, Koban MU, Dellow KA, Yacoub M, Boheler KR, Fuller SJ. Sp1 and Sp3 transcription factors are required for trans-activation of the human SERCA2 promoter in cardiomyocytes. *Cardiovasc Res* 2003 November 1;60(2):347-54.
- (184) Wen JP, Liu C, Bi WK et al. Adiponectin inhibits KISS1 gene transcription through AMPK and specificity protein-1 in the hypothalamic GT1-7 neurons. *Endocrinol* 2012 August;214(2):177-89.
- (185) Chu S, Ferro TJ. Sp1: regulation of gene expression by phosphorylation. *Gene* 2005 March 28;348:1-11.

- (186) Sulaiman M, Matta MJ, Sunderesan NR, Gupta MP, Periasamy M, Gupta M. Resveratrol, an activator of SIRT1, upregulates sarcoplasmic calcium ATPase and improves cardiac function in diabetic cardiomyopathy. *Am J Physiol Heart Circ Physiol* 2010 March;298(3):H833-H843.